学位論文内容の要旨

博士の専攻分野の名称	博士（水産学）	氏名	久万健志

学位論文題名

A Biogeochemical Study on Colloidal Ferric Oxides in Seawater

（海水におけるコロイド酸化鉄の生物地球化学的研究）

近年、分析機器の発達、分析法の改良並びに採水技術の進歩により、海水中における微量金属の正確な定量値が報告されるとともに、生物との関係についても論じられるようになった。特に第一遷移元素である鉄、マンガン、コバルト、ニッケル、銅、亜鉛は生物にとって必須微量金属と呼ばれ、生体反応に不可欠な元素である。その中でも鉄は古くからプランクトンの増殖に重要な役割を果たすと考えられ、かなり以前から必須微量元素の一つであることが報告されている。

海洋において、必須微量金属元素の大部分は溶存態で存在しているが、鉄は他の必須微量金属元素と異なり、酸化環境下における海水中では3価の水和酸化鉄として存在しており、その溶解度並びに溶解速度は極めて小さいとされている。

また、天然水及び土壌中には無定形及び種々の結晶性水和酸化鉄が存在しており水和酸化鉄の形態の違いによりそれらの溶解度及び溶解速度は異なるものと推定されている。近年報告されている外洋深層水の溶存鉄濃度は0.3-0.7nMと深度に関係なくほぼ一定値を示しており、ある種の水和酸化鉄との溶解平衡にあるものと推定される。また植物プランクトンが鉄を利用する場合、鉄を錯化出来るサイドロフォアを有する数種の赤潮プランクトンを除けば、植物プランクトンに摂取される鉄は、粒状水和酸化鉄と平衡で存在する溶存鉄及び粒状水和酸化鉄から溶解する溶存鉄である。すなわち粒状水和酸化鉄の溶解度と溶解速度は藻類による鉄の取り込み速度を支配する重要な因子である。栄養塩の枯渇しない外洋域の表層では、鉄によって植物プランクトンの成長及び増殖が制限されており、鉄を人為的に海洋に供給することで植物プランクトンの増殖を促進させ、二酸化炭素を固定し地球温暖化を抑制させるという考えが最近活発に議論され始め、地球環境を考える上でも海洋における鉄が注目されている。

以上のことから、海水における種々の水和酸化鉄の溶解度並びに溶解速度を求

めることは実際の海洋に存在する粒状水和酸化鉄の形態を知る上で、また植物プランクトンが増殖しうる水和酸化鉄の形態及びそれに取り込まれる溶存鉄の化学形態を知る上で重要である。本研究は、海水における数種の水和酸化鉄の溶解度並びに溶解速度を透析膜及びフィルター を使用して測定した。またこれらの水和酸化鉄存在下での植物プランクトンの増殖実験を行い、水和酸化鉄の溶解度及び溶解速度の観点から考察し、以下の知見を得た。

1）透析実験か得られた海水における無定形水和酸化鉄及びγ-FeOOHの溶解度は約10nM及び1.4±0.4nMであり、0.025μmのフイルターを使用して得られた溶解度とほぼ一致した。また、pH5.5から7までの酸性下ではpH上昇とともその溶解度の対数値は減少し、理論的な傾き－1を示しその主な溶存種は$Fe(OH)_4^-$である。しかしながら、pH7から海水のpH8まではpHに関係なく、ほぼ一定値を示した。これは水素イオン濃度に無関係な溶存種$Fe(OH)_3$の存在を示唆している。

2）種々の水和酸化鉄の海水における溶解度の順は、無定形水和酸化鉄（10nM）＞γ－FeOOH（1.4±0.4nM）＞$Fe_5O_7(OH)\cdot 4H_2O$（0.2－0.6nM）＞α－FeOOH（0.01nM）であり、α－FeOOHは最も安定な水和酸化鉄とされている。このことから外洋域での深層の溶存鉄濃度は準安定相の無定形水和酸化鉄よりむしろ安定相の結晶性水和酸化鉄の溶解度に支配されていると考えられる。しかしながら、溶存と粒子とを分離するために、現在一般に使用されている0.4-0.45μmフイルターでは微細コロイドを分離出来ない事、また海洋における粒状Fe（Ⅲ）の形態が明らかにされていない事等多くの問題点が残されている。

3）透析実験並びに酸性下での溶解実験から得られた種々の水和酸化鉄の溶解速度の順は溶解度の順と同じであった。これらの順は水和酸化鉄の化学組成及び結晶構造の差に由来しており、水和酸化鉄の熱力学的安定性の違いによるものである。また、溶解に必要とされる種々の水和酸化鉄の活性化エネルギーの順は、それぞれの溶解度及び溶解速度の順の逆になった。これは溶解に必要とされる活性化エネルギーが大であると、その水和酸化鉄の熱力学的安定性は大であることを意味しており、必然的に溶解度及び溶解速度は小さいことを示している。

4）種々の水和酸化鉄の存在下での植物プランクトン培養実験から、粒状水和酸化

鉄の溶解度及び溶解速度を明らかにした。また、植物プランクトンによって利用される粒状水和酸化鉄の形態を明かにし、その増殖を水和酸化鉄の溶解度、溶解速度及び熱力学的安定性と関連づけた。

鉄による増殖の度合いは、無定形水和酸化鉄＞γ－FeOOH≫$Fe_5O_7(OH)\cdot 4H_2O$＞α－FeOOHの順になり、これらの水和酸化鉄の溶解度及び溶解速度の順番と一致した。特に$Fe_5O_7(OH)\cdot 4H_2O$とα－FeOOHの水和酸化鉄の形態では植物プランクトンは栄養塩が多量に存在しているにもかかわらず殆ど増殖することが出来ず存在する水和酸化鉄の溶解度並びに溶解速度によって植物プランクトンによる鉄の取り込み速度が支配されていると考えられる。また、サイドロフォアのような鉄とキレートをつくる物質を有している植物プランクトンによる鉄の取り込みは、性に水溶洋無定さラる速定化鉄存支配以酸度で形のてク状さに本

和解域定相れン粒度性

鉄の溶解度及び溶解速度を明らかにした。また、植物プランクトンによって利用される粒状水和酸化鉄の形態を明かにし、その増殖を水和酸化鉄の溶解度、溶解速度及び熱力学的安定性と関連づけた。

A BIOGEOCHEMICAL STUDY ON COLLOIDAL FERRIC OXIDES IN SEAWATER

BY

KENSHI KUMA

A DISSERTATION
SUBMITTED IN PARTIAL FULFILMENT OF
THE REQUIREMENT FOR THE DEGREE OF
DOCTOR OF FISHERIES SCIENCE

1992

ABSTRACT

Solubilities and dissolution rates of colloidal amorphous hydrous ferric oxide ($Fe_2O_3.xH_2O$) (chapter 2) and crystalline γ-FeOOH (lepidocrocite) (chapter 3), typical ferric oxides in natural waters and soils, in seawater over pH range 5.5 to 8.2 at 20°C were experimentally determined by new dialysis techniques involving γ-activity measurements of ^{59}Fe. Within the pH range 5.5-7.0, the logarithmic solubilities of both ferric oxide phases increased linearly with decreasing pH with a slope of -1.0 in good agreement with the theoretical slope, indicating that $Fe(OH)_2^+$ is the dominant dissolved ferric species. However, in the normal pH range of seawater, the solubilities were independent of pH with values: approximately $1x10^{-8}$ and $1x10^{-9}$ mol l^{-1} for amorphous phase and γ-FeOOH, respectively. The solubilities determined by dialysis experiments are consistent with those determined by simple filtration experiments with a 0.025 μm Millipore filter (Chapter 4). The order of solubilities of various ferric oxides in seawater is amorphous hydrous ferric oxide (10 nM) > γ-FeOOH (1.4±0.4 nM) > $Fe_5O_7(OH).4H_2O$ (hydrated ferric oxyhydroxide polymer) (0.2-0.6 nM) > α-FeOOH (goethite) (0.01 nM) since α-FeOOH, the most stable iron oxyhydroxide found in soils and natural waters, is approximately three orders of magnitude less soluble than amorphous phase. The solubilities of γ-FeOOH, one of the typical iron oxyhydroxides, and/or $Fe_5O_7(OH).4H_2O$ in seawater measured at its normal pH appear to be about one order of magnitude lower than that of amorphous phase and to be nearly the

same values as the dissolved iron concentrations (0.3-0.7 nM) recently measured at deep waters in the open ocean. The implication, then, is that the deep waters in the open ocean may be in saturation equilibrium with the thermodynamically stable crystalline ferric oxide forms rather than metastable amorphous phase. This result also indicates the existence of $Fe(OH)_3^\circ$ species, which is independent of hydrogen ion concentration in the normal pH of seawater, in addition to $Fe(OH)_2^+$.

The Fe(III) dissolution rate was defined as a first-order reaction in proportion to the concentration of particulate Fe(III) in seawater. Within the pH range 7.0-8.2, the rate constants for amorphous and γ-FeOOH were independent of pH with values: 0.015 and 0.005 day^{-1}, respectively. This suggests that only water is involved in breaking the Fe-O bond on the surface of ferric oxide to form an activated complex. In the normal pH range of seawater, the dissolution rate constant of γ-FeOOH is one-third lower than that of amorphous phase. The order of dissolution rates of various ferric oxides in seawater is amorphous phase > γ-FeOOH > $Fe_5O_7(OH).4H_2O$ > α-FeOOH, a sequence that must be the result of differences in the chemical composition and crystal structure of these ferric oxides.

These above results probably suggest that thermodynamically stable γ-FeOOH, as well as α-FeOOH, β-FeOOH (akaganeite) and α-Fe_2O_3 (hematite), can not probably support phytoplankton and seaplant growth, but depending on the concentration of particulate Fe(III) as γ-FeOOH, if they can assimilate only soluble ionic species. Culture experiments with the marine flagellates and diatom demonstrate that, as an solid ferric

oxide source, amorphous hydrous ferric oxide can produce better cell yield than the more thermodynamically stable crystalline γ-FeOOH, $Fe_5O_7(OH).4H_2O$ and α-FeOOH. The order of cell yield in the culture experiments is amorphous hydrous ferric oxide > γ-FeOOH >> $Fe_5O_7(OH).4H_2O$ > α-FeOOH, which is the same orders as the solubility and dissolution rate in seawater. An increase in the thermodynamic stability of ferric oxide may reduce the dissolution rate and hence the supply of biologically available iron. The stability is important in controlling the supply of available iron by phytoplankton.

ACKNOWLEDGEMENTS

The author expresses his sincere appreciation to Dr. Katsuhiko Matsunaga for his kind and continuous guidance throughout this study. The author is very grateful to Dr. Shizuo Tsunogai, Dr. Yoshiaki Maita, Dr. Kiyotaka Ohtani and Dr. Masahiro Kajihara for critically reading the manuscript and for the coadial advices in the present study.

The author received useful suggestions from Dr. Isamu Kashiki, Mr. Minoru Koide, Dr. Mark Wells and Dr. Gustaf Arrhenius. Kind helps were also offered by Dr. Isao Kudo and Dr. Akira Usui.

CONTENTS

1 GENERAL INTRODUCTION

1.1 General introduction

Iron is one of the major components of Earth's crust and plays an important role in the biogeochemistry of natural waters. The oceanic distributions and biogeochemical behavior of dissolved and particulate iron are controlled by complex interactions among input, internal cycling and removal process. Over the last ten years, the reliable iron concentrations in seawaters have been determined by the use of clean sampling and more sensitive analytical methods (Symes and Kester, 1985; Landing and Bruland, 1987; Westerlund and Ohman, 1991). From a thermodynamic standpoint, dissolved iron should have extremely low concentrations (subnanomolar) under oxic marine conditions. It has been reported recently that the dissolved iron concentrations at mid and deep waters in the open ocean and in shallow margin waters are approximately 0.3-1x10^{-9} and 1x10^{-8} mol l^{-1}, respectively (Gordon et al., 1982; Martin and Gordon, 1988; Martin et al., 1989; Bruland et al., 1991). The principal ferric oxide phases commonly found in soils and natural waters are amorphous hydrous ferric oxide ($Fe_2O_3.xH_2O$), α-Fe_2O_3 (hematite), γ-Fe_2O_3 (maghemite), α-FeOOH (goethite) and γ-FeOOH (lepidocrocite) (Schneider, 1988; Lindsay, 1991). The solubility of the metastable amorphous phase will be generally expected to be higher than those of the stable crystalline solid phases (Stumm and Morgan,

1981). Moreover, their solubilities in seawater will be higher than those at lower ionic strengths since the activity coefficients for Fe^{3+} and OH^- lower with the increase in ionic strength. The metastable phase will be also slowly converted into the stable phase on aging (Cornell et al., 1974; Crosby et al., 1983). The solubilities of only amorphous hydrous ferric oxide in seawater were experimentally determined by simple filtration and dialysis techniques (Bryne and Kester, 1976 a), indicating that the dominant iron species is $Fe(OH)_3°$ in the normal pH range of seawater and the solubilities within the pH range 7 to 8 were independent of pH with value: approximately $1x10^{-8}$ mol l^{-1}. However, the solubilities and dissolution rates in seawater for the most common crystalline ferric oxide phases, such as γ-FeOOH, α-Fe_2O_3 and α-FeOOH, have not been reported since their solubilities and dissolution rates are extremely low and slow, respectively. The dissolved iron concentration at deep waters in the open ocean may be in equilibrium with the stable crystalline ferric oxides rather than metastable amorphous phase. To confirm this interpretation the following several problems will have to be resolved; the operationally defined concept of a dissolved (filterable) fraction with a 0.3 or 0.4 μm filter which can not quantitatively remove the smaller colloidal particles (Lewin and Chen, 1973; Zhuang et al., 1990), qualitative and quantitative analyses for solid iron phases in seawaters, atmospheric dust and colloids from rivers, the crystallization mechanism of amorphous phase to the stable form in seawater (Crosby et al., 1983), the adsorption mechanism of dissolved iron on the particles (Stumm, 1977; Stumm and Morgan, 1981; Zhuang et al., 1990), etc.

According to Duce (1986), over 95 % of the Fe supply to surface waters in the open ocean comes from the atmosphere. Zhuang et al. (1990) found that the saturated concentration of atmospheric iron in seawater passing through a 0.05 μm filter was 5-8 nM, while that passing through a 0.4 μm filter was 10-17 nM, and about 50 % of the atmospheric iron dissolved rapidly in seawater if the total iron concentration was less than 2 nM (the open Pacific Ocean is in this category). These results may indicate that the dominant ferric oxide form in atmospheric iron is probably amorphous phase and that the dissolved iron is utilized at surface photic zone in the open ocean by phytoplankton. Therefore, the dissolved iron concentrations at the surface waters in the open ocean are controlled by the atmospheric iron inputs (abundance in source media, solubility and dissolution rate depending on the iron solid form) and phytoplankton iron requirements. The iron solid form at deep waters, which is probably regenerated from oxidation of the biogenic organic flux and/or is less soluble atmospheric iron, may be less soluble oxide than amorphous phase. The implication, then, is that the dissolved iron concentration at deep waters in the open ocean may be in equilibrium with the thermodynamically stable ferric oxide forms rather than metastable amorphous phase.

Iron is also an essential micronutrient and a limiting factor for phytoplankton growth and primary production in the ocean (Glover, 1978; Finden et al., 1984; Martin and Fitwater, 1988; Martin et al., 1989, 1990 and 1991; Price et al., 1991). It has been usually assumed that phytoplankton assimilate soluble ionic species. However, the stable

form of iron in oxic seawater is Fe(III), which has a low solubility (Stumm and Morgan, 1981). Therefore, phytoplankton growth might be severely limited after initial growth had used up the small amount of soluble ionic iron in equilibrium with particulate Fe(III), since the dissolution rate of particulate Fe(III) is slow in relation to the further demands of the phytoplankton (Anderson and Morel, 1982). The crystalline ferric oxides, thermodynamically stable forms, do not support phytoplankton growth at all, while amorphous hydrous ferric oxide can induce the maximal growth and the cell yields because of faster thermal dissolution rate of amorphous phase than those of crystalline ferric oxides (Wells et al., 1983; Rich and Morel, 1990). Using three well-difined types of Fe colloids, Rich and Morel (1990) found no evidence of any direct uptake by phytoplankton. Rather, they suggested that transfer of Fe from colloids to phytoplankton is probably kinetically limited by relatively slow photoreduction and thermal dissolution processes. Waite and Morel (1984 a and b) and Rich and Morel (1990) have demonstrated the importance of photochemical reduction and solubilization of the particulate or colloidal Fe(III) as a major mechanism in maintaining a steady state dissolved iron concentration but there has been little evidence that similar photo-processes occur at natural seawater (pH 8). On recent works, however, it has been reported that Fe(III) in seawater (pH 8.0-8.1) was readily reduced to Fe(II) in sunlight in the presence of hydroxycarboxylic acids, such as sugar acids (Kuma et al; 1992 b) and that the photoconversion of synthetic colloidal iron oxyhydroxides to more available iron for phytoplankton was found to

increase in seawater (pH 8) upon irradiation with simulated and natural sunlight (Wells and Mayer, 1991; Wells et al., 1991). Moreover, dissolved Fe(II) were detected near the surface waters and/or at depths with higher concentrations of Chl a, suggesting that photochemical reduction may be an important source for Fe(II) in these waters (Nakabayashi et al, 1989; O'Sullivan et al., 1991; Kuma et al., 1992 b).

Therefore, the solubilities and dissolution rates of ferric oxides in seawater are important factors which will control the dissolved iron concentration in oxic seawater and govern the primary production of phytoplankton in seawater. In this study, the solubilities and dissolution rates of amorphous hydrous ferric oxide and γ-FeOOH in seawater at 20°C were experimentally determined by new dialysis techniques involving γ-activity measurements of ^{59}Fe. Those of hydrated ferric oxyhydroxide polymer ($Fe_5O_7(OH).4H_2O$) and α-FeOOH, in addition to amorphous phase and γ-FeOOH, in seawater were also determined by simple filtration experiments. Furthermore, the marine diatom and flagellates were cultivated in the presence of various ferric oxide forms, as described above, in order to confirm whether the phytoplankton growth is controlled by the solubilities and thermal dissolution rates of ferric oxides used.

2 SOLUBILITY AND DISSOLUTION RATE OF AMORPHOUS HYDROUS FERRIC OXIDE IN SEAWATER

2.1 Introduction

Iron is an essential micronutrient for phytoplankton growth (Finden et al., 1984; Martin and Fitzwater, 1988; Martin et al., 1989). The stable oxidation state of iron in oxic seawater is Fe(III) which has a low solubility. It has been usually assumed that phytoplankton assimilate soluble ionic species. Therefore, phytoplankton growth might be severely limited if, after initial growth, it had used up the small amount of available soluble ionic iron in equilibrium with particulate Fe(III), since the dissloution rate of particulate Fe(III) is slow in relation to the further demands of phytoplankton. The mass dissloution rate of the hydrous ferric oxide controls the free ferric ion concentration and hence the uptake rate by phytoplankton. Therefore, the solubility and dissolution rate of hydrous ferric oxide in oxic seawater are important factors which will govern the primary production of phytoplankton in seawater.

The chemical equilibria among the dissolved forms of iron and a solid phase may establish the concentration of dissolved iron in seawater. Since the most common insoluble solid phase of iron in oxic seawater is hydrous ferric oxide, the formation of this phase is expected to be a dominant feature of iron solubility equilibria in seawater. The solid

phase from solutions supersaturated with respect to Fe^{3+} is the initial formation of amorphous hydrous ferric oxide followed by a slow transformation to more stable crystalline solid phases. Ferric oxide precipitate derived from ferric iron by using conditions very similar to those encountered in natural waters was identified as amorphous in the initial phase, but containing 10-20 % α-FeOOH (goethite) on aging for 12 days, with X-ray diffraction, infrared and Mossbauer spectroscopies (Crosby et al., 1983). The composition of the amorphous hydrous ferric oxide is uncertain, but transformation to crystalline form is very slow process. In the open ocean, the most likely sources of iron colloids are atmospheric dust (Moore et al., 1984; Duce, 1986), in situ oxidation of Fe(II) (Landing and Bruland, 1987) and release of iron compounds during the degradation of organisms. The saturated concentration (filterable iron with 0.05 μm filter) of atmospheric iron in seawater was found to be 5-8 nM and the dissolution of atmospheric iron was extremely fast, probably indicating that the dominant iron solid phase in atmospheric iron is amorphous ferric oxide (Zhuang et al., 1990). In coastal waters, in addition, the input of colloids from rivers must be considered.

The metastable amorphous hydrous ferric oxide, probably a dominant iron solid phase in colloids from river and atomospheric dust, will be expected to have higher iron solubility and the faster dissolution rate than the stable crystalline ferric oxides such as α-FeOOH, γ-FeOOH (lepidocrocite) and α-Fe_2O_3 (hematite) (Stumm and Morgan, 1981). The solubility of amorphous hydrous ferric oxide in seawater was experimentally determined by filtration (Byrne and Kester, 1976 a),

indicating that the dominant iron species are $Fe(OH)_2^+$ in the pH range 5.5 to 6.5 and $Fe(OH)_3^\circ$ in the normal pH range of seawater above 7. The solubilities within the pH range 7 to 8 were independent of pH with value: approximately $1x10^{-8}$ mol l^{-1}. In this study, the solubilities and dissolution rates of amorphous hydrous ferric oxide, precipitate derived from the hydrolysis of ferric iron in seawater, in seawater over the pH range 5.5 to 8.1 at 20°C were experimentally determined by the dialysis technique involving γ-activity measurement of ^{59}Fe.

2.2 Theoretical Considerations

2.2.1 *Solubility of hydrous ferric oxide*

The solubility product of any of the hydrous ferric oxide solid phases can be conveniently formulated as follows:

$$*Kso = [Fe^{3+}] [H^+]^{-3} \quad (1)$$

The $[H^+]$ is defined on the free hydrogen ion molality. In this equation the dependence of the equilibrium on the free energy of both the solid phase and the water in the solution is incorporated into the magnitude of *Kso. Because of the dependence of *Kso on the activity of the solid phase, *Kso may decrease during the aging and transformation of a solid phase. Table 2-1 presents the solubility products of amorphous hydrous ferric oxides and α-FeOOH and the formation constants of hydroxo ferric ion complexes $[Fe(OH)_n]^{z-n}$ in water (I=0) at 25°C (Sillen

and Martell, 1964; Stumm and Morgan, 1981), but an uncertain formation constant of $Fe(OH)_3°$, and in seawater at 25°C (Byrne and Kester, 1976 a and b). Their constants can be used to construct the solubility diagrams of amorphous hydrous ferric oxide in water (I=0) and seawater as a function of pH as shown in Fig. 2-1 and 2-2, respectively.

The total concentration of dissolved Fe(III) in a solubility equilibrium also depends on the equilibria between the dissolved forms of Fe(III) in seawater. The following equation, formulated by Byrne and Kester (1976 a), can be written to approximate the solubility behavior of ferric oxide in seawater for pH>5.0.

$$T[Fe(III)d] = *Kso(*\beta_1[H^+]^2 + *\beta_2[H^+] + *\beta_3 + *\beta_4[H^+]^{-1}) \qquad (2)$$

where $*\beta_1$, $*\beta_2$, $*\beta_3$ and $*\beta_4$ are the formation constants for $Fe(OH)^{2+}$, $Fe(OH)_2^+$, $Fe(OH)_3°$ and $Fe(OH)_4^-$, respectively, represented by $*\beta_1 = [Fe(OH)^{2+}][H^+]/[Fe^{3+}]$, $*\beta_2 = [Fe(OH)_2^+][H^+]^2/[Fe^{3+}]$, $*\beta_3 = [Fe(OH)_3°][H^+]^3/[Fe^{3+}]$ and $*\beta_4 = [Fe(OH)_4^-][H^+]^4/[Fe^{3+}]$ and T[Fe(III)d] is the concentration of total dissolved Fe(III). From the constants $*\beta_1$ and $*\beta_2$ determined in various media it can be shown that above pH 4.5 the second term on the right side of eq. (2) is more significant than the first. The following solubility behavior is then predicted by eq. (2) and Fig. 2-1 and 2-2: the slope of log T[Fe(III)d] versus pH should approach -1.0 with increasing pH as the $Fe(OH)_2^+$ species becomes dominant over $Fe(OH)^{2+}$. As pH is increased further, $Fe(OH)_3°$ becomes the dominant species and the slope approaches zero. With further increase of pH, the

species $Fe(OH)_4^-$ becomes dominant and the slope should approach 1.0. The solubility product, *Kso, and the formation constant of $Fe(OH)_3°$, $*\beta_3$, are calculated from the equations $T[Fe(III)d] = *Kso*\beta_2[H^+]$ and $T[Fe(III)d] = *Kso*\beta_3$ using the results of the dialysis experiments in this study and the average value of $*\beta_2$ determined in synthetic media by Byrne and Kester (1976 b).

2.2.2 *Dissolution rate of hydrous ferric oxide*

The Fe(III) dissolution rate equation reduces to the following form, formulated by Aagaard and Helgeson (1982) and Helgeson et al. (1984), in unsaturated solutions far from equibrium.

$$\upsilon = - d[Fe(III)p]/dt = k[s.a.]a_{H^+}^{-nH^+} \qquad (3)$$

Where υ (mol l^{-1} day^{-1}) is the dissolution rate in the solution, [Fe(III)p] (mol l^{-1}) is the concentration of particulate Fe(III) in solution, k is the rate constant, [s.a.] is the effective surface area of ferric oxide, a_{H^+} is the activity of hydrogen ion and nH^+ is the exponent of the hydrogen ion activity in solution. In this study, particulate Fe(III) is defined as Fe(III) composing colloidal hydrous ferric oxide aged at least 1 week after precipitation in seawater. In this equation, the effective surface area, [s.a.], can be conveniently described by the particulate Fe(III) concentration, by supposing that the decrease of surface area by the dissolution is proportional to that of particulate Fe(III) concentration, as follows

$$k[s.a.]a_{H^+}^{-nH+} = k_1[Fe(III)p]a_{H^+}^{-nH+} \quad (4)$$

and at constant activity of hydrogen ion

$$= k_2[Fe(III)p] \quad (5)$$

Where k_1 and k_2 are the dissolution rate constants of particulate Fe(III) in the certain pH range and at constant pH, respectively. Therefore, for each pH

$$- d[Fe(III)p]/[Fe(III)p] = k_2dt \quad (6)$$

The integral of both sides between time 0 and t is then given by

$$\ln [Fe(III)p]_t = \ln [Fe(III)p]_0 - k_2t$$

$$\text{and then } \log [Fe(III)p]_t = \log [Fe(III)p]_0 - k_2t/2.3026 \quad (7)$$

where $[Fe(III)p]_t$ and $[Fe(III)p]_0$ are the concentrations of particulate Fe(III) at time t and 0, respectively.

2.2.3 *Dialysis technique*

The theoretical dialysis technique was described by Kuma et al. (1992 a). The total Fe(III) in a dialysis membrane tube is composed of dissolved (dialyzable) and particulate Fe(III). This experimental approach

assumes that, at constant pH and temperature, the dialysis rate of dissolved Fe(III) and the dissolution rate of particulate Fe(III) are in proportion to dissolved and particulate Fe(III) concentrations in the dialysis tube, respectively. In general, the dialysis rate of dissloved species from one solution to another across a dialysis membrane of constant area is proportional to the concentration of dissolved species in the membrane in case that outer solution is unsatureted far from equilibrium. If the dialysis rate is considerably faster than the dissolution rate, the logarithmic total Fe(III) concentration in the tube with time results in early non-linear change (Fig. 2-3, curve). The dotted and dot-dash lines indicate the logarithmic linear change with time resulting from dialysis of the dissolved Fe(III) in equilibrium with particulate Fe(III) at time 0 and that from dissolution of the particulate Fe(III), respectively. Therefore, the sum of dotted and dot-dash lines represents the observable early non-linear change (curve) of total Fe(III) concentration in the tube with time. After several days the linear part of the curve predominantly represents the dissolution of particulate Fe(III) in the tube and, therefore, can be used to determine the rate constant, k_2, from the slope. The particulate Fe(III) concentration in the tube at time 0 can be estimated by extrapolating the linear part of curve after several days to time 0. Therefore, the solubility of particulate Fe(III) can be determined by subtracting the particulate Fe(III) concentration at time 0 from the total Fe(III) concentration at time 0 in the tube since the dissolved Fe(III) concentration at time 0 is in equilibrium with particulate Fe(III).

From the results of the dialysis dissolution experiments, the solubility

product and the formation constant of $Fe(OH)_3^\circ$ were determined according to the calculating procedure of Byrne and Kester (1976 a,b) and the dissolution rate constants and nH^+ were calculated from the above eqs. (4), (5) and (7). Furthermore, the dissolution rate of particulate Fe(III) as amorphous hydrous ferric oxide in seawater was finally determined from eq. (5).

2.3 Experimental Procedure

In this study, the dialysis technique was used to distinguish between dissolved Fe(III) and particulate Fe(III) in seawater. Total Fe(III) concentration in a dialysis membrane tube was measured with time by γ-activity counting of ^{59}Fe. The dissolution rate and solubility experiments of particulate Fe(III) in seawater within the pH range 5.5-8.1 were conducted in the following manner.

(1) To eliminate the dissolved Fe(III), seawater collected from Funka Bay in Japan (salinity = 33.6 ‰) was passed through a silica-immobilized 8-hydroxyquinoline column (Sturgeon et al., 1981) after being filtered through an acid-cleaned Millipore membrane filter with a pore size of 0.45 μm. The 8-hydroxyqunoline has a large formation constant with iron (10^{38}) and other metals, it has been usually used to preconcentrate trace metals from seawater.

The iron concentration in seawater prepared in this procedure was determined by a graphite furnace atomic absorption spectrophotometer (Hitachi 180-70) after preconcentration by APDC/DDDC-chloroform

organic extraction (Landing and Bruland, 1987). The iron concentration was below 1 nM.

(2) For each dialysis experiment, radioactive ferric ^{59}Fe (New England Nuclear Corp.) solution was added to 50 ml pretreated seawater in a 100 ml polyethylene bottle previously cleaned with 6 N HCl in quantity over the solubility of Fe(III) at a given pH. Small volumes of diluted subboiled HCl (S-HCl) solution were then added to the seawater solutions a few times per day for 1 week at 20°C to obtain a desired pH within the range 5.5-7.6. For pH less than 6.6, the desired pH was obtained within 1 week as a result of buffering systems in the seawater. For the pH range 6.6-7.6, S-HCl solution was added to the seawater solution until the pH was within a desired range of values. Subboiled water (S-water) was used for the dilution of reagents and the washing of apparatus. S-HCl and S-water were produced by subboiling in a clean room.

(3) For each experiment, 600 ml of pretreated seawater (procedure (1)) was added to an Erlenmeyer flask, followed by stirring with aTeflon-coated magnetic stirrer and immersed in a constant-temperature water bath (Yamato-Komatsu Coolnics Circulator CTE42A) at 20±0.2°C. Small volumes of S-HCl solution were added to the seawater several times per day for a period of 1 week in order to obtain a desired pH within the range 5.5-7.6. For pH less than 6.6, the desired pH was attained within 1 week.

(4) For each experiment 1 ml of pretreated seawater containing ^{59}Fe as prepared in procedure (2) was added to a 7.6 mm diameter cellulosic

dialysis tube which excludes solids with molecular weights greater than 1000 Da (Spectrum). Each tube was inserted into a counting vial to measure the γ-activity of solution in the tube at time 0. The tube was then immersed in the 600 ml seawater solution prepared in procedure (3) with the same pH as the seawater in the tube.

(5) Each dialysis tube was withdrawn from the seawater solution twice a day and inserted into a counting vial to measure the γ-activity for a duration of 12 days. After each radiomeasurement, the dialysis tube was reimmersed in the seawater solution till the time for the next measurement. During this dialysis experiment, the pHs of the solutions in the flasks in the pH range 6.6-7.6 were continually adjusted to the desired pH range by adding S-HCl solution.

(6) The γ-activity of each dialysis tube, containing ^{59}Fe solution, in counting vials, was measured by Aloka ARC-310B with an average counting efficiency for ^{59}Fe (CE-I). In addition, the counting efficiency (CE-II) due to the insertion of a dialysis tube containing ^{59}Fe solution into a counting vial is approximately 70 % of that for the ^{59}Fe solution directly added into a vial. Therefore, the measured counts were corrected for CE-II for each tube. Finally, the total Fe(III) concentration in each dialysis tube with time for a duration of 12 days was calculated from the counts corrected for CE-II, CE-I of the scintillation counter, volume of solution added in the tube and amount of Fe per count.

The concentration of dialyzed Fe(III) in 600 ml seawater solution is negligibly low for the determination of solubility and dissolution rate constants in the sense of being far from equilibrium. After dialysis

experiments, the iron concentration in 600 ml seawater in each flask at pH 6.80-8.06 was also determined by the same analytical method described in procedure (1). The iron concentration was below 1 nM.

To confirm the ferric oxide form produced in procedure (2), it was produced by adding ferric chloride solution to the seawater, adjusting to pH 8.0 with NaOH and then aging for 1 week at 20°C. X-ray diffraction analysis with filtered Cu Kα radiation (40 kv, 20 mA) confirmed that the product was amorphous solid phase, which is defined as colloidal hydrous ferric oxide, with two broad peaks in the X-ray diffractogram (Fig. 2-4).

2.4 Results and Discussion

Fig. 2-5 and 2-6 show the results of dissolution experiments for 12 days at pHs 5.50-6.25 and 6.50-8.06, respectively. Each curve is in excellent agreement with the theoretical curve shown in Fig. 2-3; the linear part after day 5 primarily represents the dissolution of particulate Fe(III) in each tube. The dissolution rate constant, k_2, in the eq. (7) and the solubility at each pH (Table 2-2) were determined from the slope and the particulate Fe(III) concentration at time 0, respectively, using a least-squares linear regression of the dialysis data after day 5. The two dialysis results, with different total Fe(III) concentrations at time 0, at pH 6.50 (Fig. 2-6) indicated nearly the same dissolution rate constant and solubility (Table 2-2), suggesting that the dissolution rate of particulate Fe(III) is in proportion to the particulate Fe(III) concentration and that

the dissolved Fe(III) concentration at time 0 is in equilibrium with the colloidal hydrous ferric oxide in this study. Fig. 2-7 shows the dialysis data at pH 5.50 (solid line), the dissolution of particulate Fe(III) (dot-dash line) calculated from the data after day 5 and the dialysis of dissolved Fe(III) at time 0 (dotted line) obtained by subtraction of the dot-dash line from the solid line. This result indicates that the dialysis rate of dissolved Fe(III) is in proportion to the dissolved Fe(III) concentration and the dialysis rate of dissolved Fe(III) is considerably faster than the dissolution rate of particulate Fe(III) within the pH range in this study.

2.4.1 *Solubility of colloidal hydrous ferric oxide in seawater*

The solubility results are presented graphically in Fig. 2-8 as a plot of log T[Fe(III)d] (mol l^{-1}) vs. pH. The line labeled $Fe(OH)_2^+$ was determined over the pH range 5.50-6.50 and is representative of the equation $T[Fe(III)d] = {}^*Kso^*\beta_2[H^+]$ assuming that within this pH range only the species $Fe(OH)_2^+$ is significant.The constant term, ${}^*Kso^*\beta_2 = 4.3\pm0.4\times10^{-2}$, in this equation was calculated from an average of the values of $T[Fe(III)d]/[H^+]$ within the pH range 5.50-6.50. A least-squares linear regression of log T[Fe(III)d] vs. pH gives a slope of -1.01±0.08 in good agreement with the theoretical slope of -1.0. Using the procedure of Byrne and Kester (1976 a) and the average value of ${}^*\beta_2$ (8.6×10^{-8}) determined in synthetic media by them (1976 b), the stoichiometric solubility product, *Kso, and the thermodynamic product, Kso, were calculated to be $5.0\pm0.5\times10^5$ and $10^{-37.47\pm0.04}$, respectively. The calculated Kso in this study is consistent with the value of $10^{-37.5\pm0.1}$ obtained from

the results of simple filtration experiments for a freshly precipitated hydrous ferric oxide (Byrne and Kester, 1976 a) and $10^{-37.1}$ > Kso > $10^{-38.3}$ obtained for a fresh, rapidly precipitated amorphous solid phase (Langmuir, 1969). Published equilibrium constants for ferric hydroxide complexes indicate that only the monomeric species, $Fe(OH)_2^+$, can exist in significant concentrations in the pH range 5.50-6.50 (Fox, 1988).

The solubility over the pH range 6.8-8.06 is relatively pH independent with $1.05\pm0.05\times10^{-8}$ mol l^{-1} as an average value between pHs 7.57 and 8.06. This result indicates that the dominant iron species in oxic seawater at the normal pH of seawater is probably $Fe(OH)_3°$ in addition to $Fe(OH)_2^+$. The concentration of $Fe(OH)_2^+$ in equilibrium with colloidal hydrous ferric oxide at pH 8.0, obtained by extrapolation to pH 8.0, is about 4.4×10^{-10} mol l^{-1} and is only about 4 % of the solubility at pH 8.0. The formation constant of $Fe(OH)_3°$, $*\beta_3$, was calculated to be $2.1\pm0.7\times10^{-14}$ from $*Kso*\beta_3 = 1.05\pm0.05\times10^{-8}$ and $*Kso = 5.0\pm0.5\times10^{5}$. This is consistent with the value of $2.4\pm1.0\times10^{-14}$ obtained from the acidification followed by filtration experiments of Byrne and Kester (1976 a). However, the concentration of $Fe(OH)_3°$ at the normal pH of seawater obtained in this study may be overestimated since organic complexes with ferric ion in seawater could exist in significant concentrations. The problem is mainly confined to small organic complexes, with molecular weights smaller than 1000 Da, which could cross the dialysis membrane, since most humic material is large enough to be excluded by the dialysis membrane (Fox, 1988).

It has been reported recently that the dissolved iron concentrations in

mid and deep waters in the open ocean and in the shallow margin waters are approximately $1x10^{-9}$ mol l^{-1} and $1x10^{-8}$ mol l^{-1}, respectively (Gordon et al., 1982; Martin and Gordon, 1988; Martin et al., 1989). The solubility in seawater measured at its normal pH in this experimental study appears to be an order of magnitude higher than the dissolved iron concentration measured in mid and deep waters in the open ocean. The implication, then, is that the open waters may not be in saturation equilibrium with a metastable colloidal hydrous ferric oxide as found in this study. The dominant iron solids found in open water are probably the stable clay minerals, ferric oxide and oxyhydroxide of atmospheric input. The iron solubilities of these stable iron compounds in seawater are possibly lower than that of metastable hydrous ferric oxide in this study (Stumm and Morgan, 1981). Moreover, the dissolved Fe(III) forms polynuclear hydrolysis products, $Me_q(OH)_n^{+z}$, which are absorbed readily at particle-water interfaces (Stumm, 1977; Stumm and Morgan, 1981). It may be also interpreted that the dominant iron solid phase in the shallow margin and coastal waters is the metastable amorphous phase supplied from sediments and rivers and that their waters is in saturation equilibrium with the amorphous ferric oxide phase. The biogeochemical cycling of iron will, therefore, be a function of the inputs (abundance in source media and rate of transfer to dissolved forms depending on the solid form, its effective surface area and photoreduction at organic surfaces) and residence time in the aquatic environment (reactivity towards particle surfaces, organisms, etc.).

2.4.2 *Dissolution rate of colloidal hydrous ferric oxide in seawater*

The dissolution rate constants, k_2, determined from the slopes (Figs. 2-5 and 2-6) are presented in Table 2-2. A plot of log k_2 vs. pH, Fig. 2-9, allows the calculation of nH^+ and the dissolution rate constant, k_1, from the equation $\log k_2 = \log k_1 + nH^+pH$. Within the pH range 5.5-6.80, log k_2 increases with an increase in the activity of the hydrogen ion and fitted by a line whose slope corresponds to $nH^+ = -0.55\pm0.06$. The increase as a function of pH is consistent with that of solubility. For the corresponding mechnism in seawater at 20°C, we calculate a value for the dissolution rate constant, $k_1 = 95\pm16$ day^{-1}. Within the pH range 6.8-8.06, k_2 is relatively independent of pH with a value of $k_2 = k_1 = 0.015\pm0.002$ day^{-1} with $nH^+ = 0$. This suggests that only water is involved in breaking the Fe-O bond on the surface of hydrous ferric oxide to form an activated complex. The Fe(III) dissolution rate of colloidal amorphous hydrous ferric oxide in the normal pH range of oxic seawater at 20°C is 0.015x[Fe(III)p] (conc. day^{-1}), which was determined from eqn. (5) by the particulate Fe(III) concentration and the dissolution rate constant.

Particle size distributions of hydrous ferric oxide may depend on the Fe(III) concentration added to seawater and the pH of seawater. The different distributions may influence the dissolution rates, although it was supposed that decrease of surface area due to dissolution is proportional to particulate Fe(III) concentration in eqn. (4). Regrettably, the particle size distribution at each pH could not be measured because the particulate Fe(III) concentration in this dialysis experiment is extremely low.

2.5 Conclusions

Solubilities and dissolution rate constants of colloidal amorphous hydrous ferric oxide in seawater over the pH range 5.5-8.1 at 20°C were experimentally determined by dialysis techniques involving γ-activity measurements of ferric ^{59}Fe. The Fe(III) dissolution rate was defined as a first-order reaction in proportion to the concentration of particulate Fe(III) in seawater. These rate constants and solubilities within the pH range 6.8-8.1 were independent of pH with values: 0.015±0.002 day^{-1} and 1.05±0.05x10^{-8} mol l^{-1}, respectively. This results probably indicates the existence of $Fe(OH)_3°$ as well as $Fe(OH)_2^+$ in the normal pH range of seawater. The concentration of $Fe(OH)_2^+$ in equilibrium with amorphous hydrous ferric oxide at pH 8.0 is about 4.4x10^{-10} mol l^{-1} and is only about 4 % of the solubility at pH 8.0. At lower pHs, the logarithmic dissolution rate constants and solubilities increased linearly with decreasing pH with a slope of -0.55 and -1.0, respectively. The Fe(III) dissolution rate of colloidal hydrous ferric oxide at the normal pH of seawater can be estimated from 0.015x[Fe(III)p] (conc. day^{-1}) by the concentration of particulate Fe(III) in seawater.

Table 2-1 Stability constant for solubility equilibria of hydrous ferric oxides in water and seawater at 25°C

Oxide and Hydroxides	Symbol for Equilibria Constants	logK at 25°C
(I) I=0 (Stumm and Morgan, 1981; Sillen and Martell, 1964)		
$(am)FeOOH\ (s) + 3H^+ = Fe^{3+} + 2H_2O$	*Kso	2.5
α-$FeOOH\ (s) + 3H^+ = Fe^{3+} + 2H_2O$	*Kso	0.5
$Fe^{3+} + H_2O = FeOH^{2+} + H^+$	$*\beta_1$	-2.19
$Fe^{3+} + 2H_2O = Fe(OH)_2^+ + 2H^+$	$*\beta_2$	-5.67
$Fe^{3+} + 3H_2O = Fe(OH)_3^\circ + 3H^+$	$*\beta_3$	< -12
$Fe^{3+} + 4H_2O = Fe(OH)_4^- + 4H^+$	$*\beta_4$	-21.6
(II) in seawater (Byrne and Kester, 1976 a and b)		
$(am)Fe(OH)_3\ (s) + 3H^+ = Fe^{3+} + 3H_2O$	*Kso	5.67
$Fe^{3+} + H_2O = FeOH^{2+} + H^+$	$*\beta_1$	-2.71
$Fe^{3+} + 2H_2O = Fe(OH)_2^+ + 2H^+$	$*\beta_2$	-7.07
$Fe^{3+} + 3H_2O = Fe(OH)_3^\circ + 3H^+$	$*\beta_3$	-13.62
$Fe^{3+} + 4H_2O = Fe(OH)_4^- + 4H^+$	$*\beta_4$	-26.4

The possible occurence of polynuclear complexes, for example, $Fe(OH)_2^{4+}$, has been ignored. Such complexes do not change the solubility characteristics markedly for the solids considered here.

Table 2-2 Iron solubilities and dissolution rate constants determined by dialysis experiments on colloidal hydrous ferric oxide in seawater at 20°C

pH	solubility (mol l^{-1})	Dissolution rate constant k_2 (day^{-1})
5.50	$1.37\pm0.03\times10^{-7}$	$8.19\pm0.32\times10^{-2}$
5.75	$7.97\pm0.17\times10^{-8}$	$6.26\pm0.16\times10^{-2}$
6.00	$5.94\pm0.33\times10^{-8}$	$5.72\pm0.42\times10^{-2}$
6.25	$2.19\pm0.32\times10^{-8}$	$4.29\pm0.34\times10^{-2}$
6.50	$1.43\pm0.06\times10^{-8}$	$2.25\pm0.15\times10^{-2}$
6.50	$1.41\pm0.23\times10^{-8}$	$2.86\pm0.14\times10^{-2}$
6.80	$1.23\pm0.09\times10^{-8}$	$1.58\pm0.10\times10^{-2}$
7.57	$1.10\pm0.18\times10^{-8}$	$1.61\pm0.22\times10^{-2}$
8.06	$1.00\pm0.15\times10^{-8}$	$1.33\pm0.20\times10^{-2}$

The error values of solubility and dissolution rate constant at each pH were estimated from the standard deviations of particulate Fe(III) concentration at time 0 and the slope, respectively, obtained by using a least-squares linear regression of the dialysis data after day 5.

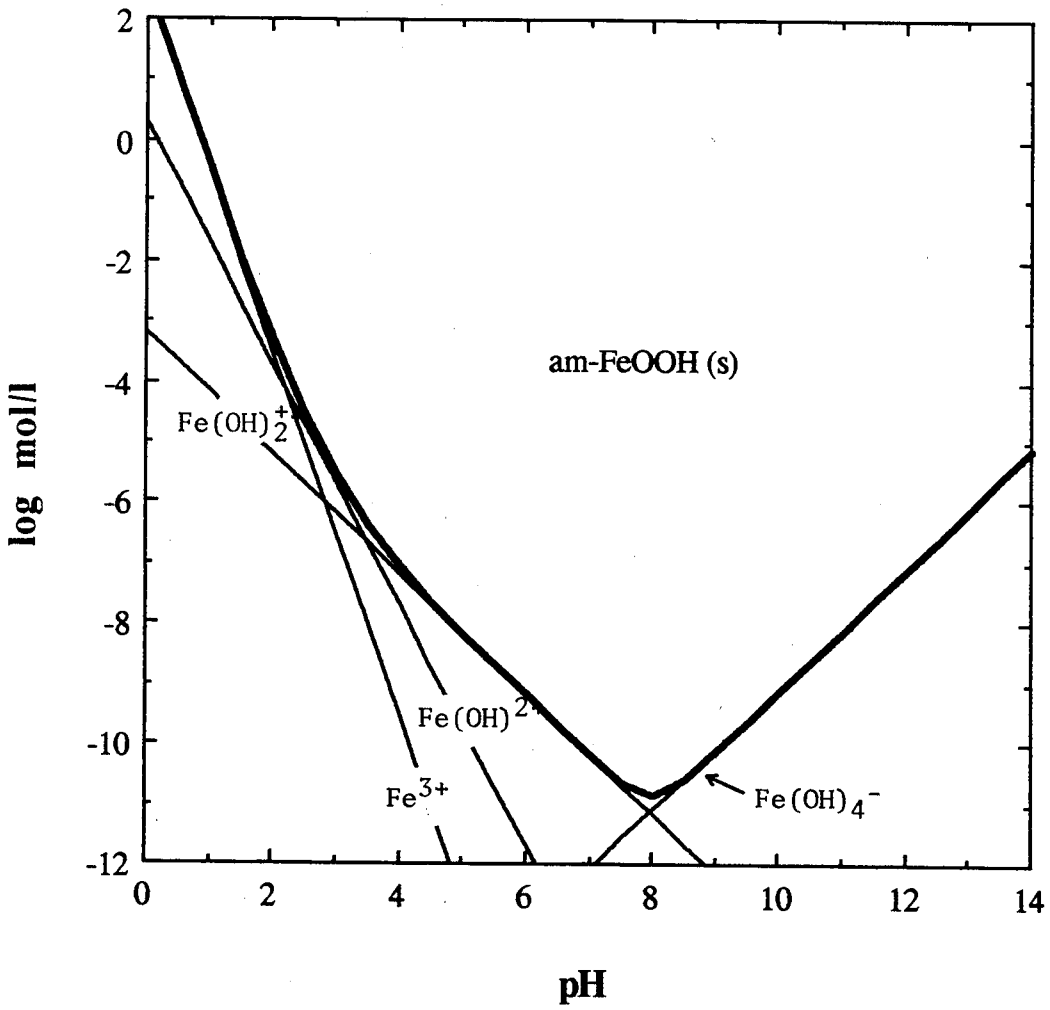

Fig. 2-1 Iron solubility of am-FeOOH at 25°C I=0 (Stumm and Morgan, 1981)

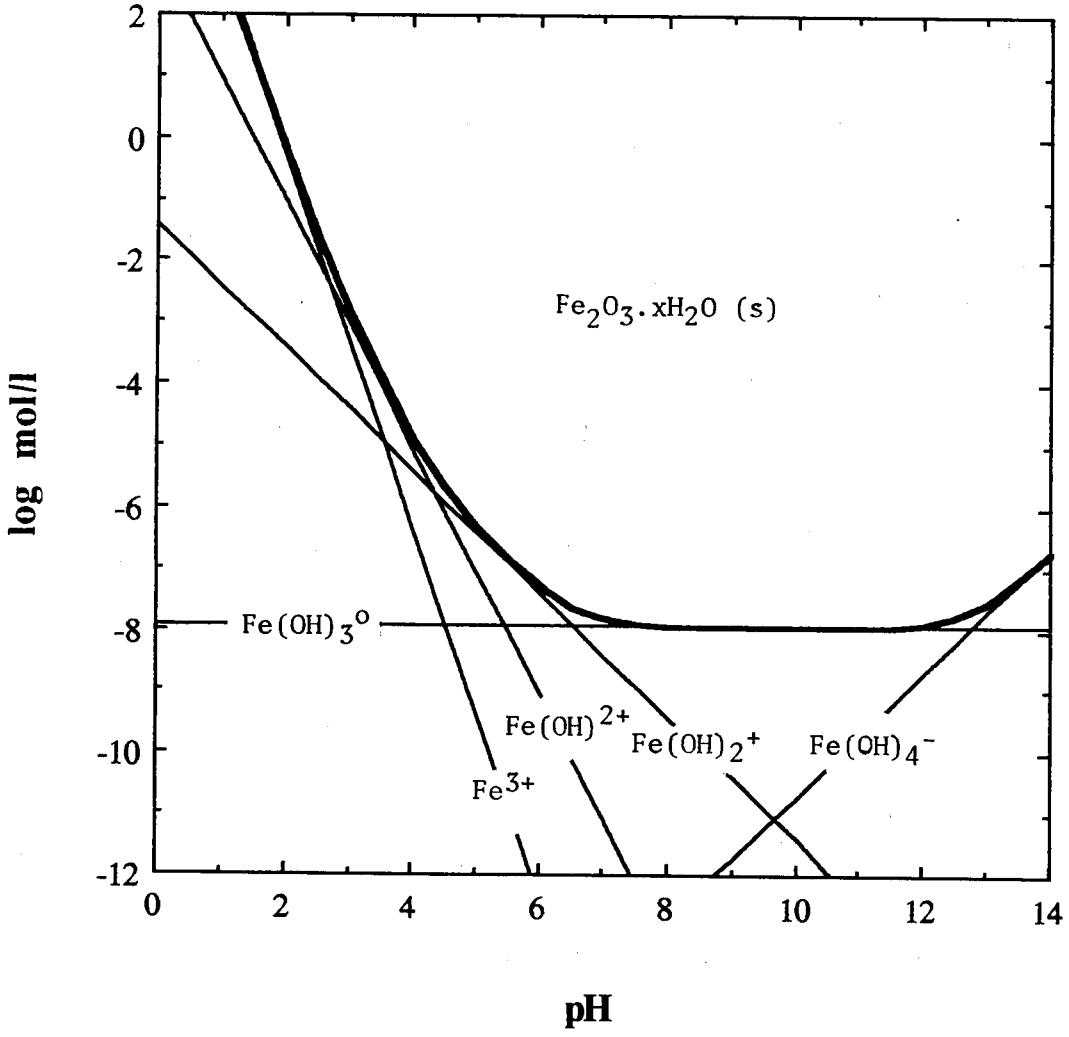

Fig. 2-2 Iron solubility of hydrous ferric oxide at 25°C in seawater (Byrne and Kester, 1976 a and b)

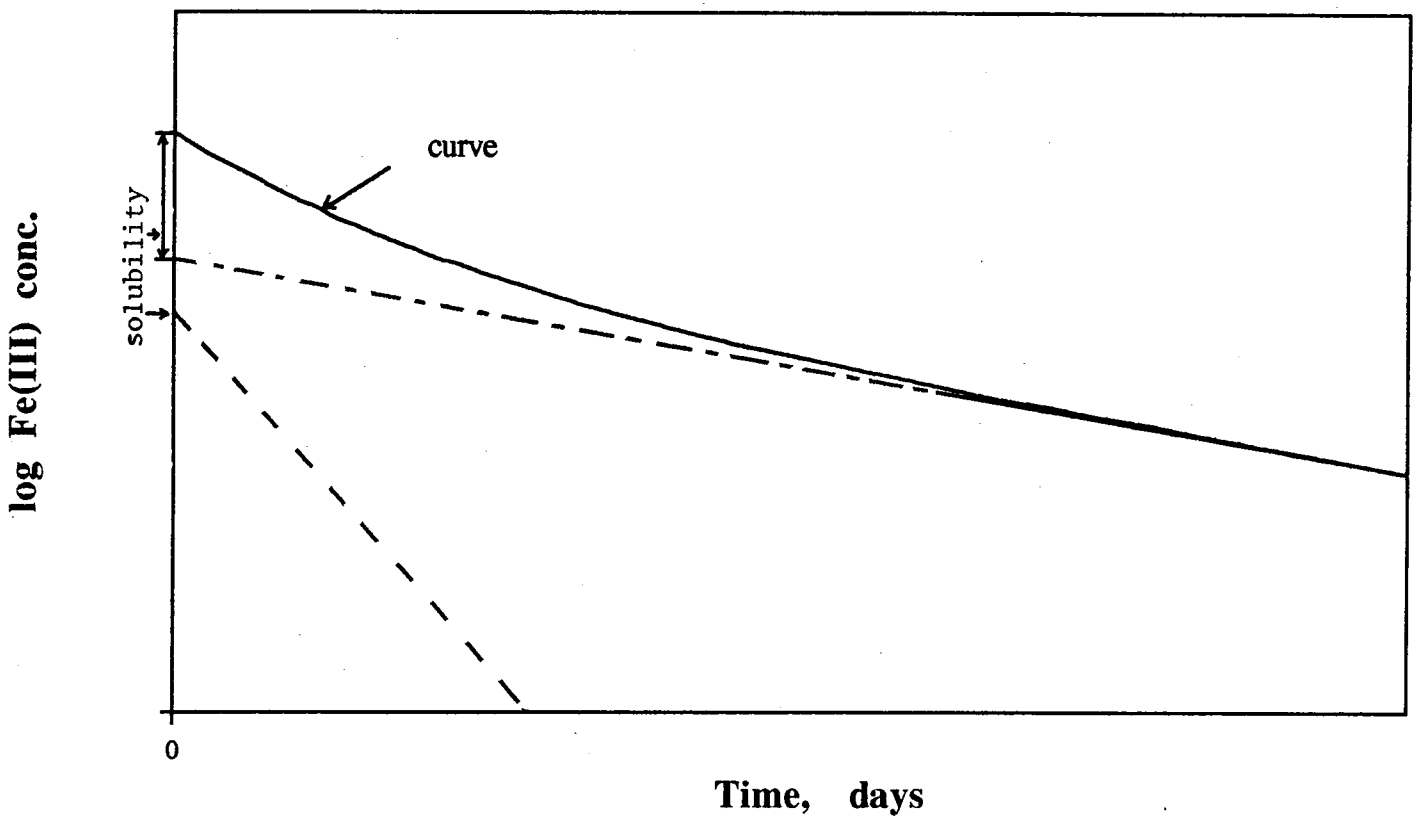

Fig. 2-3 Dialysis model profile of Fe(III) concentration in the dialysis tube with time at constant pH

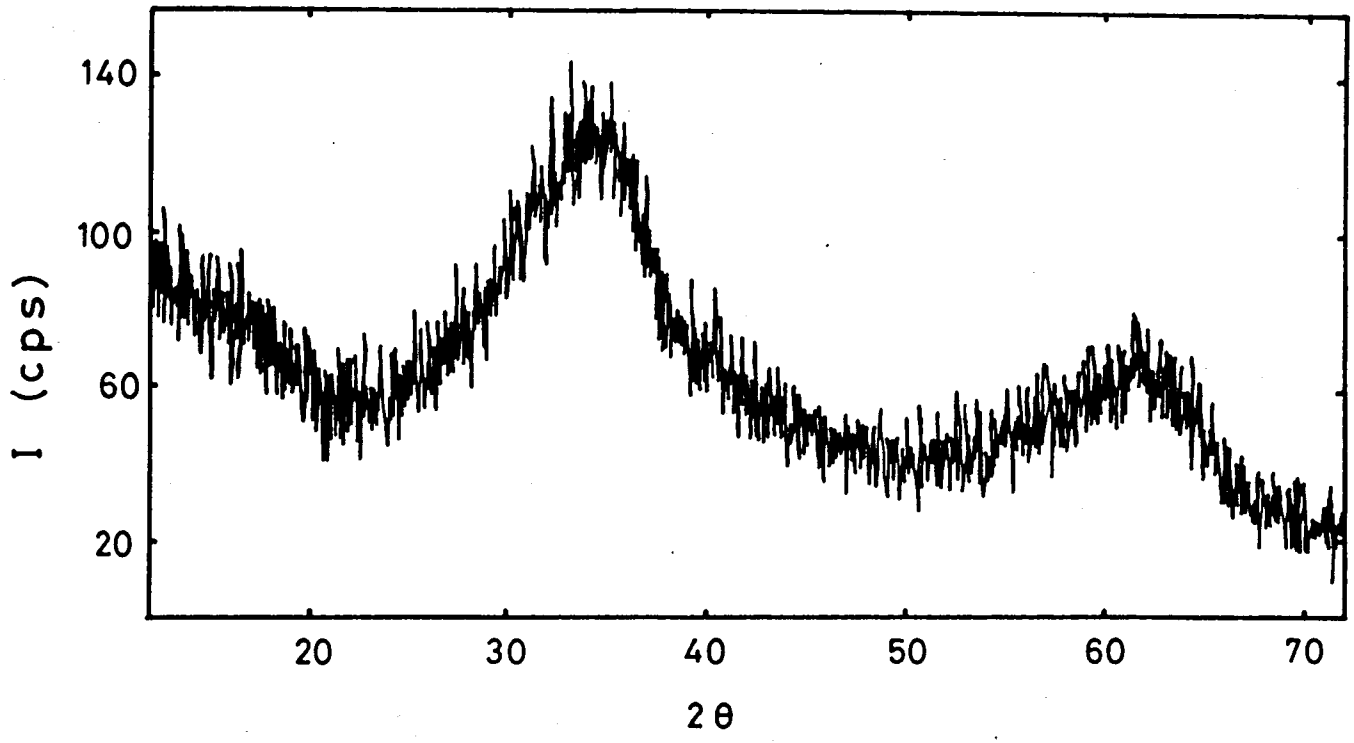

Fig. 2-4 X-ray diffractogram of amorphous phase defined as hydrous ferric oxide

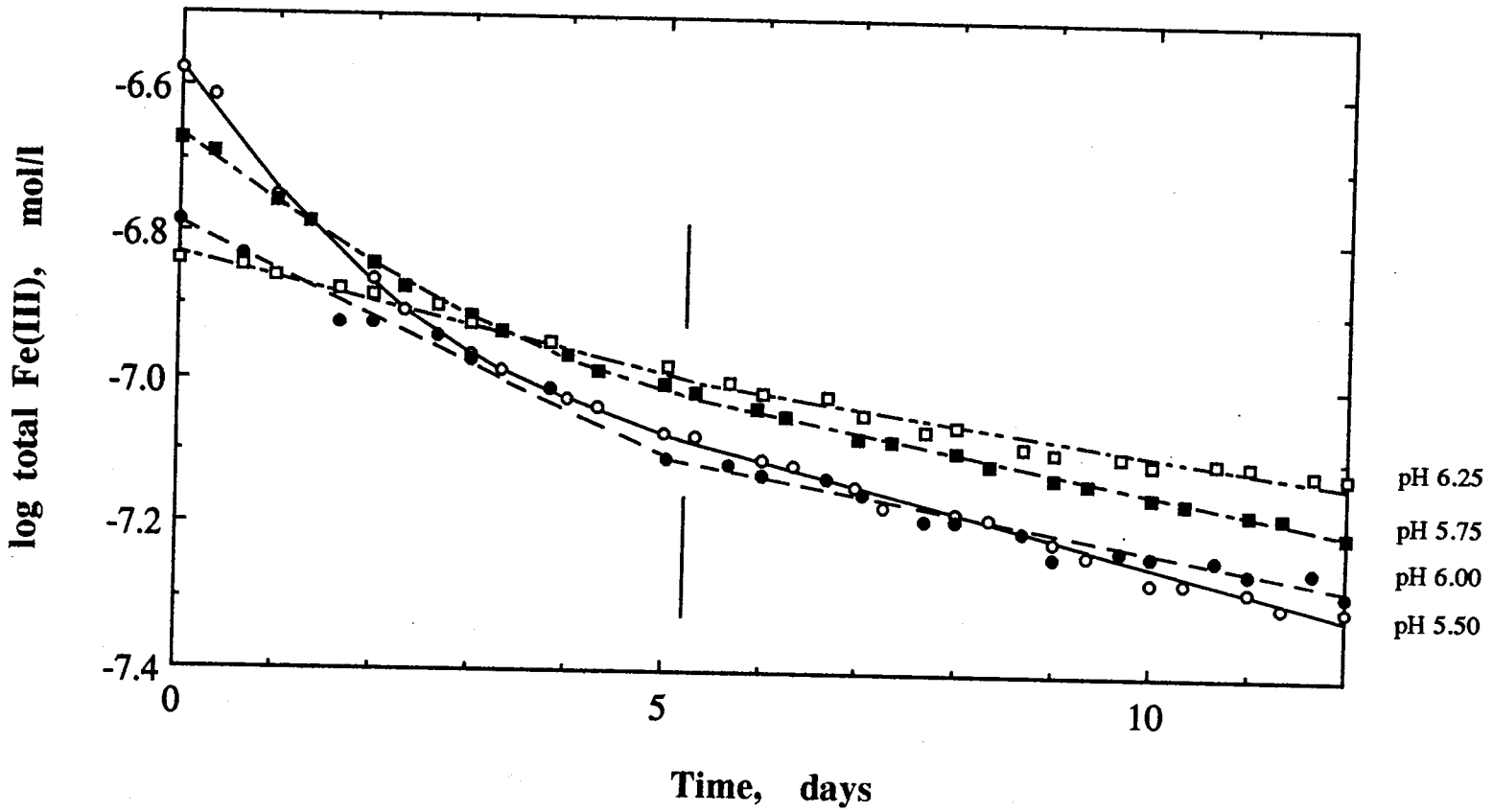

Fig. 2-5 Results of dialysis experiments at 20°C in the pH range 5.50-6.25

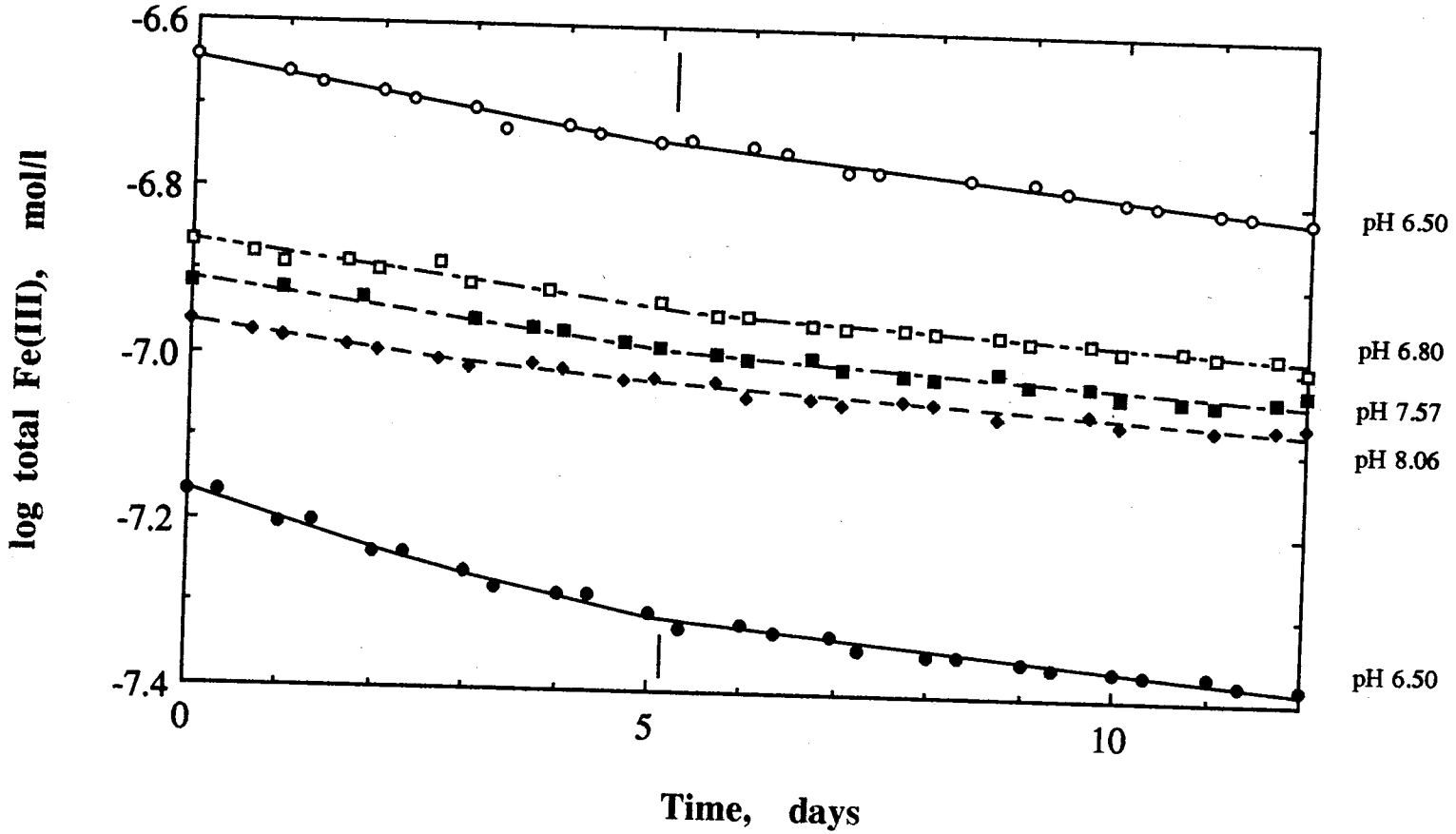

Fig. 2-6 Results of dialysis experiments at 20°C in the pH range 6.50-8.06

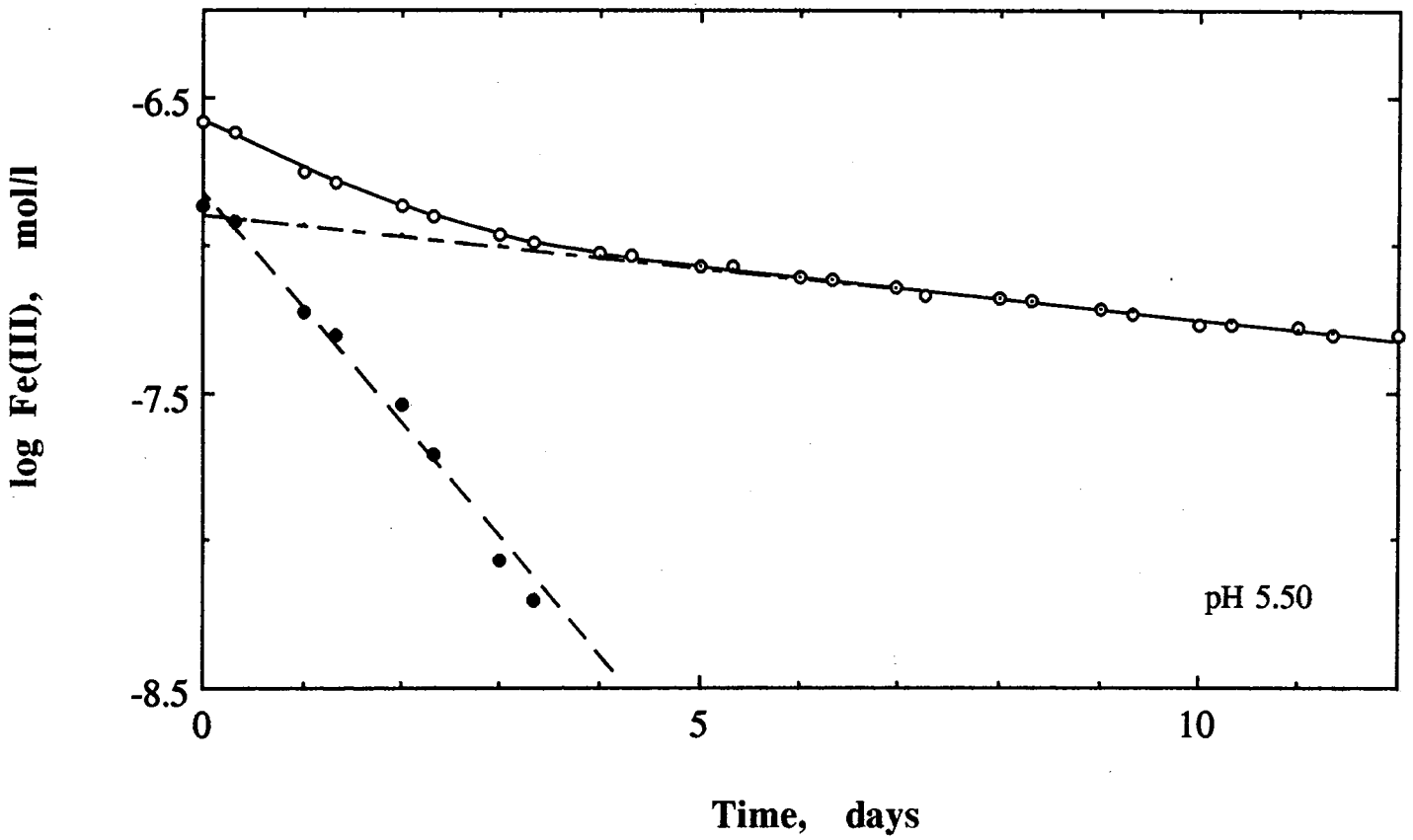

Fig. 2-7 Dissolution of particulate Fe(III) and dissolved Fe(III) in the dialysis tube calculated from the result of dialysis experiment at pH 5.50

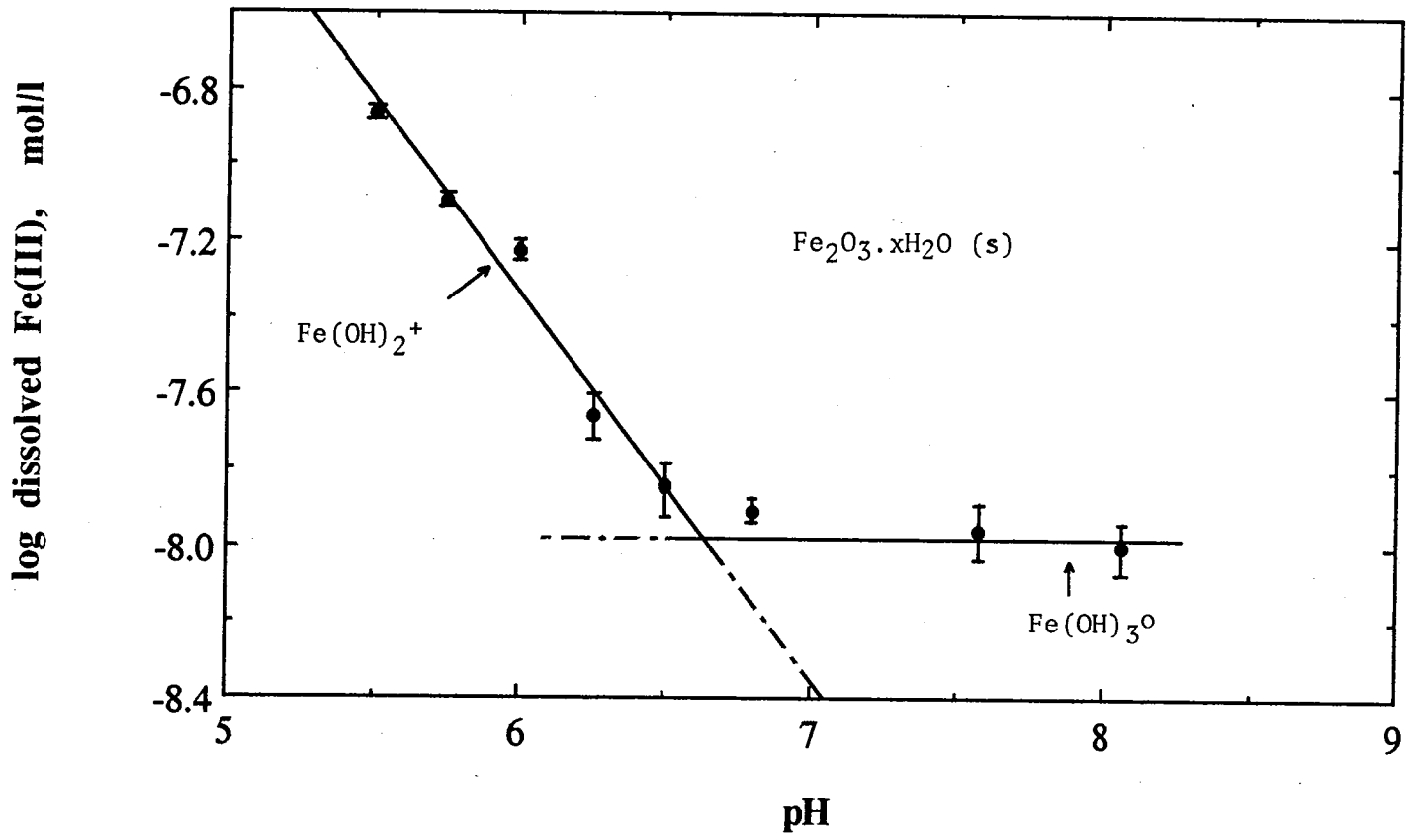

Fig. 2-8 Iron solubility in seawater at 20°C obtained by dialysis experiments

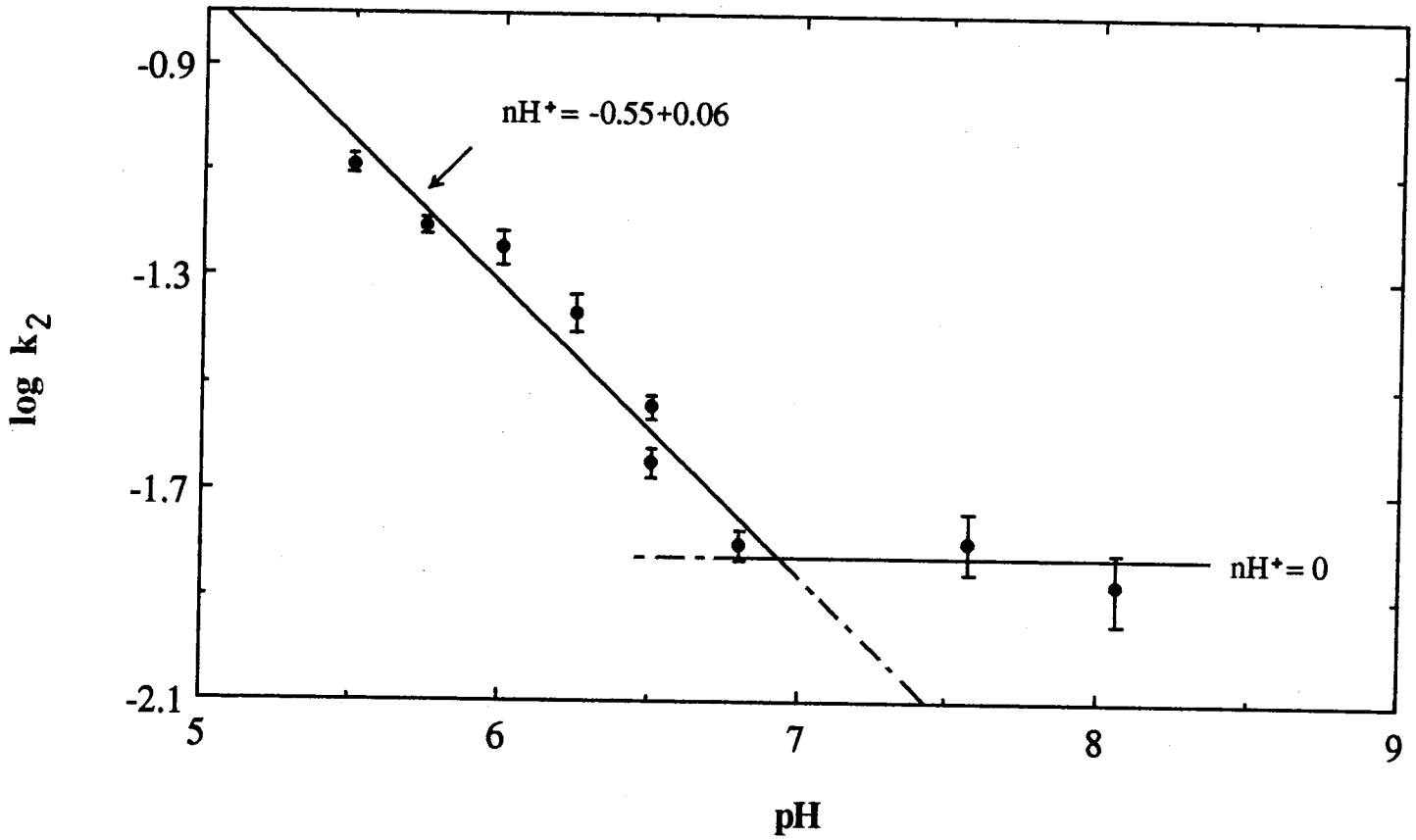

Fig. 2-9 Dissolution rate constant vs. pH in seawater at 20°C obtained by dialysis experiments

3. SOLUBILITY AND DISSOLUTION RATE OF COLLOIDAL γ-FeOOH IN SEAWATER

3.1 Introduction

Iron is one of the major components of the Earth's crust and plays an important role in the biogeochemistry of natural waters. Iron is also an essential micronutrient for phytoplankton growth (Finden et al., 1984; Martin and Fitzwater, 1988; Martin et al., 1989). The stable oxidation state of iron in oxic seawater is Fe(III) with a low solubility. Therefore, phytoplankton growth might be severely controlled by the solubility and the dissolution rate of particulate Fe(III) since it has usually been assumed that most species of phytoplankton assimilate soluble ionic species. The principal phases commonly found in soils and natural waters are amorphous hydrous ferric oxide ($Fe_2O_3.xH_2O$), α-Fe_2O_3 (hematite), γ-Fe_2O_3 (maghemite), α-FeOOH (goethite) and γ-FeOOH (lepidocrocite), whereas β-FeOOH (akaganeite) is rarher rare (schneider, 1988; Lindsay, 1991). The order of solubilities of crystalline ferric oxides is γ-Fe_2O_3 > γ-FeOOH > α-Fe_2O_3 > α-FeOOH. For comparison, amorphous ferric oxide is approximately three order of magnitude more soluble than α-FeOOH (Lindsay, 1991). The dissolution rates per unit surface area of various crystalline iron oxides in 0.5 N HCl at 25°C are in the order: γ-FeOOH > Fe_3O_4 (magnetite) > β-FeOOH > γ-Fe_2O_3 > α-Fe_2O_3 > α-FeOOH, a sequence that must be the result of differences in the chemical composition

and crystal structure of these minerals (Sidhu et al., 1981). The crystalline ferric oxides such as α-FeOOH, β-FeOOH and α-Fe_2O_3, thermodynamically stable forms, do not support phytoplankton (diatoms:*Thalassiosira pseudonana* and *Thalassiosira weissflogii*) growth at all, while amorphous hydrous ferric oxide can induce the maximal growth and the cell yields because of faster thermal dissolution rate of amorphous phase than those of crystalline ferric oxides (Wells et al., 1983; Rich and Morel, 1990). Their thermal dissolution rates were spectrophotometrically determined over time by adding the iron chelating reagents, such as sulphosalicylic acid (Wells et al., 1983) and 8-hydroxyquinoline-5-sulfonic acid (Rich and Morel, 1990) into iron colloid solutions. Therefore, the solubilities and dissolution rates of ferric oxides in seawater are important factors which will govern the primary production of phytoplankton in seawater.

An operational distinction is usually made between particulate and dissolved (0.4 μm filterable) iron. The dissolved fraction consists of inorganic complexes, organically bound iron and colloids with sizes < 0.4 μm (Lewin and Chen, 1973). It has been reported recently that the dissolved iron concentrations in mid and deep waters in the open-ocean and in shallow margin waters are approximately 0.3-1x10^{-9} and 1x10^{-8} mol l^{-1}, respectively (Gordon et al., 1982; Martin and Gordon, 1988; Martin et al., 1989; Bruland et al., 1991). Colloidal ferric oxide in seawater may have widely varying origins, chemical compositions and sizes. In the open ocean, the most likely sources of iron colloids are atmospheric dust (Moore et al., 1984; Duce, 1986), in situ oxidation of

Fe(II) (landing and Bruland, 1987) and release of iron compounds during the degradation of organisms. In coastal waters, in addition, the input of colloids from rivers must be considered. Iron oxyhydroxide precipitates derived from ferric and ferrous iron by using conditions very similar to those encountered in natural waters were identified as amorphous in the initial phases, but containing 10-20% α-FeOOH on aging for 12 days, and as poorly crystalline γ-FeOOH, respectively, with X-ray diffraction, infrared and Mossbauer spectroscopies (Crosby et al., 1983). The above results suggest that the dissolved iron concentrations in oxic seawaters may be controlled by the dominant iron solid phase, which will govern the iron solubility and dissolution rate in seawater, on site.

The solubilities of amorphous hydrous ferric oxide in seawater were experimentally determined by filtration (Byrne and Kester, 1976 a) and dialysis techniques (Kuma et al., 1992 a), indicating that the dominant iron species are $Fe(OH)_2^+$ in the pH range 5.5 to 6.5 and $Fe(OH)_3^\circ$ in the normal pH range of seawater above 7. The solubilities within the pH range 7 to 8 were independent of pH with value: approximately $1x10^{-8}$ mol l^{-1}. The dissolution rate constants within the same pH range were also independent of pH with value: 0.015 day^{-1} (Kuma et al., 1992 a). The previous dissolution studies of several ferric oxide forms were performed with acidification, reduction and/or complexation using inorganic acids (Cornell et al., 1976; Sidhu et al., 1981; Cornell and Giovanoli, 1988; Schwertmann, 1991), organic acids such as oxalate and ascorbate (Zinder et al., 1986; Sulzberger et al., 1989; Schwertmann,

1991) and chelating reagents (Wells et al., 1983; Rich and Morel, 1990). However, the solubilities and dissolution rates in seawater for the most common crystalline ferric oxide phases, such as γ-FeOOH, α-FeOOH and α-Fe_2O_3, have not been reported since their solubilities and dissolution rates are extremely low and slow, respectively, in the normal pH range of seawater. In general, the solubilities of the stable crystalline solid phases will be expected to be lower than that of metastable amorphous phase (Stumm and Morgan, 1981). In this study, the solubilities and dissolution rates of γ-FeOOH, one of the typical iron oxyhydroxides and precipitate derived from the oxidation of ferrous iron in seawater, in seawater over the pH range 5.5 to 8.2 at 20°C were experimentally determined by the dialysis technique involving γ-activity measurement of ^{59}Fe. In addition, the dissolution experiments at the pH range 2.4 to 3.4 were conducted by adding acetic acid in γ-FeOOH suspended seawater solutions.

3.2 Theoretical Considerations

The theoretical solubilty, dissolution rate and dialysis technique are described in 2.2 Theoretical Considerations (Chapter 2).

3.3 Experimental Procedure

3.3.1 *Dialysis experiments*

In this study, the dialysis technique was used to distinguish between

dissolved Fe(III) and particulate Fe(III) in seawater. Total Fe(III) concentration in a dialysis membrane tube was measured with time by γ-activity counting of ^{59}Fe. The dialysis experiments of γ-FeOOH in seawater within the pH range 5.5-8.2 were conducted in the following manner.

(1) To eliminate the dissolved Fe(III), seawater collected from Funka Bay in Japan (salinity = 33.6 ‰) was passed through a silica-immobilized 8-hydroxyquinoline column (Sturgeon et al., 1981) in a clean room after being filtered through an acid-cleaned 0.45 μm Millipore membrane filter.The iron concentration in seawater prepared in this procedure was determined by a graphite furnace atomic absorption spectrophotometer (Hitachi 180-70) after preconcentration by APDC/DDDC-chloroform organic extraction (Landing and Bruland, 1987). The iron concentration was below 0.2 nM.

(2) For each dialysis experiment, radioactive ferrous ^{59}Fe (New England Nuclear Corp.) solution, into which a small known amount of stable ferrous iron (Mohr's salt) solution was already added, was added to 50 ml pretreated seawater in a 100 ml polyethylene bottle previously cleaned with 6 N HCl in quantity over the solubility of Fe(III) and the possibly adsorbable amount of particulate Fe(III) on the wall of bottle.

The seawater solutions (pH 7.5-8.2) were standed for 1 week at 20°C in order to complete the oxidation of ferrous iron, resulting in the precipitation of γ-FeOOH. The half-life, $T_{1/2}$, of ferrous iron in seawater at 20°C is around 7.1 and 1.4 min at pH 7.5 and 8.2, respectively (Roekens and Van Grieken, 1983). Therefore, the ferrous iron

concentration remained in seawater solutions after standing for 1 week can be negligibly low for the following dialysis experiments.

To confirm the ferric oxide form produced in this produce, it was produced by adding ferrous iron (Mohr's salt) solution to the seawater, bubbling air, adjusting to pH 8.0 with NaOH and then aging for 1 week at 20°C. In general, the obtainable ferric oxide form is dependent on the preparative conditions, such as acidity, reaction temperature, the concentration of ferrous iron added, etc. (Hamada and Kuma, 1976). X-ray diffraction analysis with filtered Cu Kα radiation (40 kv, 20 mA) confirmed that the product was poorly crystalline γ-FeOOH (Table 3-1 and Fig. 3-1). This result was consistent in that by Crosby et al. (1983), indicating that the precipitate derived from ferrous iron by using conditions similar to those encountered in natural waters was identified as poorly crystalline γ-FeOOH.

(3) Small volumes of diluted subboiled HCl (S-HCl) solution were then added to the seawater solutions a few times per day for 1 week at 20°C to obtain a desired pH within the range 5.5-7.5. For pH less than 7.0, the desired pH was obtained within 1 week as a result of buffering systems in the seawater. For the pH range 7.0-7.5, S-HCl solution was added to the seawater solution until the pH was within a desired range of values. Subboiled water (S-water) was used for the dilution of reagents and the washing of apparatus. S-HCl and S-water were produced by subboiling in a clean room.

(4) For each experiment, 600 ml of pretreated seawater (procedure (1)) were added to an Erlenmeyer flask, followed by stirring with a

magnetic stirrer and immersed in a constant-temperature water bath at 20 ± 0.2°C. Small volumes of S-HCl solution were added to the seawater several times per day for a period of 1 week in order to obtain a desired pH within the range 5.5-7.5. For pH less than 7.0, the desired pH was attained within 1 week.

(5) For each experiment, 1 ml of pretreated seawater containing ^{59}Fe as prepared in procedure (3) was added to a 7.6 mm diameter dialysis tube which excludes solids with molecular weights greater than 1000 Da. Each tube was inserted into a counting vial to measure the γ-activity of solution in the tube at time 0. The tube was then immersed in the 600 ml seawater solution prepared in procedure (4) with the same pH as the seawater in the tube.

(6) Each dialysis tube was withdrawn from the seawater solution twice a day and inserted into a counting vial to measure the γ-activity for a duration of 12 days. After each radiomeasurement, the dialysis tube was reimmersed in the seawater solution till the time for the next measurement. During this dialysis experiment, the pHs of the solutions in the flasks in the pH range 7.0-7.5 were continually adjusted to the desired pH range by adding S-HCl solution.

(7) The γ-activity of each dialysis tube, containing ^{59}Fe solution, in counting vials, was measured by Aloka ARC-301B with an average counting efficiency for ^{59}Fe (CE-I). In addition, the counting efficiency (CE-II) due to the insertion of a dialysis tube containing ^{59}Fe solution into a counting vial is approximately 70 % of that for the ^{59}Fe solution directly added into a vial. Therefore, the measured counts were corrected

for CE-II for each tube. Finally, the total Fe(III) concentration in each dialysis tube with time for a duration of 12 days was calculated from the counts corrected for CE-II, CE-I of the scintillation counter, volume of solution added in the tube and amount of Fe per count.

After dialysis experiments, the iron concentration in 600 ml seawater in each flask at pHs 7.00-8.20 was also determined by the same analytical method described in procedure (1). The iron concentration was below 0.2 nM.

3.3.2 *Filtration experiments*

The 0.45 μm Millipore membrane filter was used to distinguish between dissolved Fe(III) and particulate Fe(III) in seawater. The dissolution rate of γ-FeOOH in seawater within the pH range 2.4-3.5 were conducted in the following manner.

(1) Seawater collected from Funka Bay in Japan (salinity = 33.6 ‰) was filtered through an acid cleaned 0.45 μm Millipore filter. A small amount of ferrous (Mohrs's salt) solution was added to 240-250 ml filtered seawater at 20°C in an Erlenmeyer flask, followed by adjusting pH to 8.10±0.01 with NaOH solution. The iron concentration in seawater solution is 10 μM. The seawater solutions were aged for 1 week at 20°C in order to complete the precipitation of γ-FeOOH.

(2) The concentrated acetic acids (0.5, 1.25, 2.5, 5 and 10 ml) were directly added to the γ-FeOOH suspended seawater solutions stirred with a magnetic stirrer at 20±0.2°C. Fifteen ml of each sample in the flask was immediately withdrawn at the appropriate time for 90 min and

filtered through a 0.45 μm filter. The dissolved (filterable) iron concentrations during the dissolution experiments by acidification in the pH range 2.4-3.4 were determined by the ferrozine method (Stookey, 1970). After the dissolution experiments, the total iron concentrations and pHs of the seawater solutions were measured by the same method as described above and a pH meter, respectively.

(3) To know the effect of temperature on the dissolution rate at pH 2.6, 5 ml concentrated acetic acids were added to 245 ml γ-FeOOH suspended seawater solutions, aged for 1 week at 20°C, at 5, 10, 15, 20 and 25°C. The dissolved and total iron concentration were determined by the method in the procedure (2). The pH of the seawater solutions were measured by the pH meter immediately after the dissolution experiments.

3.4 Results and Discussion

Figs. 3-2 and 3-3 show the logarithmic changes of total Fe(III) concentrations in the tubes with for 12 days at pHs 5.50-6.25 and 6.50-8.20, respectively. Each curve is in excellent agreement with the theoretical curve shown in Fig. 2-3 (Chapter 2); the linear part after day 5 primarily represents the dissolution of particulate Fe(III) in each tube. The dissolution rate constant, k_2, in the eqn. (7) and the solubility at each pH (Table 3-2) were determined from the slope and the particulate Fe(III) concentration at time 0, respectively, using a least-squares linear regression of the dialysis data after day 5. The two dialysis results, with

extremely different total Fe(III) concentrations at time 0, at nearly same pH (7.95 and 8.2) (Fig. 3-3) indicated nearly the same dissolution rate constant and solubility (Table 3-2), suggesting that the dissolution rate of particulate Fe(III) is in proportion to the particulate Fe(III) concentration and that the dissolved Fe(III) concentration at time 0 is in equilibrium with γ-FeOOH in this study. Figs. 3-4, 3-5 and 3-6 show the dialysis data at pH 5.50, 5.75 and 6.00 (solid line), respectively, the dissolution of particulate Fe(III) (dot-dash line) at each pH calculated from the data after day 5 and the dialysis of dissolved Fe(III) (dotted line) obtained by substraction of the dot-dash line from the solid line at each pH. The dialysis rate constants of dissolved Fe(III) at pH 5.50, 5.75 and 6.00 were determined to be 0.360 (r^2=0.991), 0.358 (r^2=0.992) and 0.313 day^{-1} (r^2=0.965), respectively from the slope of dotted line at each pH. This result suggests that the dialysis rate of dissolved Fe(III) is in proportion to the dissolved Fe(III) concentration in the tube and is considerably faster than the dissolution rate of particulate Fe(III) in the pH range in this study. Moreover, the dialysis rate constant is relatively independent of pH, indicating the character of dialysis membrane tube used.

3.4.1 *Solubility of colloidal γ-FeOOH in seawater*

The solubility results are presented graphically in Fig. 3-7, including those of colloidal amorphous hydrous ferric oxide in Chapter 2 (Kuma et al., 1992 a), as a plot of log T[Fe(III)d] (mol l^{-1}) vs. pH. The line labeled $Fe(OH)_2^+$ was determined over the pH range 5.50-7.00 and is

representative of the equation $T[Fe(III)d]=*Kso\ *\beta_2[H^+]$ assuming that within this pH range only the species $Fe(OH)_2^+$ is significant. The constant term, $*Kso*\beta_2=2.5\pm0.7\times10^{-2}$, in this equation was calculated from an average of the values of $T[Fe(III)d]/[H^+]$ within the pH range 5.50-7.00. A least-squares linear regression of log T[Fe(III)d] vs. pH gives a slope of -1.05±0.06 in good agreement with the theoretical slope of -1.0. Using the calculating procedure of Byrne and Kester (1976 a) and the average value of $*\beta_2$ (8.6×10^{-8}) determined in synthetic media (Byrne and Kester,1976 b), the stoichiometric solubility product, *Kso, and the thermodynamic product, Kso, were calculated to be $2.9\pm0.8\times10^5$ and $10^{-37.7\pm0.1}$, respectively. The calculated Kso is consistent with the values of $10^{-37} > Kso > 10^{-44}$ for the ferric oxides (Schwertmann, 1991) and is slightly lower than the values of $10^{-37.5}$ obtained from the results of simple filtration experiments (Byrne and Kester, 1976 a) and dialysis experiments (Kuma et al., 1992 a) for amorphous hydrous ferric oxide in seawater. Published equilibrium constants for ferric hydroxide complexes indicate that only the monomeric species, $Fe(OH)_2^+$, can exist in significant concentrations in the pH range 5.50-6.50 (Fox, 1988).

In dissolution experiments, the solubility may depend upon the quality of the solid present (Feitknecht and Schindler, 1963). An active form of the precipitate, usually a very fine crystalline or amorphous solid phase with a disordered lattice is formed from oversaturated solutions. Such an active precipitate may persist in metastable equilibrium with the solution; it is more soluble than the stable solid phase and may slowly convert into the stable phase such as inactive amorphous and crystalline

forms (Stumm and Morgan, 1981). The precipitate derived from ferric iron was identified as amorphous in the initial phases, but containing 10-20 % α-FeOOH on aging for 12 days (Crosby et al., 1983). In Chapter 2, the amorphous hydrous ferric oxide may have slowly and partly converted into the stable phase during acidification to adjust the desired pH for 1 week (Kuma et al., 1992 a). In addition, the acidifying treatment may have primarily dissolved the active amorphous phase which is more soluble than the stable phases. Therefore, the conversion into stable phase and the acidification may have resulted in lowering the solubilities especially at lower pHs (dotted line at pH 5.50-6.50 in Fig. 2-8 in Chapter 2) and Kso of active amorphous phase may be slightly larger than that obtained in Chapter 2. Futhermore, Kso of particles < 1 μm in diameter may increase by several orders of magnitude with decreasing particle size (Schwertmann, 1991). Regrettably, the particle size distribution at each pH could not be measured because the particulate Fe(III) concentration in this dialysis experiment is extremely low.

The solubility over the pH range 7.0 to 8.2 is relatively pH independent with $1.4\pm0.4\times10^{-9}$ mol l^{-1} as an average value between pHs 7.50 and 8.20. The solubility of γ-FeOOH at the normal pH of seawater appears to be about an order of magnitude lower than that (1.0×10^{-8} mol l^{-1}) of amorphous hydrous ferric oxide (Byrne and Kester, 1976 a; Kuma et al., 1992 a). This result also indicates that the dominant dissolved iron species in oxic seawater at the normal pH of seawater is probably $Fe(OH)_3^\circ$ in addition to $Fe(OH)_2^+$. The concentration of $Fe(OH)_2^+$ in equilibrium with colloidal γ-FeOOH at pH 8.0, obtained by extrapolation

of the line labeled $Fe(OH)_2^+$ (Fig. 3-7) to pH 8.0, is about $1.9x10^{-10}$ mol l^{-1} and is only 14 % of the solubility at pH 8.0. The formation constant of $Fe(OH)_3°$, $*\beta_3$, was calculated to be $5.7\pm3.0x10^{-15}$ from $*Kso*\beta_3=1.4\pm0.4x10^{-9}$ and $*Kso=2.9\pm0.8x10^{5}$. This value is about one-fourth lower than those of amorphous phase obtained from the acidification followed by filtration experiments of Byrne and Kester (1976 a) and from the dialysis experiments of Kuma et al. (1992 a). This results from the difference between calculated *Kso values of γ-FeOOH and amorphous phase probably because of the partly conversion of metastable amorphous into stable phase for the dialysis experiments of amorphous phase, as mentioned above.

It has been reported recently that the dissolved iron concentrations in mid and deep waters in the open ocean and in the shallow margin waters are approximately $0.3\text{-}1x10^{-9}$ mol l^{-1} and $1x10^{-8}$ mol l^{-1}, respectively (Gordon et al., 1982; Martin and Gordon, 1988; Martin et al., 1989; Bruland et al., 1991). The solubility of γ-FeOOH in seawater measured at its normal pH in this experimental study appears to be nearly the same value as the dissolved iron concentrations measured in mid and deep waters in the open ocean. The implication, then, is that the open waters may be in saturation equilibrium with stable crystalline ferric oxides, such as γ-FeOOH, α-Fe_2O_3 and α-FeOOH, rather than metastable amorphous phase. However, to confirm this interpretation, the following several problems will have to be resolved; the operationally defined concept of a dissolved (filterable) fraction with 0.4 μm filter which can not quantitatively remove the smaller colloidal particles (Lewin and

Chen, 1973; Zhuang et al., 1990), qualitative and quantitative analyses for solid iron phases in seawaters, atmospheric dust and colloids from rivers, the crystallization mechanism of metastable to the stable forms in seawater (Crosby et al., 1983), the adsorptin mechanism of dissolved iron on the particles (Stumm, 1977; Stumm and Morgan, 1981; Zhuang et al., 1990), etc. The biogeochemical cycling of iron will, therefore, be a function of the inputs (abundance in source media, solubility and rate of transfer to dissolved forms depending on the solid form and its effective surface area and photoreduction at organic surfaces) and residence time in the aquatic environment (reactivity towards particle surfaces and organisms, conversion rate of metastable into the stable form, etc.).

3.4.2 *Dissolution rate of colloidal γ-FeOOH in seawater*

The dissolution rate constants, k_2, determined from the slopes after day 5 (Figs. 3-2 and 3-3) are presented in Table 3-1. A plot of log k_2 vs. pH, Fig. 3-8, allows the calculation of nH^+ and the dissolution rate constant, k_1, from the equation $\log k_2 = \log k_1 + nH^+pH$. Within the pH range 5.50-7.00, log k_2 increases with an increase in the activity of the hydrogen ion and is fitted by a line whose slope corresponds to $nH^+ = -0.95\pm0.06$. The increase as a function of pH is consistent with that of solubility. For the corresponding mechanism in seawater at 20°C we calculate a value for the dissolution rate constant, $k_1=2.3\pm0.5\times10^4$ day^{-1}.

Fig. 3-9 presents the dissolution rates of γ-FeOOH within the pH range 2.46-3.40, obtained by the filtration experiments at 20°C, indicating

that the Fe(III) dissolution rate at each pH was a first-order reaction in proportion to the particulate Fe(III) concentration in seawater. The dissolution rate constants, k_2, determined from the slopes are presented in Table 3-3. A plot of log k_2 vs. pH, Fig. 3-10, allows the calculation of nH^+. Within this pH range, 2.4-3.4, log k_2 increases linearly with an increase in the activity of the hydrogen ion and is fitted by a line whose slope corresponds to $nH^+ = -0.89 \pm 0.07$. The nH^+ value within the pH range 2.46-7.00 was also calculated to be -0.80 ± 0.02 from a plot of log k_2 vs. pH (Fig. 3-11) obtained by the dialysis (pH 5.50-7.00) and filtration data (pH 2.46-3.40). These results suggest that the dissolution mechanism of γ-FeOOH with an increase in the activity of the hydrogen ion is same within the pH range 2.46-7.00. However, the nH^+ value is approximately twice larger than that (-0.55) for amorphous phase in the pH range 5.50-7.00 (Kuma et al., 1992 a). The implication is that the inactive amorphous and/or stable crystalline phases by conversion of active amorphous phase may have been dominant at lower pH, as mentioned above, and their nH^+ values may be lower than that of γ-FeOOH in this study.

Within the pH range 7.00-8.20, k_2 is relatively independent of pH with a value of $k_2 = k_1 = 0.005 \pm 0.001$ day^{-1} with $nH^+ = 0$ (Fig. 3-8). This suggests that only water is involved in breaking the Fe-O bond on the surface of γ-FeOOH to form an activated complex. In the normal pH range of oxic seawater, the dissolution rate constant of γ-FeOOH is one-third lower than that of amorphous hydrous ferric oxide (Kuma et al., 1992 a). The Fe(III) dissolution rate of colloidal γ-FeOOH in

seawater at 20°C is 0.005x[Fe(III)p] (conc. day^{-1}), which was determined from eqn. (5) by the particulate Fe(III) concentration as γ-FeOOH and the dissolution rate constant. This result may suggest that thermodynamically stable γ-FeOOH, as well as α-FeOOH, β-FeOOH and α-Fe_2O_3 (Wells et al., 1983; Rich and Morel, 1990), in comparison with metastable amorphous hydrous ferric oxide will be expected not to support phytoplankton growth, but depending on the particulate Fe(III) concentration as γ-FeOOH, if phytoplankton can assimilate only soluble iron species. The dissolution rates of various iron oxides in 0.5 M HCl at 25°C are in the order: γ-FeOOH > Fe_3O_4 > β-FeOOH > γ-Fe_2O_3 > α-Fe_2O_3 > α-FeOOH, a sequence that must be the result of differences in the chemical composition and crystal structure of these minerals (Sidhu et al., 1981). γ-FeOOH has a more open structure than α-FeOOH and dissolves more rapidly. In γ-FeOOH double sheets of octahedra are hydrogen-bonded together by zig-zag chains of -O-H-O-H-O in planes parallel to the octahedral sheets. Between each double sheet of octahedra there are channels oriented parallel to the x-axis. During HCl dissolution proton attack may occur along these channels as well as on the surface. Cornell and Giovanoli (1988) reported that acid attack was most pronounced at the edges of the crystals of γ-FeOOH and appeared to involve a disruption of the hydrogen bonds that link the sheets of octahedra making up the structure. There are no similar channels in α-FeOOH.

In comparison with fresh waters, it is expected that a large amount of Cl^- in seawater may accelerate dissolution. A Fe-Cl complex has been

suggested that forms on the oxide surface with a consequent reduction in the surface positive charge (Cornell et al., 1976). Such a complex reduces the repulsion between the oxide surface and protons in solution and thereby increases the dissolution rate. Complex formation may also weaken the attractive force between the surface Fe^{3+} and neighboring O^{2-} ions and, hence, facilitate the breakdown of Fe-O bonds (Sidhu et al., 1981).

3.4.3 *Effect of temperature on the dissolution rate of colloidal γ-FeOOH*

To know the effect of temperature on the dissolution rate, the dissolution rate measurements of γ-FeOOH in seawater were carried out by the filtration experiments (pH 2.60) after addition of acetic acid into γ-FeOOH suspended seawater solutions, aged for 1 week at 20°C, at 5, 10, 15, 20 and 25°C (Fig. 3-12). The dissolution rate at each temperature was a first-order reaction and the rate constant, k_2, was calculated from the slope (Table 3-4). The relationship between dissolution rate constant and temperature for γ-FeOOH is described by Arrhenius equation:

$$k_2 = A\exp(-E/RT)$$

$$\log k_2 = \log A - E/2.303RT$$

where k_2= dissolution rate constant, A = frequency factor, E = activation energy, T = absolute temperature and R = gas constant. The values of E and A are calculated from the slope and intercept of log k_2 vs. 1/T plot

(Fig. 3-13), respectively. The activation energy for the dissolution of γ-FeOOH in seawater at pH 2.60 is calculated to be 11.8±0.7 kcal mol^{-1}. If the activation energy for the dissolution in seawater is nearly the same at overall pH, we can estimate the dissolution rate constants at the different temperatures in the normal pH range of seawater, using the equation given below.

$$E=2.303R(\log k_a - \log k_b)/(1/T_b - 1/T_a)$$

where k_a and k_b are the dissolution rate constants at T_a and T_b, respectively. The dissolution rate constants, k_2,of γ-FeOOH at 5,10, 15 and 25°C in the normal pH of seawater are calculated to be 0.0017, 0.0024, 0.0035 and 0.0070 day^{-1}, respectively, from the rate constant (0.005 day^{-1}) determined from the dissolution data in the normal pH of seawater at 20°C (Fig. 3-3 and 3-8) by dialysis experiments and activation energy (E=11.8 kcal mol^{-1}) determined from the dissolution data in seawater (pH 2.60) at various temperatures (Fig. 3-12 and 3-13) by filtration experiments.

3.5 Conclusions

Solubilities and dissolution rates of colloidal γ-FeOOH, one of the typical iron oxyhydroxides, in seawater over pH range 5.5 to 8.2 at 20°C were experimentally determined by dialysis techniques involving γ-activity measurements of ^{59}Fe. The Fe(III) dissolution rate was defined

as a first-order reaction in proportion to the concentration of particulate Fe(III) in seawater from the dialysis and filtration experiments. The solubilities and dissolution rate constants within the pH range 7.0 to 8.2 were independent of pH with values: approximately $1x10^{-9}$ mol l^{-1} and 0.005 day^{-1}, respectively. This result probably indicates the existence of the $Fe(OH)_3^\circ$ as well as $Fe(OH)_2^+$ in the normal pH range of seawater. The solubility and dissolution rate constant were one order of magnitude and one-third, respectively, lower than those of amorphous hydrous ferric oxide. The Fe(III) dissolution rate of colloidal γ-FeOOH in the normal pH of seawater can be estimated from 0.005x[Fe(III)p] (conc. day^{-1}) by the concentration of particulate Fe(III) as γ-FeOOH in seawater. At lower pHs 5.5-7.0, the logarithmic solubilities and dissolution rate constants increased linearly with decreasing pH with a slope of -1.0 and -0.95, respectively, indicating that $Fe(OH)_2^+$ is the dominant dissolved ferric species. The dissolution mechanism at pHs 5.5-7.0 was nearly the same as that at lower pH 2.46-3.6 obtained by the filtration experiments. The effect of temperature on the dissolution rate constant in the normal pH of seawater is probably estimated from the activation energy (11.8 kcal mol^{-1}) obtained by the filtration experiments at pH 2.60.

Table 3-1. The observed X-ray diffraction lines compared to that of γ-FeOOH.

	Observed XRD lines		ASTM No. 8-98 (γ-FeOOH)		
line No.	intensity (obs.) (I/Io) x100	d(obs.) Å	d(ref.) Å	intensity (ref.) (I/Io) x100	(h k l)
1	80	6.260	6.262	100	0 2 0
2	100	3.285	3.289	90	1 2 0
	----	----	2.970	10	0 1 1
3	100	2.471	2.470	80	0 3 1
4	70	2.374	2.360	20	1 1 1
5	20	2.092	2.090	20	1 3 1, 0 6 0
6	80	1.940	1.937	70	0 5 1, 2 0 0
	----	----	1.848	20	2 2 0
7	40	1.735	1.732	40	1 5 1
	----	----	1.566	20	0 8 0
	----	----	1.535	20	0 0 2
8	60	1.528	1.524	40	2 3 1
9	40	1.480	1.496	10	0 2 2
	----	----	1.449	10	1 8 0
	----	----	1.433	20	1 7 1
	----	----	1.418	10	2 6 0
10	30	1.388	1.389	10	1 2 2

Crystal system of γ-FeOOH: orthorhombic (a=3.83, b=12.54, c=3.07 Å)

Table 3-2. Iron solubilities and dissolution rate constants determined by dialysis experiments of colloidal γ-FeOOH in seawater at 20°C.

pH	Solubility (mol l^{-1})	Dissolution rate constant k_2 (day^{-1})
5.50	$1.00\pm0.06\times10^{-7}$	$1.07\pm0.04\times10^{-1}$
5.75	$4.40\pm0.24\times10^{-8}$	$8.77\pm0.22\times10^{-2}$
6.00	$2.14\pm0.17\times10^{-8}$	$5.22\pm0.22\times10^{-2}$
6.25	$1.10\pm0.11\times10^{-8}$	$3.00\pm0.19\times10^{-2}$
6.50	$8.35\pm0.81\times10^{-9}$	$1.35\pm0.16\times10^{-2}$
7.00	$2.36\pm0.95\times10^{-9}$	$4.82\pm1.50\times10^{-3}$
7.50	$1.77\pm0.55\times10^{-9}$	$5.78\pm0.85\times10^{-3}$
7.95	$1.06\pm0.08\times10^{-9}$	$4.23\pm2.21\times10^{-3}$
8.20	$1.35\pm0.80\times10^{-9}$	$4.86\pm1.69\times10^{-3}$

The error values of solubility and dissolution rate constant at each pH were estimated from the standard deviations of particulate Fe(III) concentration at time 0 and the slope, respectively, obtained by using a least-squares linear regression of the dialysis data after day 5 (Figs. 3-2 and 3-3).

Table 3-3. Iron dissolution rate constants determined by filtration experiments of colloidal γ-FeOOH in seawater at 20°C

pH	Dissolution rate constant (k_2)		
	min^{-1}	day^{-1}	r^2
2.46	0.0213±0.0001	30.7±0.1	1.00
2.60	0.0154±0.0001	22.2±0.1	1.00
2.80	0.0094±0.0004	13.5±0.6	0.99
3.04	0.0077±0.0002	11.1±0.3	1.00
3.40	0.0029±0.0002	4.2±0.3	0.98

The error values of dissolution rate constant at each pH were estimated from the standard deviations of the slope obtained by using a least-squares linear regression of the filtration data from 5 to 90 min (Fig. 3-9).

Table 3-4. Iron dissolution rate constants determined by filtration experiments of colloidal γ-FeOOH in seawater at pH 2.60

Temperature		Dissolution rate constant (k_2)		
°C	1/T (x1000)	min^{-1}	day^{-1}	r^2
5	3.5952	0.0051±0.0001	7.3±0.1	1.00
10	3.5317	0.0074±0.0001	10.7±0.1	1.00
15	3.4704	0.0121±0.0002	17.4±0.3	1.00
20	3.4112	0.0154±0.0001	22.2±0.1	1.00
25	3.3540	0.0210±0.0007	30.2±1.0	0.99

The error values of dissolution rate constant at each temperature (pH 2.60) were estimated from the standard deviations of the slope obtained by using a least-squares linear regression of the filtration data from 5 to 90 min (Fig. 3-11).

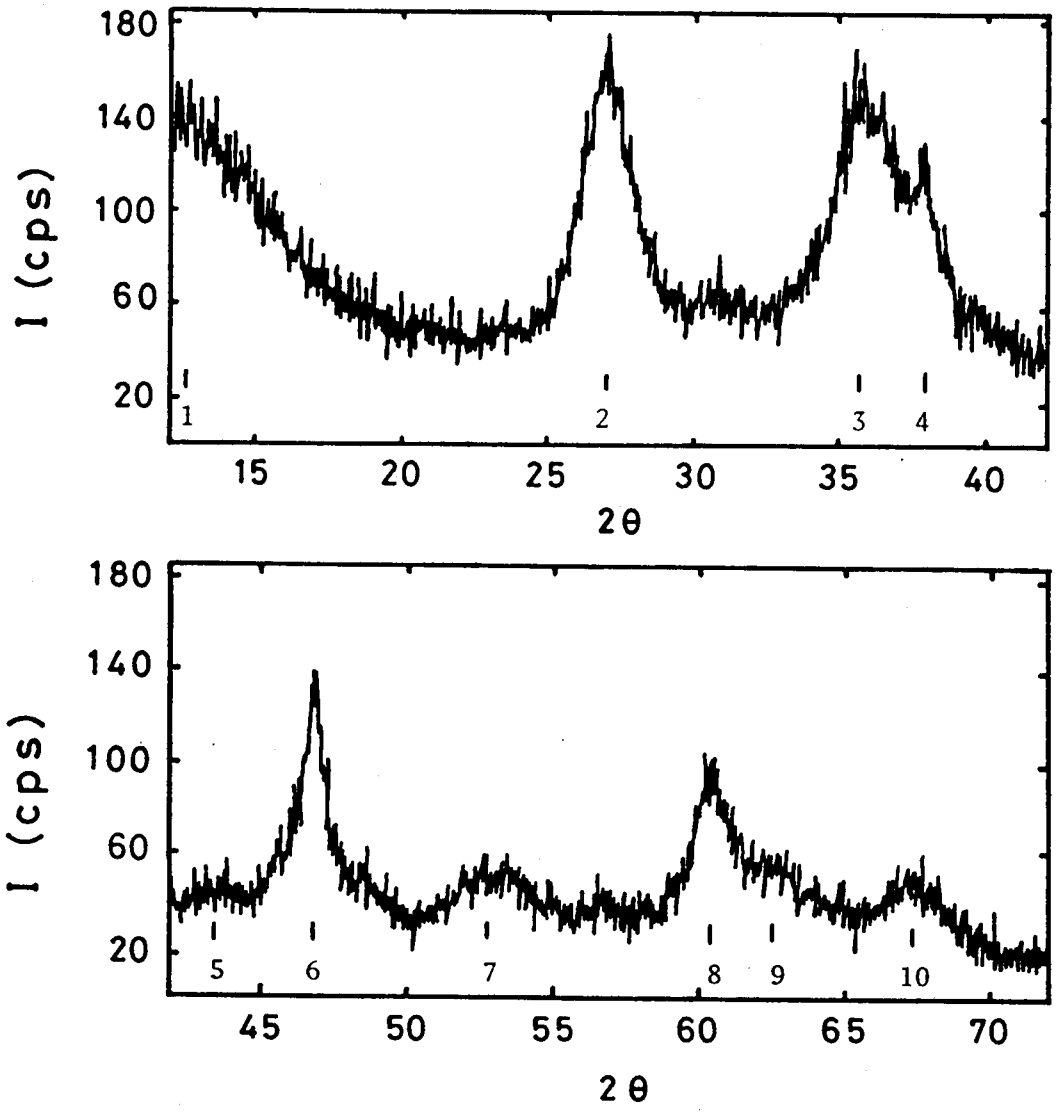

Fig. 3-1 X-ray diffractogram of poorly crystalline iron oxyhydroxide defined as γ-FeOOH (Table 3-1)

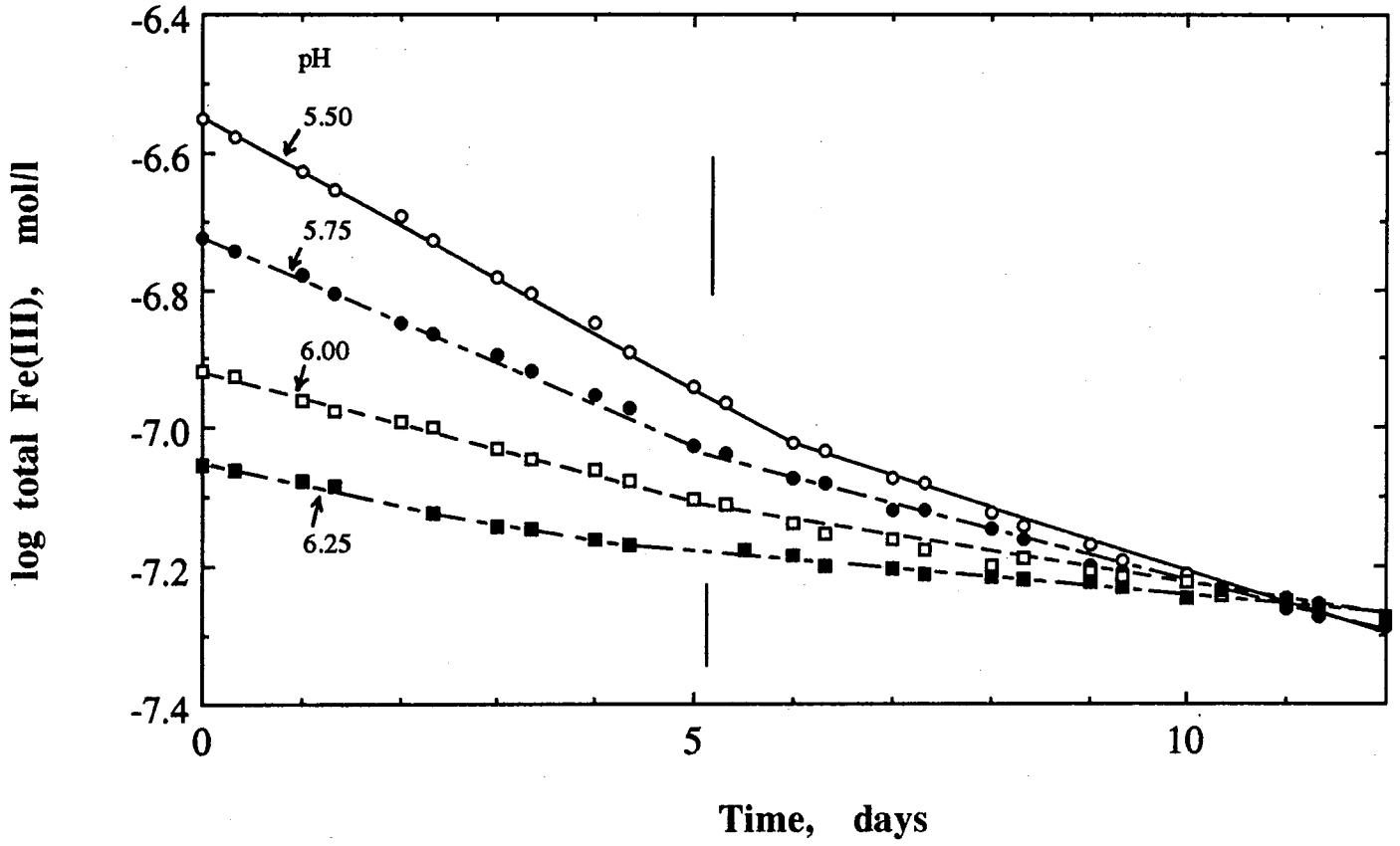

Fig. 3-2 Results of dialysis experiments at 20°C in the pH range 5.50-6.25

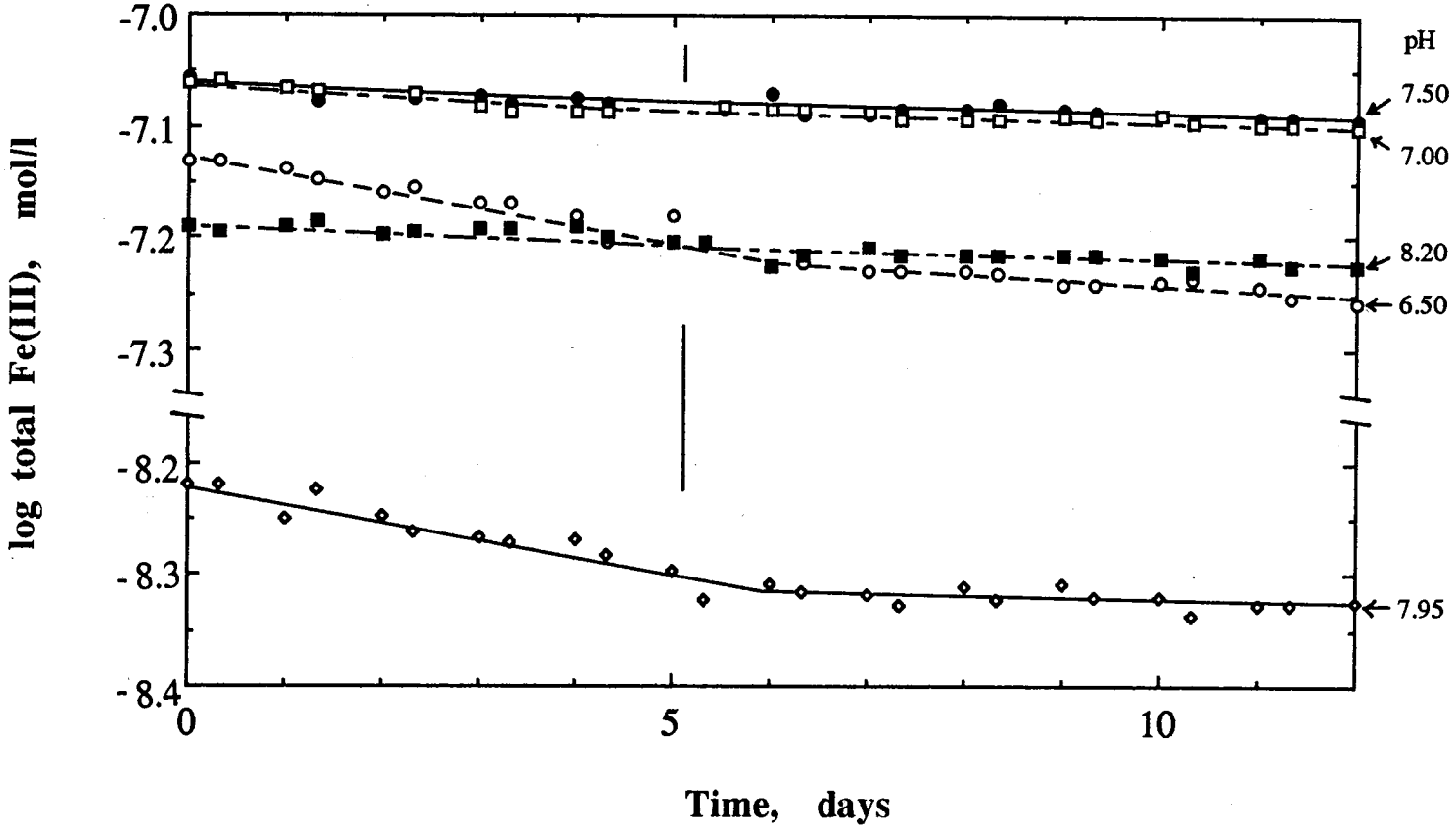

Fig. 3-3 Results of dialysis experiments at 20°C in the pH range 6.50-8.20

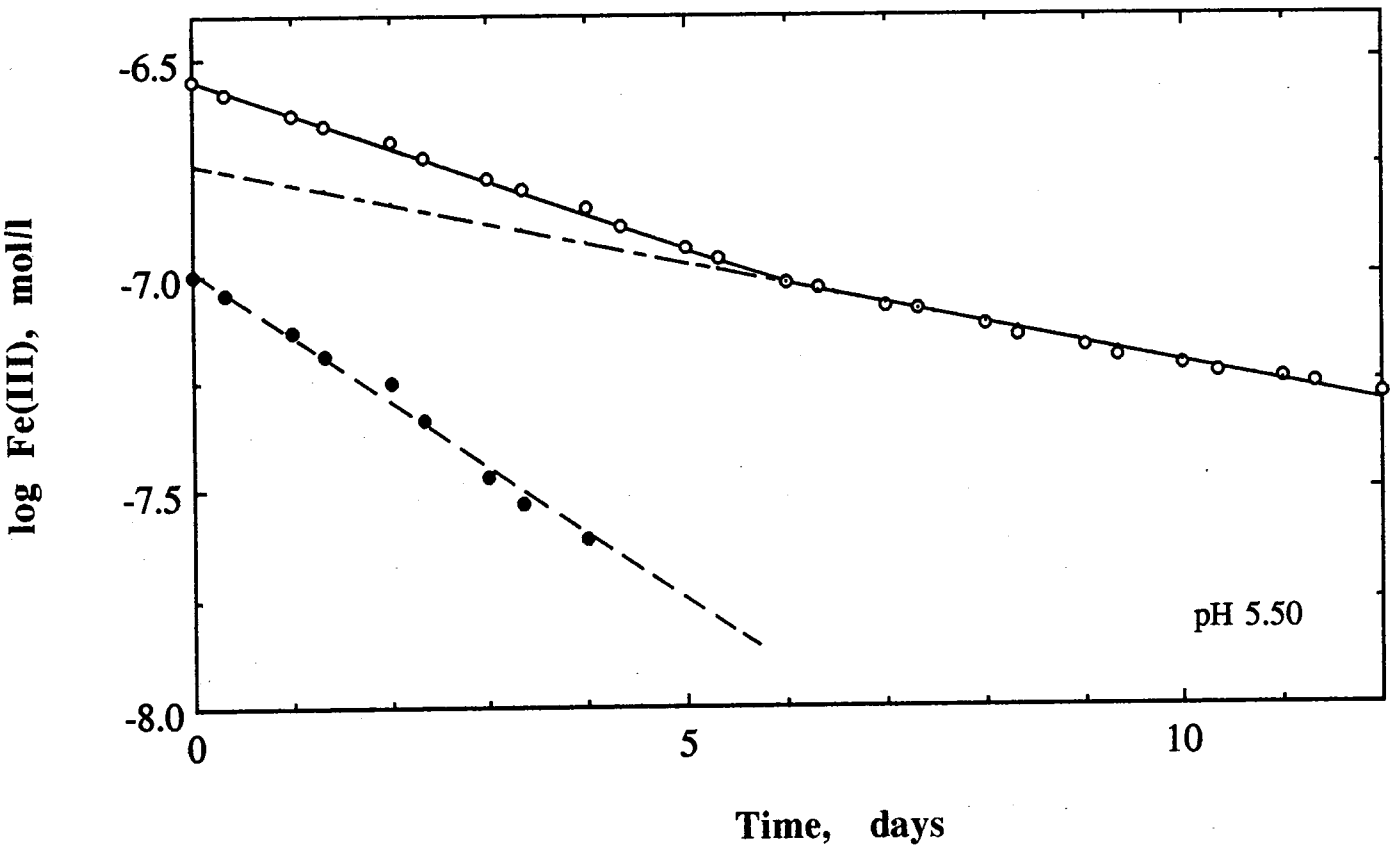

Fig. 3-4 Dissolution of particulate Fe(III) and dissolved Fe(III) in the dialysis tube calculated from the result of dialysis experiment at pH 5.50

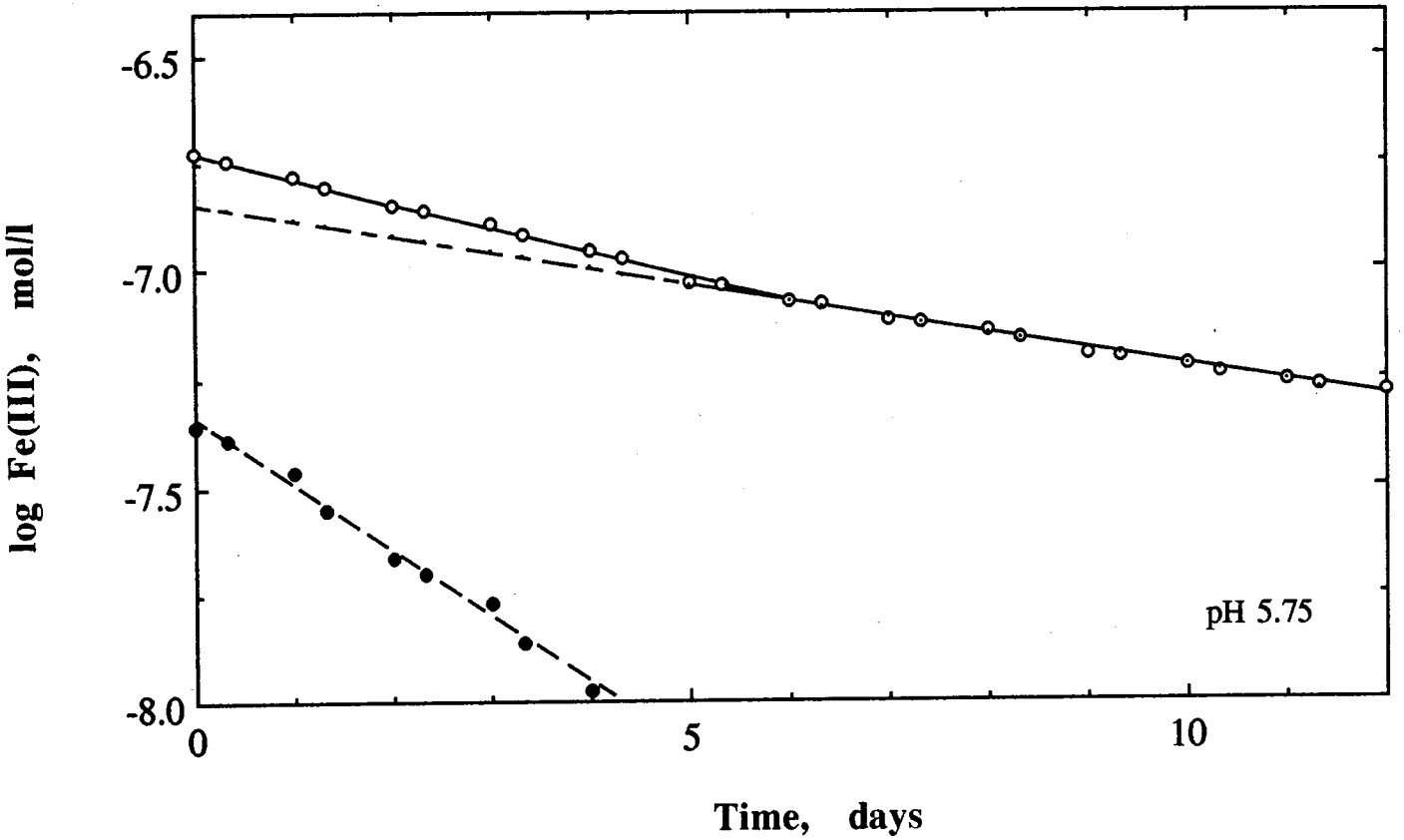

Fig. 3-5 Dissolution of particulate Fe(III) and dissolved Fe(III) in the dialysis tube calculated from the result of dialysis experiment at pH 5.75

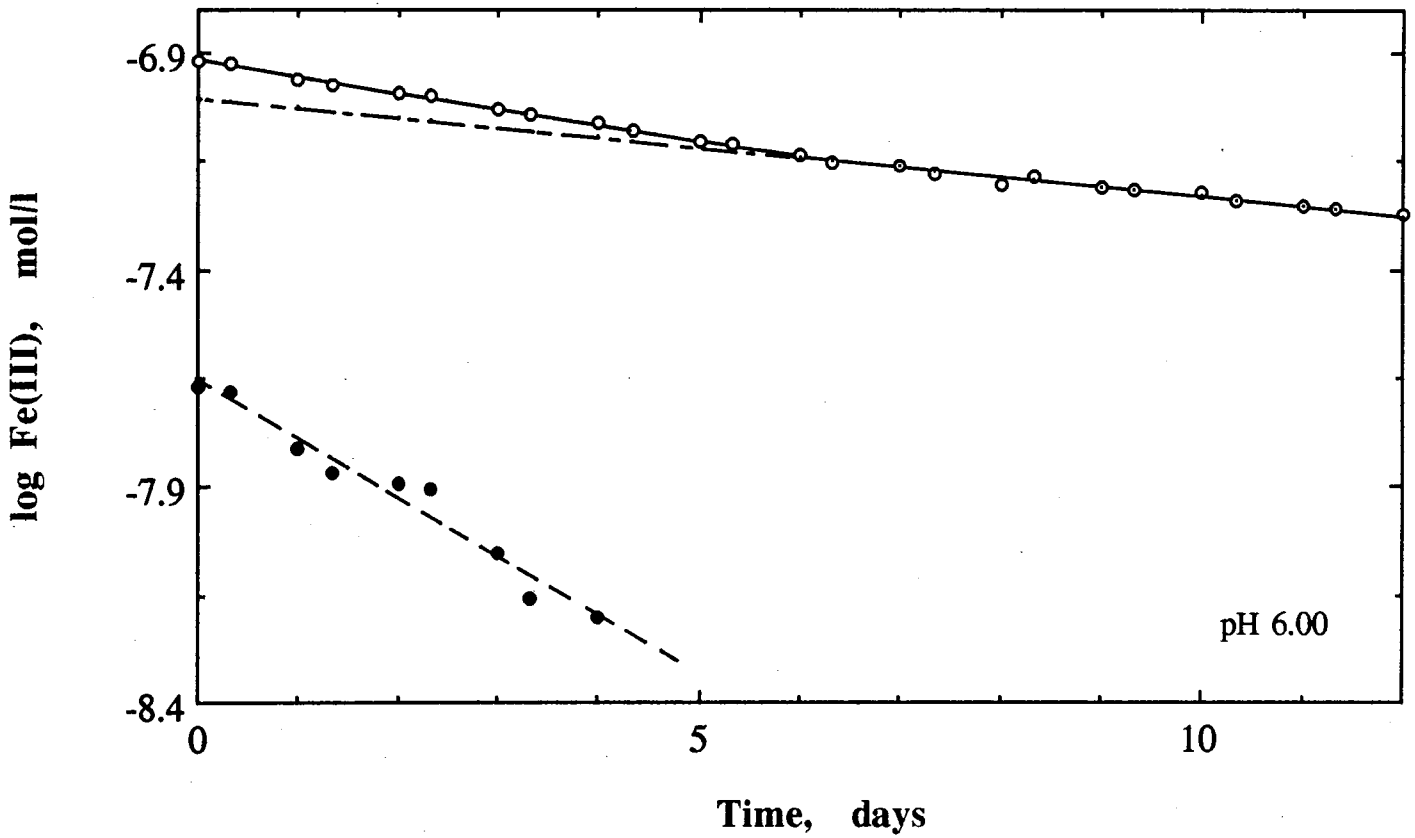

Fig. 3-6 Dissolution of particulate Fe(III) and dissolved Fe(III) in the dialysis tube calculated from the result of dialysis experiment at pH 6.00

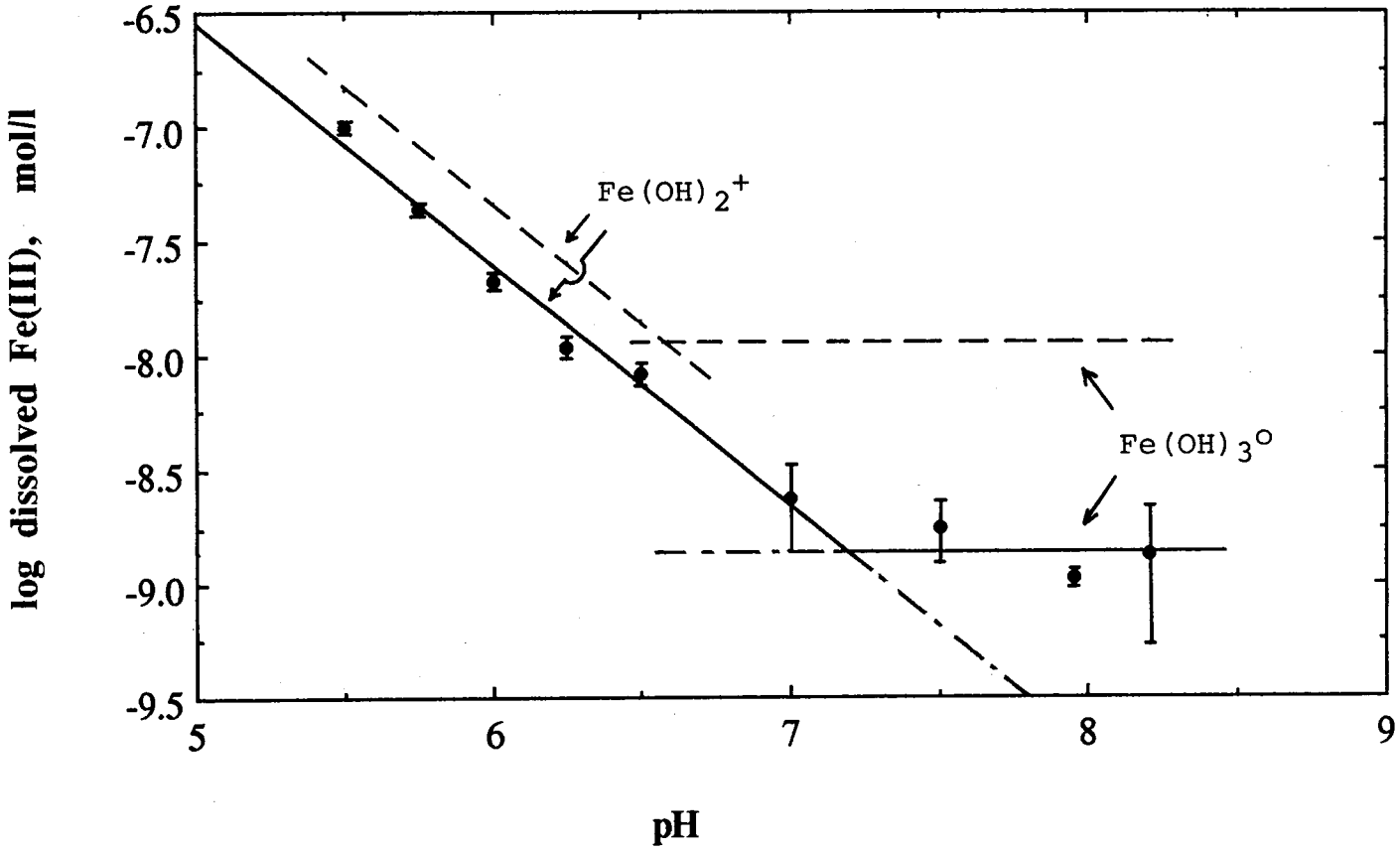

Fig. 3-7 Iron solubility in seawater at 20°C obtained by dialysis experiments ——, r-FeOOH; - - - -, amorphous hydrous ferric oxide

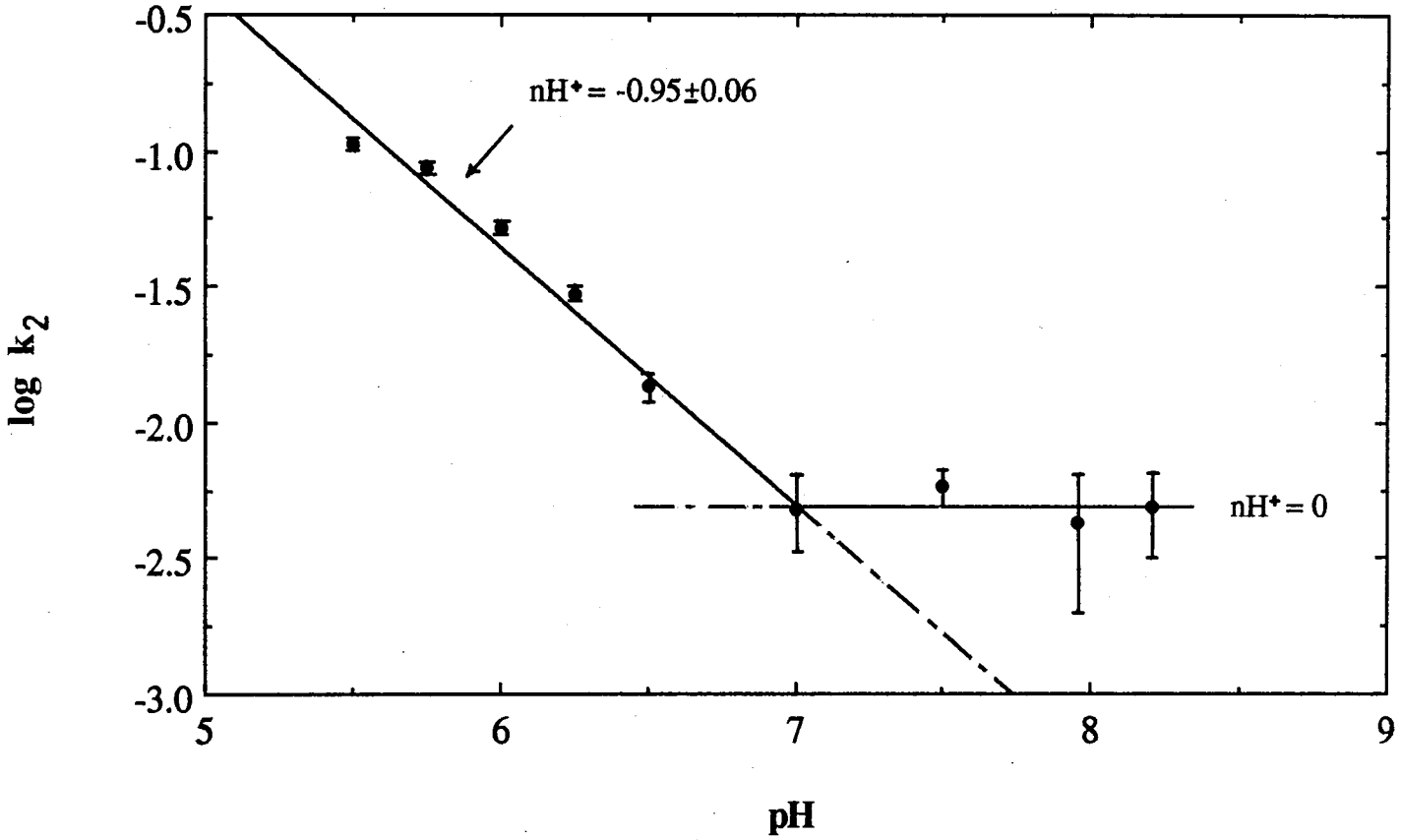

Fig. 3-8 Dissolution rate constant vs. pH in seawater at 20°C obtained by dialysis experiments

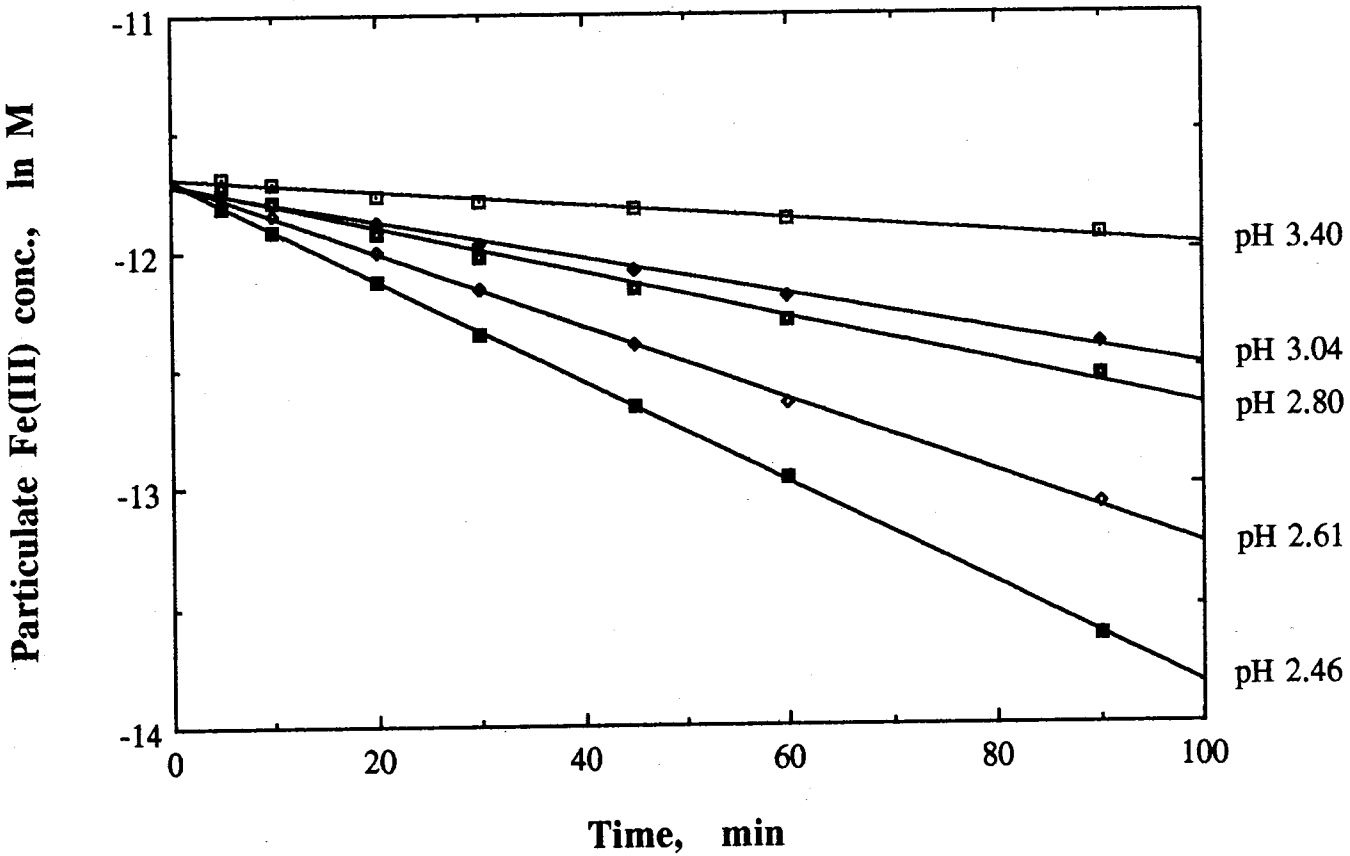

Fig. 3-9 Fe(III) dissolution rate of r-FeOOH in seawater at 20°C obtained by filtration experiments

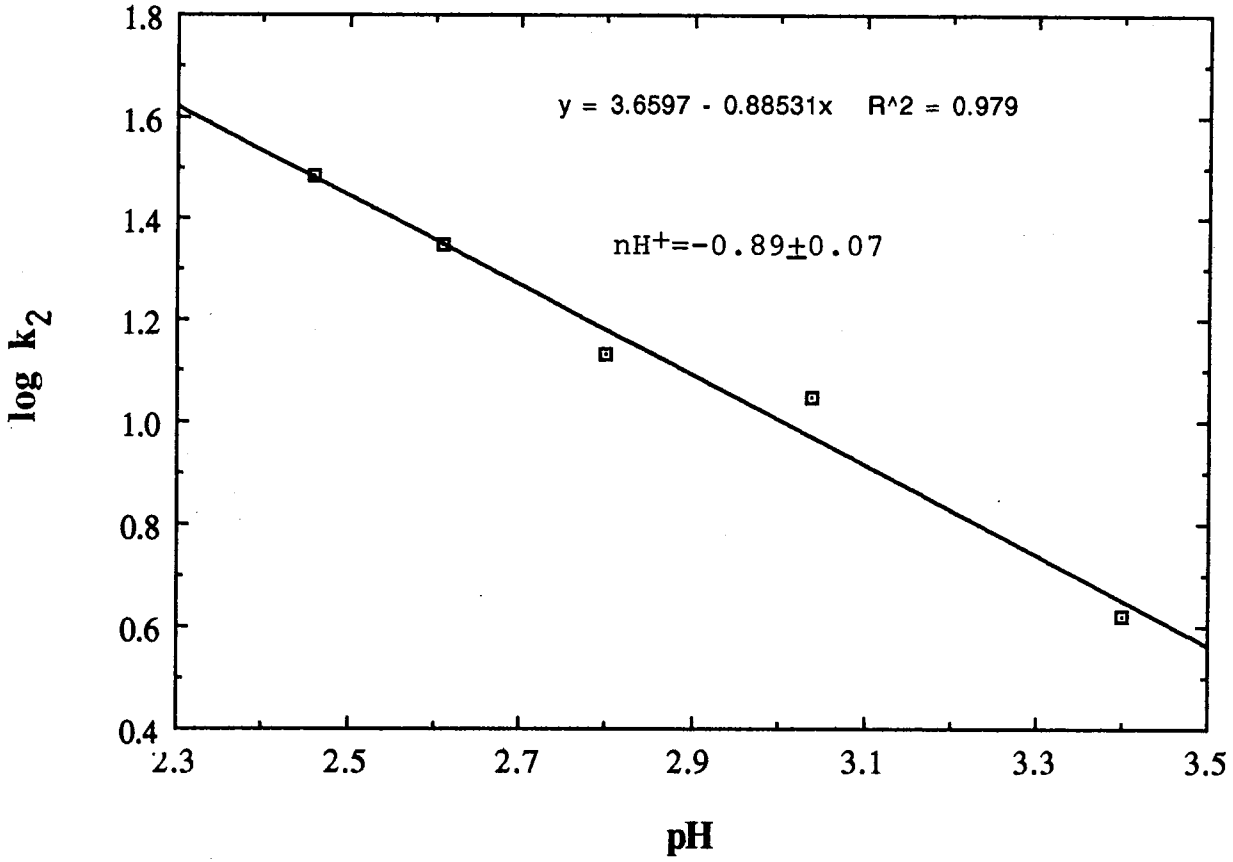

Fig. 3-10 Dissolution rate constant vs. pH in seawater at 20°C obtained by filtration experiments

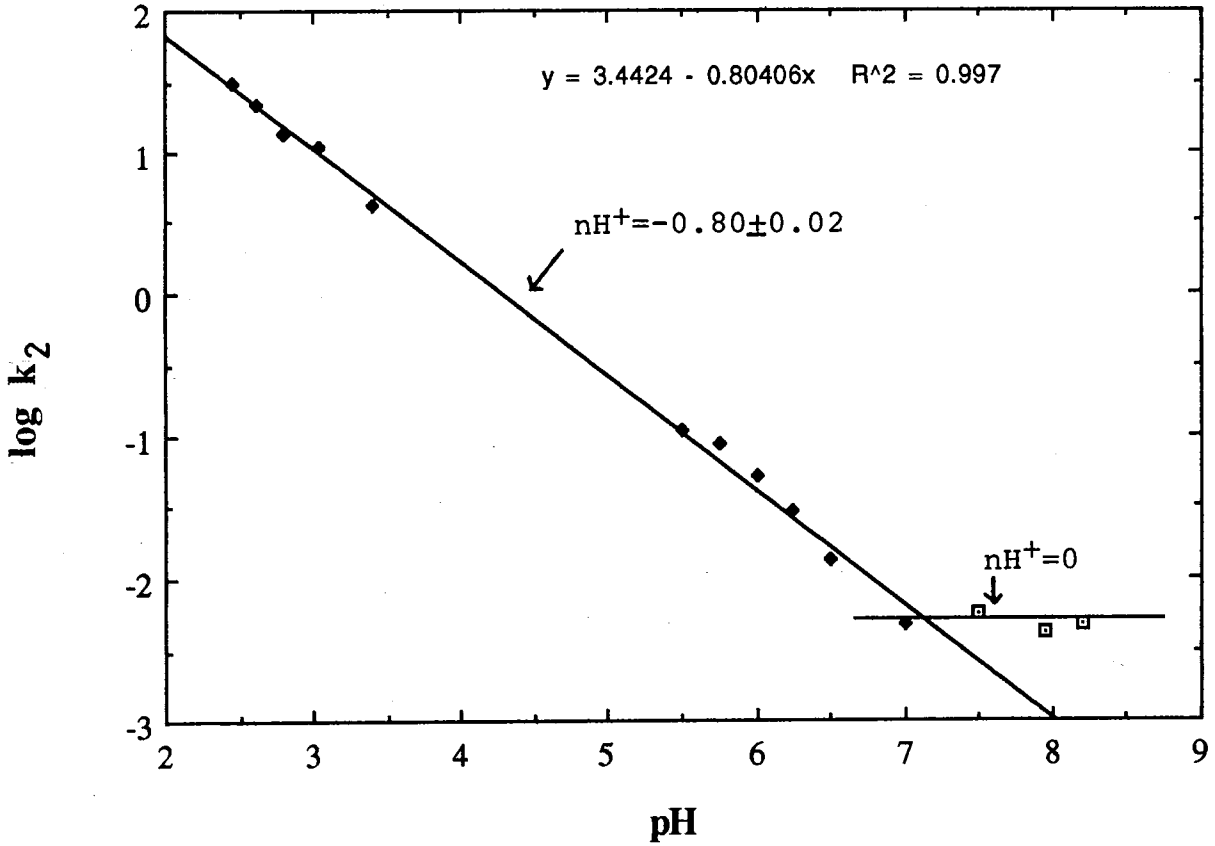

Fig. 3-11 Dissolution rate constant vs. pH in seawater at 20°C obtained by filtration and dialysis experiments

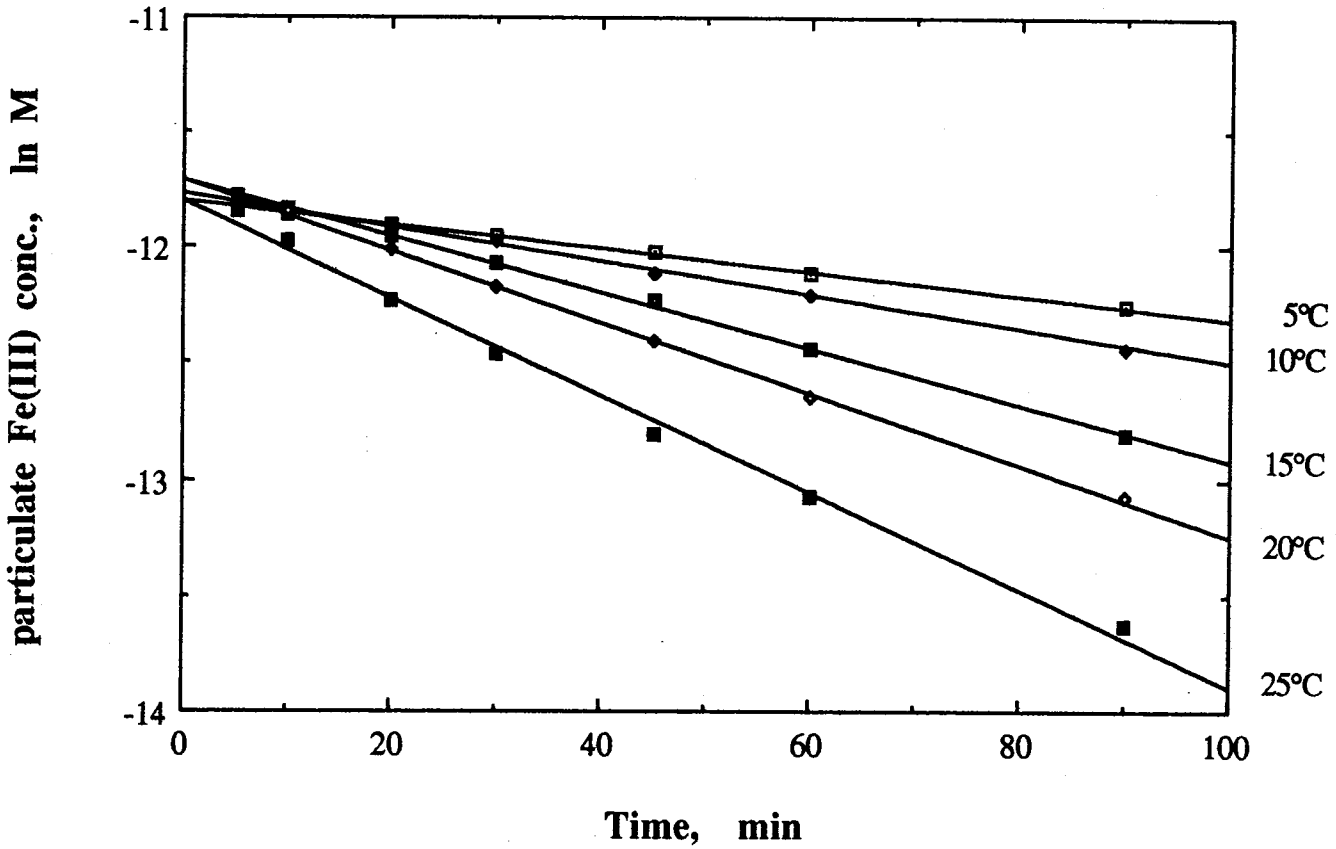

Fig. 3-12 Fe(III) dissolution rate of r-FeOOH in seawater at pH 2.60 obtained by filtration experiments

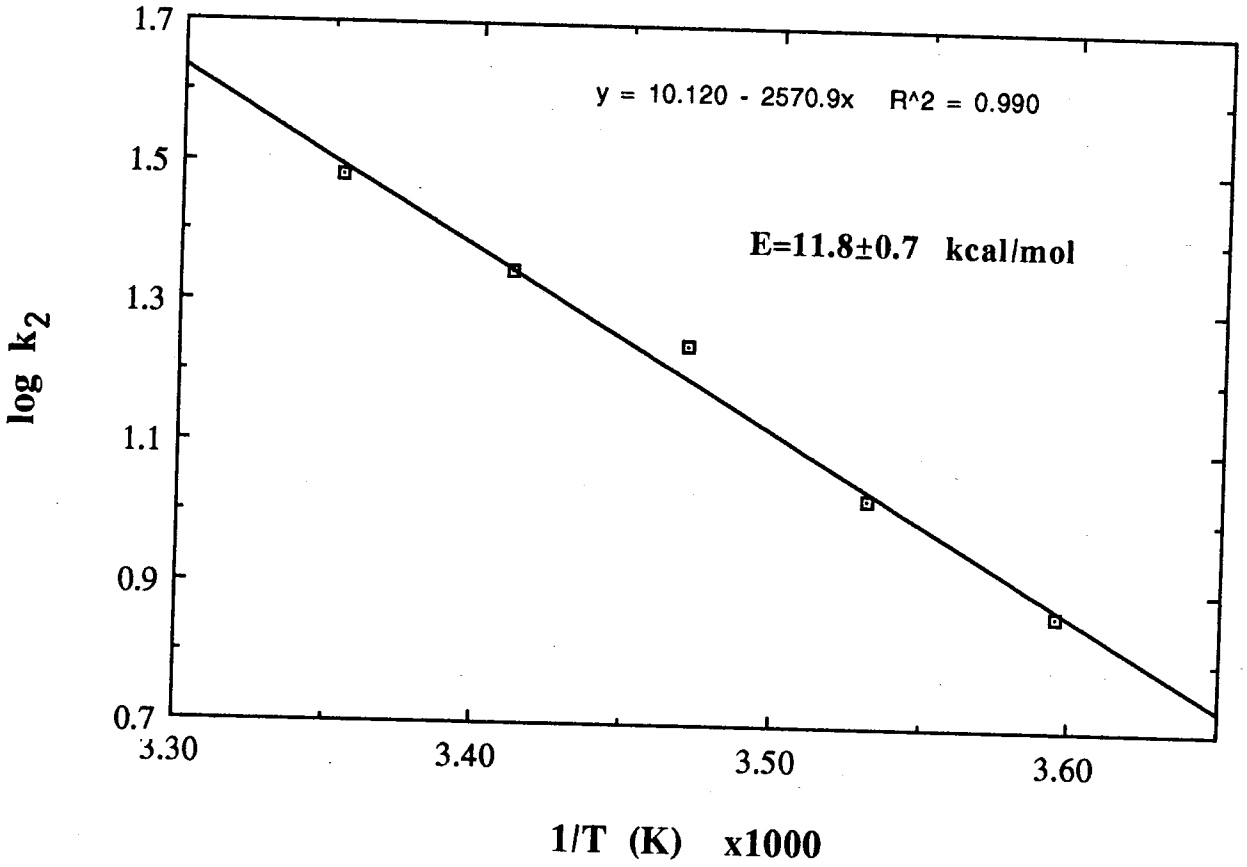

Fig. 3-13 The effect of temperature on the dissolution rate constant in seawater at pH 2.60 obtained by filtration experiments

4 SOLUBILITIES OF COLLOIDAL FERRIC OXIDES AND OBSERVED DISSOLVED IRON CONCENTRATIONS IN SEAWATER

4.1 Introduction

The solubilities of amorphous hydrous ferric oxide and γ-FeOOH in seawater over pH 5.5 to 8.2 at 20°C were experimentally determined by dialysis techniques in Chapter 2 and 3. In this Chapter, the solubilities of hydrated ferric oxyhydroxide polymer ($Fe_5O_7(OH).4H_2O$), in addition to those of amorphous phase and γ-FeOOH, in seawater (around pH 8) at 20°C were determined by simple filtration techniques involving γ-activity measurements of filterable ^{59}Fe. The ferric oxide forms derived from ferric and ferrous iron in seawater were identified as amorphous in the initial phases and poorly crystalline γ-FeOOH, respectively (Chapter 2 and 3; Crosby et al., 1983). The suspensions in seawater were easily obtained by adding ferric and ferrous iron in seawater. However, it is difficult to obtain α-Fe_2O_3 and α-FeOOH, commonly found in soils and natural waters, suspensions in seawater without contamination and to carry out the dialysis experiments of ^{59}Fe in Chapter 2 and 3. Hematite (α-Fe_2O_3) is generally formed by directly dehydration of α-FeOOH and by dehydration and/or transformation of other ferric oxides, such as amorphous hydrous ferric oxide, γ-Fe_2O_3, and γ-FeOOH, with heating (Hamada and Kuma, 1977; Sidhu et al., 1981). Goethite (α-FeOOH) is also obtained by oxidation of ferrous iron (Hamada and Kuma, 1976 and 1977) and by aging Fe(III) hydroxide gels (Atkinson et al., 1968) in

strong alkaline solutions.

The order of solubilities of ferric oxides is amorphous phase > γ-FeOOH > α-Fe_2O_3 > α-FeOOH, which is approximately three order of magnitude more insoluble than amorphous phase (Lindsay, 1991), although their solubilities, except for those of amorphous phase (Byrne and Kester, 1976 a; Kuma et al., 1992 a) and γ-FeOOH (Chapter 3), in seawater have not been reported. In seawater, the dominant ferric oxide solid form at the coastal region and the shollow margins will be expected to be metastable amorphous phase originated from river input and sediments. However, the dominant solid form at the mid and deep waters in the open ocean may be stable crystalline form such as γ-FeOOH (the oxidation product of ferrous ion probably released by the decomposition of organism in seawater), α-Fe_2O_3 or α-FeOOH.

In this study, the solubilities of amorphous phase, γ-FeOOH and $Fe_5O_7(OH).4H_2O$ in seawater were determined by simple filtration technique involving γ-activity measurements of filterable ^{59}Fe in order to compare with the results of dialysis experiments (Chapter 2 and 3) and the dissolved iron concentrations observed in seawaters.

4.2 Experimental Procedure

In this study, the simple filtration (acid-cleaned 0.45 and 0.025 μm Millipore membrane filters) was used to distinguish between dissolved Fe(III) and particulate Fe(III) in seawater. The filtered seawater (0.45 μm), which was collected from Funka Bay in Japan, was used in this

study. Hydrated ferric oxyhydroxide polymer ($Fe_5O_7(OH).4H_2O$) was prepared by autoclaving the amorphous hydrous ferric oxide suspended in seawater at 120°C for 1 hr (1.1 kg cm^{-2}). X-ray diffraction analysis with filtered Co Kα radiation (40 kv, 20 mA) confirmed that the air-dried product was poorly crystalline $Fe_5O_7(OH).4H_2O$ (Fig.4-1 and Table 4-1).

4.2.1 *Solubility measurements of ferric oxides in seawater by filtration*

Radioactive ferric and ferrous ^{59}Fe solutions, in quantity over the solubilities of amorphous hydrous ferric oxide and γ-FeOOH, respectively, were added to100 ml pretreated seawater in 100 ml polyethylene bottles previously cleaned with 6 N HCl. Hydrated ferric oxyhydroxide polymer ($Fe_5O_7(OH).4H_2O$) was prepared by autoclaving the amorphous hydrous ferric oxide suspended in seawater at 120°C for 1 hr (1.1 kg cm^{-2}). The seawater solutions (around pH 8) were filtered through acid-cleaned Millipore filters with pore size of 0.45 and 0.025 μm after allowing to stand for 3 days, 1, 3 and 5 weeks at 20°C. The γ-activity of 2.5 ml filtered solutions was measured after being acidified by addition of a small amount of concentrated HCl in order to prevent the adsorption of filtered Fe(III) on the walls. The filtered Fe(III) concentrations were calculated from the counts corrected with an average counting efficiency for ^{59}Fe, volume of filtered solution and amount of Fe per count.

4.2.2 *Dissolved (filterable) iron concentrations in the open ocean*

Water samples were collected with Go-Flo samplers hung on a

Kevlar line at 40 and 49° N on the 180° longitude line in the North Pacific Ocean in June, 1990 and were immediately filtered through an acid-cleaned 0.45 μm Millipore filter in a clean bench. All water samples were acidified to pH 2.9 with 4 ml of 1 M Ultrapur HCl and stored until analysis in a clean room. Quartz-sub-boiled distilled water was produced by sub-boiling in a clean room and used for the dilution of reagents and for the washing of apparatus. The dissolved iron concentration of each filtered and acidified seawater sample was determined by a graphite furnace atomic absorption spectrophotometer after preconcentration by APDC/DDDC-chloroform organic extraction (Landing and Bruland, 1987). The overall extraction efficiency, determined using ^{59}Fe radiotracer, was 94.8±0.15 % (n=5). The precisions for Fe analysis was ±4.4% at 2 nM Fe level.

4.3 Results and Discussion

4.3.1 *Soulbilities of ferric oxides in seawater determined by filtration*

The results of the filtration and dialysis experiments in seawater at 20°C for various ferric oxide forms and atmospheric dust are summarized in Table 4-2. The filterable iron concentrations in seawater determined by using 0.45 and 0.4 μm filters were about two to three times higher than those by using 0.05 and 0.025 μm filters and dialysis membrane. In this study, the 0.45 μm filterable iron concentrations decreased extremely with aging time indicating that the filterable fraction contains iron colloids with size < 0.45 μm. However, the solubilities of amorphous

hydrous ferric oxide and γ-FeOOH obtained by using 0.025 μm filters are in good agreement with those obtained by the dialysis experiments (Kuma et al., 1992 a and 1992 c). In addition, the solubilities of amorphous phase in this study are consistent with the values obtained from the acidification followed by ultrafiltration and the dialysis experiments by Byrne and Kester (1976 b) and from the 0.05 μm filtration experiments for atmospheric iron by Zhuang et al. (1990). The order of solubilities of ferric oxides forms in seawater at 20°C in this study is amorphous hydrous ferric oxide (8-13 nM) > γ-FeOOH (1-2 nM) > $Fe_5O_7(OH).4H_2O$ (0.2-0.6 nM). The solubility of α-FeOOH, the most stable iron oxyhydroxide found in soils and natural waters, in seawater will be expected to be extremely low (about 0.01 nM) since α-FeOOH is approximately three orders of magnitude less soluble than amorphous phase (Lindsay, 1991).

4.3.2 *Dissolved iron concentrations in the open ocean*

Fig. 4-2 shows the vertical distributions of dissolved iron concentrations at two stations (40° N, 180° W and 49° N, 180° W). In surface waters (about 0-25 m), the dissolved iron concentrations were approximately 1-2 nM and twice higher than those at deep waters. At deeper waters (100 to 1000 m), the concentrations were constant at a range 0.4-0.9 nM. A typical dissolved Fe profile from the North Pacific central gyre is presented in Fig. 4-3 A (Bruland et al., 1991). This vertical profile exhibits the influence of aeolian input, similar to that observed for Mn and Al. The mixed-layer concentrations are as high as 0.37 nM, but

decrease sharply through the upper seasonal thermocline to a subsurface minimum of only 0.02-0.05 nM at depths of 75-100 m. According to Duce (1986), over 95 % of the Fe supply to surface waters in open ocean comes from the atmosphere. These extremely low values in the subsurface are consistent with both the uptake of this required metal by phytoplankton and with the reactivity of particulate Fe. The concentrations at depths from 100 to 800 m increase gradually with depth, exhibiting a nutrient-type profile, and those below 800 m are constant at a range 0.3-0.4 nM. Dissolved Fe and NO_3^- have very different chemistries in the deep waters. NO_3^- regenerated into intermediate or deep waters is chemically unreactive and eventually mixes back into the surface waters ready to be reassimilated. Fe, however, is a chemically reactive species that is scanvenged from the deep sea. Thus, most of the Fe regenerated into the deep sea from oxidation of the biogenic organic flux is probably rescanvenged and efficiently removed to the sediments rather than mixed back into the surface (Bruland et al., 1991).

A vertical profile of dissolved Fe from the subarctic Pacific is presented in Fig. 4-3 B to show the low dissolved Fe found throughout the surface photic zone. It is in these nutrient-rich, open ocean having low atmospheric Fe inputs that Fe is suggested to be a biolimiting nutrient (Martin and Fitzwater, 1988; Martin and Gordon, 1988; Martin et al., 1989, 1990, 1991). At the depths from 500 to 4000 m, the dissolved Fe concentrations are within a narrow range 0.6-0.7 nM. The dissolved Fe concentrations at deep waters in open ocean may be in equilibrium with more stable crystalline ferric oxide, such as γ-FeOOH, $Fe_5O_7(OH).4H_2O$ or α-Fe_2O_3

rather than metastable amorphous hydrous ferric oxide (Table 4-2). The metastable amorphous phase would slowly convert into the more stable phases (FeOOH, Fe_2O_3 or both) (Crosby et al., 1983; Bruland et al., 1991). In the open ocean, the most likely sources of iron colloids are atmospheric dust (Moore et al., 1984; Duce, 1986; Zhuang et al., 1990), in situ oxidation of Fe(II) (Landing and Bruland, 1987) and release of iron compounds during the degradation of organisms. Zhuang et al. (1990) reported that the saturated concentration (filterable with 0.05 μm filter) of dissolved atmospheric iron in seawater was found to be 5-8 nM (Table 4-2) and about 50 % of the atmospheric iron dissolved rapidly in seawater if the total iron concentration was less than 2 nM (the open Pacific Ocean is in this category). These results may indicate that the dominant ferric oxide form in atmospheric iron is probably amorphous phase and that the dissolved iron at surface photic zone in the open ocean decrease rapidly because of the uptake by phytoplankton. In coastal waters, in addition, the input of colloids from rivers and sediments must be considered. The dissolved iron concentrations were observed to be approximately 5-10 nM at the shallow margin and on the shelf (Martin and Gordon, 1988; Nolting et al., 1991). The dominant iron solid phase, which will govern the dissolved iron concentration and dissolution rate in oxic seawater, will be probably metastable amorphous phase, originated from atmospheric dust, river and/or sediment, with the highest solubility (5-20 nM) among the other ferric oxide forms. The dissolved iron concentration in seawater will, therefore, be a function of the inputs (abundance in source media, solubility and rate of transfer

to dissolved forms depending on the solid form and its effective surface area and photoreduction at organic surfaces) and residence time in the aquatic environment (reactivity towards particle surfaces and organisms, conversion rate of metastable into the stable form, etc.).

4.4 Conclusions

The solubilities of various ferric oxides in seawater at 20°C determined by dialysis experiments (1000 Da) are consistent with those determined by filtration experiments (0.025 μm). The order of solubilities of various ferric oxides is amorphous hydrous ferric oxide (10 nM) > γ-FeOOH (1.4±0.4 nM) > $Fe_5O_7(OH).4H_2O$ (0.2-0.6 nM). The solubility of α-FeOOH, the most stable iron oxyhydroxide found in soils and natural waters, in seawater will be expected to be extremely low (about 0.01 nM) since α-FeOOH is approximately three orders of magnitude less soluble than amorphous phase.

In the open ocean, the dissolved iron concentrations at the surface waters are controlled by the atmospheric iron inputs (abundance in source media, solubility and dissolution rate depending on the iron solid form) and phytoplankton iron requirements. The solublities of γ-FeOOH and/or $Fe_5O_7(OH).4H_2O$ in seawater measured at its normal pH appear to be nearly the same values as the dissolved iron concentrations (0.3-0.7 nM) measured at deep waters in the open ocean. The implication, then, is that the deep waters in the open ocean may be in saturation equilibrium with the thermodynamically stable ferric oxide forms rather than metastable amorphous phase.

Table 4-1. The observed X-ray diffraction lines compared to that of $Fe_5O_7(OH).4H_2O$.

	Observed XRD lines		hydrated ferric oxyhydroxide polymer $Fe_5O_7(OH).4H_2O$	
line No.	intensity (obs.) (I/Io) x100	d(obs.) Å	d(ref.) Å	intensity (ref.) (s, m or w)
1	100	2.53	2.52	s
2	40	2.25	2.25	m
3	12	1.99	1.97	w
	----	----	1.72	w
4	42	1.48	1.48	m

Crystal system of $Fe_5O_7(OH).4H_2O$: hexagonal (a=5.08, c=9,4 Å)

Table 4-2. Dissolved (filterable and/or dialyzable) iron concentrations in amorphous hydrous ferric oxide, γ-FeOOH, $Fe_5O_7(OH).4H_2O$ and atmospheric dust suspended in seawaters.

(1) filterable iron concentration in seawater at 20°C (pH 7.8-8.0)

material	amorphous		γ-FeOOH		$Fe_5O_7(OH).4H_2O$	
filter size (μm)	0.45	0.025	0.45	0.025	0.45	0.025
	filterable iron concentration (nM)					
aging time (day)						
3	37.3	12.5	----	----	1.40	0.53
7	28.6	10.7	6.97	2.42	1.74	0.55
21	24.2	9.42	3.93	1.78	0.42	0.34
35	21.1	8.49	3.21	1.42	0.22	0.17

(2) dialyzable (1000 Da) iron concentrations in seawater at 20°C (pH 7-8) (Kuma et al., 1992 a and 1992 c)

material	amorphous	γ-FeOOH
aging time (day)		
7-	10.5±0.5 nM	-------
14-	-------	1.4±0.4 nM

(3) freashly precipitated hydrous ferric oxide in seawater at 25°C (Byrne and Kester, 1976 a)

dialyzable (pH 8.12 and 8.13) 12.4-17.5 nM

acidification followed by ultrafiltration (pH 5.99-8.28) 5-20 nM

(4) atmospheric dust in seawater at 20°C (pH 8.11) (Zhuang, 1990)

0.4 μm Nuclepore filter 10-17 nM

0.05 μm Millipore filter 5-8 nM

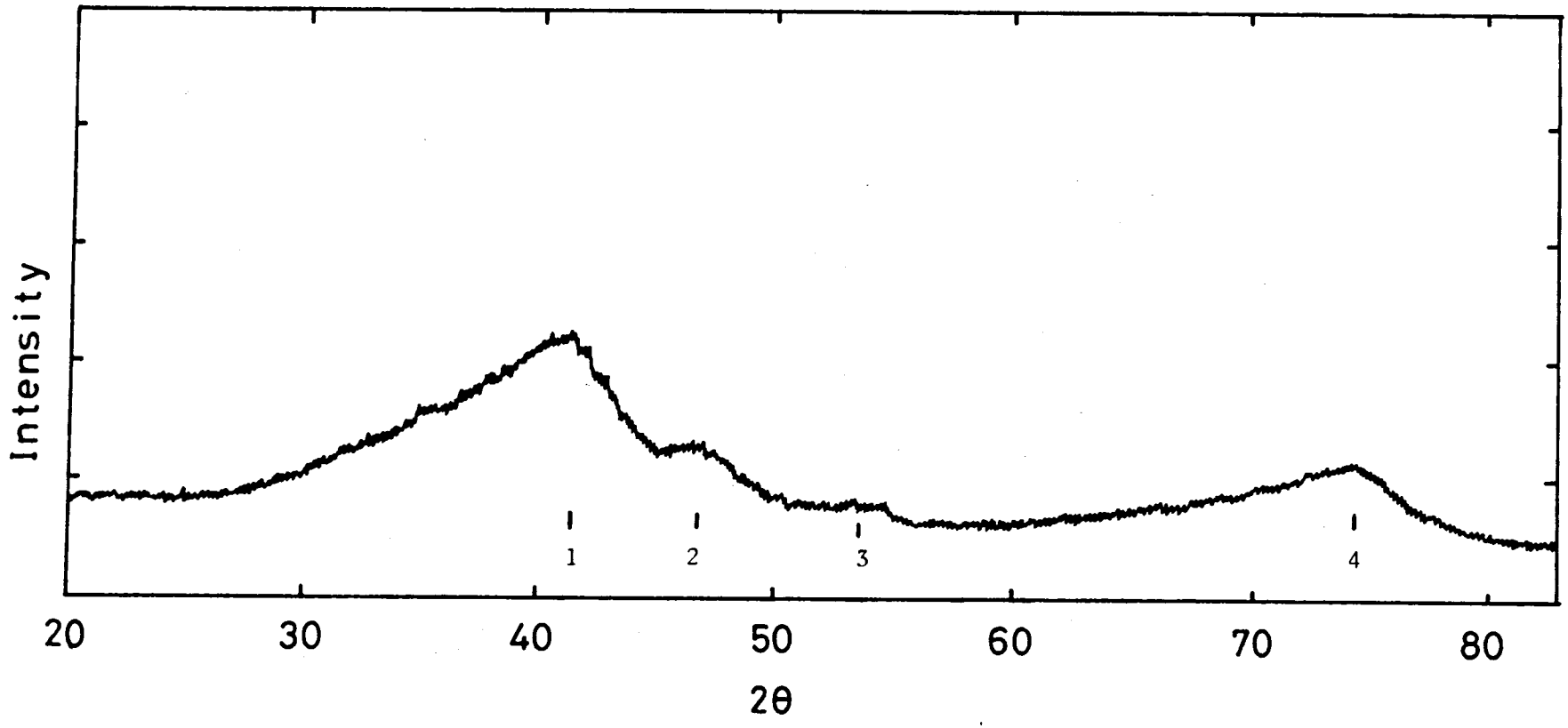

Fig. 4-1 X-ray diffractogram of hydrous ferric oxide autoclaved at 120°C for 1 hr defined as hydrated ferric oxyhydroxide polymer ($Fe_5O_7(OH).4H_2O$) (Table 4-1)

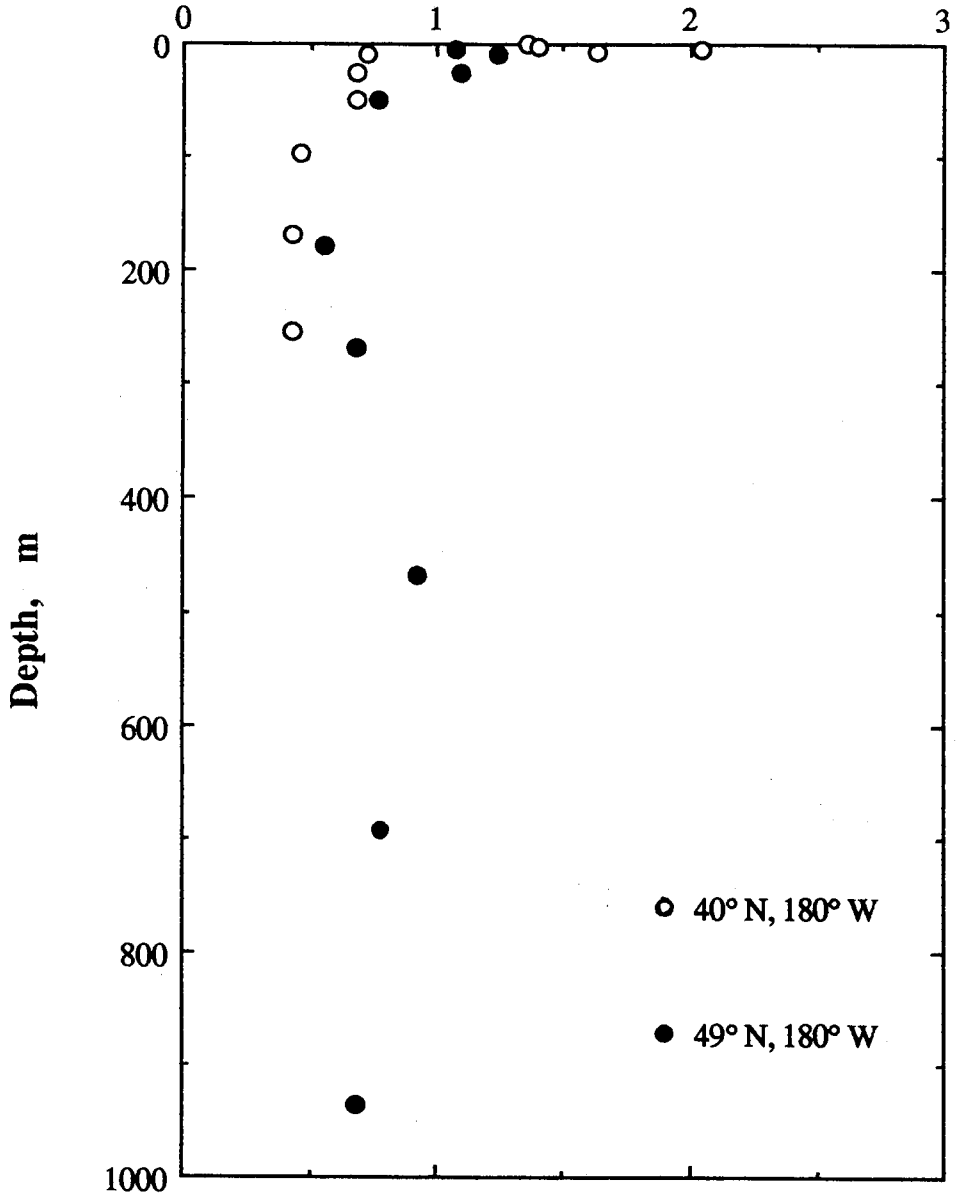

Fig. 4-2 Vertical distributions of dissolved Fe at 180° W line in the North Pacific Ocean

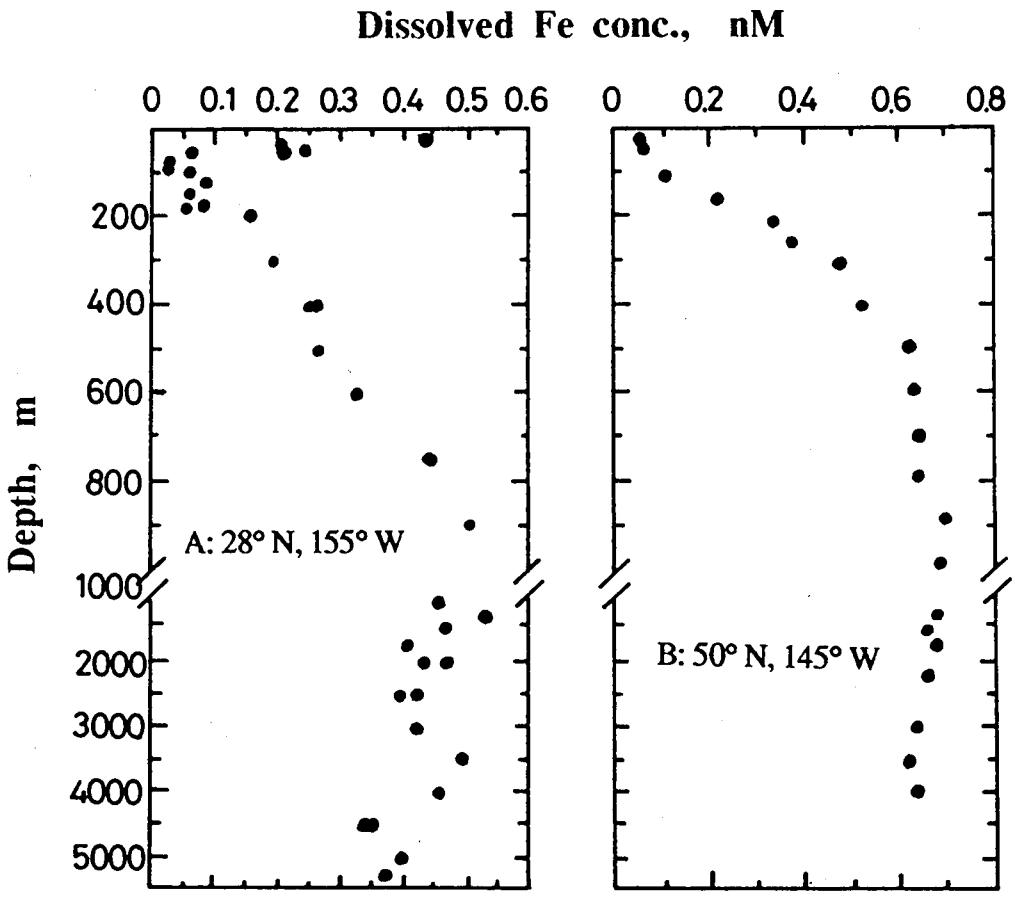

Fig. 4-3 Typical profiles for dissolved Fe in the North Pacific central gyre (Bruland et al., 1991) and in the subarctic Pacific (Martin et al., 1989)

5 AVAILABILITY OF COLLOIDAL FERRIC OXIDES IN PROVIDING A SOURCE OF IRON TO PHYTOPLANKTONS

5.1 Introduction

In oxic seawater, iron colloids may exist in a number of crystalline and noncrystalline ferric oxide forms. The principal phases commonly found in soils and natural waters are amorphous hydrous ferric oxide ($Fe_2O_3.xH_2O$), α-Fe_2O_3, α-FeOOH and γ-FeOOH, whereas β-FeOOH is rather rare (Schneider, 1988; Lindsay, 1991). Since the internal structure of the colloid affects its thermodynamic stability, it will also influence the iron uptake rate by phytoplankton at which the colloid is able to provide biologically available inorganic species of iron. With phytoplankton, the biologically available species of iron appear to include dissolved ionic species (Anderson and Morel, 1982) as well as some dissolved organic complexes (Lewin and Chen, 1971). In flagellate cultures, the addition of soluble chelated Fe(III)-EDTA to culture media induces the phytoplankton to grow (Lewin and Chen, 1971; Iwasaki and Iwasa, 1982; Yamochi, 1983). These biologically available species exist in equilibrium with the more dominant colloidal ferric oxides in seawater. The crystalline ferric oxides such as α-FeOOH, β-FeOOH and α-Fe_2O_3, thermodynamically stable forms, do not support phytoplankton growth at all, while amorphous hydrous ferric oxide can induce the maximal growth and the cell yields because of faster thermal dissolution rate of

metastable amorphous phase than those of stable crystalline ferric oxides (Wells et al., 1983; Rich and Morel, 1990).

This investigation tested the hypothesis that differences in the thermal dissolution rates of ferric oxide colloids will affect their ability to supply iron for the growth of the red tide flagellates *Chattonella marina* (Osaka bay (1982-08), Axenic, Clonal) and *Gymnodinium nagasakiense* (Harima-Nada (1980-08), Axenic, Clonal) and the marine diatom *Phaeodactylum tricornutum*.. The ferric oxide forms used in this study were amorphous hydrous ferric oxide obtained by adding ferric iron to filtered seawater, hydrated ferric oxyhydroxide polymer ($Fe_5O_7(OH).4H_2O$) obtained by autoclaving amorphous phase suspended seawater solution, colloidal γ-FeOOH obtained by adding ferrous iron to filtered seawater and α-FeOOH obtained by aerial oxidation of ferrous iron in strong alkaline solution.

5.2 Experimental Procedure

5.2.1 *Cultivation experiments of phytoplanktons in the presence of different ferric oxide forms*

The flagellates *C. marina* and *G. nagasakiense* and the diatom *P. tricornutum* were grown in f/2 medium (Guillard and Ryther, 1962) without trace metals and EDTA, which was already autoclaved at 121°C for 20 min (1.1 kg cm^{-2}), at 20°C under 3000 lux fluorescent light (12 h light, 12 h dark). The f/2 medium contains 880 μM nitrate, 38 μM phosphate, 35 μM silicate and small amounts of vitamins in filtered

seawater. The cultivation experiments were carried out under the same conditions, as described above, using f/2 medium in the presence of different colloidal ferric oxide forms. Amorphous hydrous ferric oxide and γ-FeOOH suspended seawaters were directly prepared by aging 1 day at 20°C after adding ferric and ferrous iron, respectively, in 50 ml of autoclaved filtered seawaters. $Fe_5O_7(OH).4H_2O$ suspended seawater was prepared by autoclaving at 120°C for 1 hr after adding ferric iron to the filtered seawater. The ferric oxides growth media were then prepared by addition of concentrated f/2 stock to the ferric oxides suspended seawaters. α-FeOOH medium was prepared by directly adding a dilute colloidal α-FeOOH suspended solution to the f/2 medium. In addition, soluble Fe(III)-EDTA (1:2) and control (without adding iron) media were also prepared to compare the growth rates with those for colloidal ferric oxide forms. The iron concentrations in the media are 0.2 μM for the flagellates and 0.02 μM for the diatom cultivation experiments.

At start of the cultivation experiments a small amount of each culture in the stationary growth phase was added to 50 ml of each pretreated medium. Flagellates and diatom cell concentrations are approximately 300 and 5000 cells ml^{-1}, respectively. During experiments the cell concentrations were optically counted by using an optical microscope on a daily or weekly basis.

α-FeOOH suspended seawater solution was obtained by aerial oxidation of ferrous iron (Mohr's salt) in strong alkaline solution (1N NaOH) at 45°C and then washing several times with distilled water. X-ray

diffraction analysis with filtered Co Kα radiation (40 kv, 20 mA) confirmed that the air-dried product was crystalline α-FeOOH (Fig. 5-1 and Table 5-1).

5.2.2 *Dissolution rate measurements of ferric oxides in seawater at acidic pH by filtration*

The 0.45 μm Millipore membrane filter was used to distinguish between dissolved (filterable) Fe(III) and particulate Fe(III) in seawater. The dissolution rates of amorphous hydrous ferric oxide, $Fe_5O_7(OH).4H_2O$ and α-FeOOH, in addition to γ-FeOOH (Chapter 3), in seawater at acidic pHs were conducted in the following manner.

(1) For amorphous hydrous ferric oxide, a small amount of ferric iron solution was added to 250 ml filtered seawater at 20°C in an Erlenmeyer flask, followed by adjusting pH to 8.10±0.01 with NaOH solution. The seawater solutions were aged for 1 day at 20°C. For $Fe_5O_7(OH).4H_2O$ and α-FeOOH, their suspended water solution were produced by same methods in Chapter 4 and as described above, respectively. The total iron concentrations of $Fe_5O_7(OH).4H_2O$ and α-FeOOH stocks were determined by the ferrozine method (Stookey, 1970) after strong acidic digestion (2 N HCl).

(2) The concentrated acetic acid (0.125, 0.25, 0.5 or 1.25 ml) was directly added to each amorphous ferric oxide suspended seawater solution, after aging for 1 day, stirred with a magnetic stirrer at 20°C. For $Fe_5O_7(OH).4H_2O$ and α-FeOOH, a small amount of each stock was added to each 250 ml seawater solution at 20°C acidified with conc. acetic acid

(10, 25 or 62.5 ml) or conc. HCl (1 or 2 ml) and acetic acid (62.5 ml) or HCl (2, 5, 10, 20 or 42 ml), respectively. The total iron concentration in 250 ml seawater solutions is ca. 10 μM. Fifteen ml of each sample in the flask was immediately withdrawn at the appropriate time for 90 min and passed through a 0.45 μm filter. The dissolved (filterable) iron concentrations during the dissolution experiments were determined by the ferrozine method. After the experiments, the total iron concentrations and pHs of the seawater solutions were measured by the modified ferrozine method (adding more conc. HCl and heating longer to dissolve extremely less soluble $Fe_5O_7(OH).4H_2O$ and α-FeOOH) and a pH meter, respectively.

(3) The active amorphous hydrous ferric oxide in the solution converts slowly and partly into the inactive phase and/or most stable form such as α-FeOOH (Stumm and Morgan, 1981; Crosby et al., 1983). Therefore, the dissolution experiments were also conducted at 20°C for 90 min by adding 1.25 ml acetic acid to 250 ml amorphous phase suspended seawater solutions (pH 3.04) which were aged for 3 hr and 1, 3 and 7 days at 20°C. The dissolved and total iron concentrations in the solutions were determined by the ferrozine method.

(4) To know the effect of temperature on the dissolution rate in seawater at acidic pH, the dissolution experiments were conducted at 2.5, 5, 10, 15, 20 and/or 25°C for 90 min by adding 0.5 ml acetic acid to 250 ml amorphous phase suspended seawater solutions (pH 3.30), 2 ml HCl to 248 ml for $Fe_5O_7(OH).4H_2O$ (pH 1.02) and 42 ml HCl to 208 ml for α-FeOOH (pH -0.21). The dissolved and total iron concentrations in seawater solutions were determined by the same method in the precedure

(2).

5.3 Results and Discussion

5.3.1 *Cultivation of phytoplanktons in the presence of different ferric oxide forms*

Fig. 5-2, 5-3 and 5-4 present the cultivation results on the effect of various ferric oxide forms for *C. marina, G. nagasakiense* and *P. tricornutum,* respectively. Among solid ferric oxide forms, cell yields for all species used are significantly higher in the presence of amorphous hydrous ferric oxide than $Fe_5O_7(OH).4H_2O$, α-FeOOH and no iron (control). The cell yields in the presence of γ-FeOOH are the same as or less than those in the presence of amorphous phase. The order of cell yield is amorphous phase > γ-FeOOH >> $Fe_5O_7(OH).4H_2O$ > α-FeOOH. α-FeOOH and α-Fe_2O_3 are probably the most stable ferric oxyhydroxide and oxide, respectively, under earth surface conditions (Langmuir and Whittemore, 1971). The heating of amorphous phase, ultimately resulting in the formation of crystalline products, decreases the rate of colloid solubilization as a consequence of enhanced thermodynamic stability. Amorphous hydrous ferric oxide, in constrast, consists of aggregates of hydrated ferric ions that have a much lower thermodynamic stability. Therefore, the thermodynamic stability may be important in controlling the supply of biologically available iron. On the other hand, the addition of soluble chelated Fe(III)-EDTA to culture media for all species induces the maximum cell yields.

5.3.2 *Dissolution rates of ferric oxides in seawater at acidic pH*

(1) Dissolution rates of several ferric oxide forms in acidic pHs at 20°C

Fig. 5-5 presents the acid dissolution rates of amorphous hydrous ferric oxides, which were aged for 1 and 3 hr and 1, 3 and 7 days at 20°C, at pH 2.91 (by adding 1.25 ml conc. acetic acid to 250 ml seawater). The rates decreased rapidly with aging time and did not obey the first-order reaction in proportion to the concentration of particulate Fe(III) different from those of γ-FeOOH (Chapter 3), $Fe_5O_7(OH).4H_2O$ and α-FeOOH as described below. This probably results from the slowly and partly conversion of the fleshly precipitated active amorphous phase to the stable phase by aging (Crosby et al., 1983; Wells et al., 1983; Wells and Mayer, 1991). The each dissolution rate of amorphous phase, on aging for 1 day at 20°C, within pH range 2.67-3.82 at 20°C was closely a first-order reaction at early dissolution stage from 5 to 30 min (Fig. 5-6). The dissolution rate constants, k_2, determined from the slopes at early stage are presented in Table 5-2. Within this pH range, log k_2 increases linearly with an increase in the activity of the hydrogen ion and is fitted by a line whose slope corresponds to nH^+=-1.3±0.1 (Fig. 5-7). The nH^+ value within the pH range 2.67-6.80 was also calculated to be -0.96±0.03 from a plot of log k_2 vs. pH (Fig. 5-8) obtained by the dialysis (pH 6.01-6.80) and filtration data (pH 2.67-3.82). The data at pH 5.50 and 5.75 in the dialysis experiments turn aside from the line with nH^+=-0.96. This result indicates that the inactive amorphous and/or stable crystalline phases by conversion of active amorphous phase may have been dominant at lower pH in the

dialysis experiments (pH 5.50-8.06) and their nH^+ values may be lower than that of active phase.

The iron dissolution rates of $Fe_5O_7(OH).4H_2O$ and α-FeOOH as well as γ-FeOOH (Chapter 2) were a first-order reaction in proportion to the particulate Fe(III) concentration. Fig. 5-9 and Table 5-3 present the dissolution rates of $Fe_5O_7(OH).4H_2O$ in seawater at several acidic pHs at 20°C and the dissolution rate constants, k_2, calculated from the slopes of ln [Fe(III)p] vs. min (Fig. 5-9), respectively. Within this pH range 1.02-2.35, log k_2 increases linearly with an increase in the activity of the hydrogen ion whose slope corresponds to nH^+=-0.64±0.04 (Fig. 5-10). Fig. 5-11 and Table 5-4 present the dissolution rates of α-FeOOH and the rate constants, respectively. The log k_2 also increases linearly with an decrease of pH, within pH range -0.05 to 0.97, with nH^+=-0.38±0.04, while the log k_2 at pH -0.21 was extremely large probably because of the formation of Fe(III)-Cl complex resulting in accelerating dissolution (Fig. 5-12). The dissolution reaction in high concentration of HCl is considered to involve the rapid establishment of equilibrium between α-FeOOH surface and chloride ion which adsorbs from solution, followed by a rate determining reaction between a proton and the surface Fe(III)-Cl complex (Cornell et al., 1976).

On the assumption that the dissolution rate constants in the pH range 7.0-8.0 is independent of pH as shown in the dialysis data of amorphous phase and γ-FeOOH (Chapter 2 and 3), the rate constants of ferric oxides at pH 7.0 were estimated by extrapolating the lines of log k_2 vs. pH to pH 7.0 (Fig. 5-13). The dissolution rate constants at pH 7.0 and

the -nH^+ values (Table 5-5) are in the order: amorphous hydrous ferric oxide > γ-FeOOH > $Fe_5O_7(OH).4H_2O$ > α-FeOOH, a sequence that must be the result of differences in the chemical composition and crystal structure of these ferric oxides. This order is in good agreement with that of dissolution rates for several ferric oxides in 0.5 N HCl at 25°C (Sidhu et al., 1981). γ-FeOOH has a more open structure than α-FeOOH, which is probably the most stable ferric oxyhydroxide, and dissolves more rapidly. γ-FeOOH consists of corrugated sheets of $Fe(O, OH)_6$ octahedra held together only by hydrogen bonds. These bonds are probably readily disrupted by proton attack, leading to the formation of holes at the edges of the crystals (Cornell and Giovanoli, 1988).

(2) Effect of temperature on dissolution rates of several ferric oxides

The dissolution rates of amorphous phase, γ-FeOOH, $Fe_5O_7(OH).4H_2O$ and α-FeOOH were presented in Fig. 5-14, 3-12 (Chapter 3), 5-15 and 5-16, respectively. The dissolution rate of amorphous phase was closely a first-order reaction at early dissolution stage from 5 to 30 min because of the partly and slowly conversion of active amorphous phase to the inactive and/or stable crystalline phases (Stumm and Morgan, 1981; Crosby et al., 1983), while those of others obeyed first-order from 5 to 90 min at overall temperatures. The dissolution rate constant, k_2, at each temperature was calculated from each slope of ln [Fe(III)p] vs. min plot (Table 5-6). The relationship between rate constant and temperature is described by Arrhenius equation (Chapter 3) and then each activation energy, E, for the acid dissolution was calculated from

the slope of log k_2 vs. 1/T (Fig.5-17). The activation energies (Table 5-7) for the dissolution of these ferric oxides vary in the following order: α-FeOOH > $Fe_5O_7(OH).4H_2O$ > γ-FeOOH > amorphous hydrous ferric oxide. This order is consistent with that obtained by Sidhu et al. (1981). On the basis of activation energies alone, dissolution rates should vary in the reverse order. Actually, the dissolution rate constants were in the order: amorphous phase > γ-FeOOH > $Fe_5O_7(OH).4H_2O$ > α-FeOOH as described above. If each activation energy obtained for the acid dissolution is nearly the same at overall pH, we can estimate the dissolution rate constants at the different temperatures in the normal pH range of seawater, using the equation given below.

$$E=2.303R(\log k_a - \log k_b)/(1/T_b - 1/T_a)$$

where k_a and k_b are the dissolution rate constants at T_a and T_b, respectively.

5.4. Conclusions

The order of cell yield in the culture experiments in the presence of various ferric oxide forms is amorphous hydrous ferric oxide > γ-FeOOH >> $Fe_5O_7(OH).4H_2O$ > α-FeOOH, which is the same orders as the solubilities and dissolution rates of these ferric oxides in seawater. Because cell yield was especially less in cultures containing α-FeOOH or $Fe_5O_7(OH).4H_2O$ than those with amorphous phase, the thermodynamic stability may be important in controlling the supply of biologically

available iron. Since biologically available iron is believed to consist of ionic species in some mononuclear organic or inorganic complexed form (Anderson and Morel, 1982), dissolution of colloidal ferric oxide must occur to provide biologically available iron. As the thermodynamic stability of the ferric oxide colloid increases, the activation energy required for dissolution increases. On the basis of the activation energies alone, the dissolution rates should vary in the reverse order. In fact, the activation energies reguired for the acid dissolution of various ferric oxides were in the order: α-FeOOH > $Fe_5O_7(OH).4H_2O$ > γ-FeOOH > amorphous phase. Therefore, an increase in the thermodynamic stability may reduce the dissolution rate and hence the supply of biologically available iron.

Table 5-1. The observed X-ray diffraction lines compared to that of α-FeOOH.

line No.	Observed XRD lines intensity (obs.) (I/Io) x100	d(obs.) Å	ASTM No. 17-536 (α-FeOOH) d(ref.) Å	intensity (ref.) (I/Io) x100	(h k l)
1	15	5.03	4.93	10	0 2 0
2	100	4.20	4.18	100	1 1 0
3	10	3.38	3.38	10	1 2 0
4	43	2.69	2.69	30	1 3 0
5	30	2.58	2.58	8	0 2 1
6	13	2.52	2.52	4	1 0 1
	----	----	2.490	16	0 4 0
7	93	2.45	2.452	25	1 1 1
8	26	2.25	2.252	10	1 2 1
9	29	2.19	2.192	20	1 4 0
10	4	2.01	2.009	2	1 3 1
11	8	1.92	1.920	6	0 4 1
12	11	1.80	1.799	8	2 1 1
13	4	1.77	1.770	2	1 4 1
14	36	1.72	1.721	20	2 2 1
15	12	1.69	1.694	10	2 4 0
16	4	1.66	1.661	4	0 6 0
17	8	1.60	1.606	6	2 3 1
18	24	1.56	1.564	16	1 5 1, 1 6 0
19	23	1.51	1.509	10	2 5 0, 0 0 2

Crystal system of α-FeOOH: orthorhombic (a=4.596, b=9.957, c=3.021)

Table 5-2. Iron dissolution rate constants of amorphous hydrous ferric oxides, aged for 1 day at 20°C, in seawater at 20°C by adding acetic acid.

pH	Dissolution rate constant (k_2)		
	min^{-1}	day^{-1}	r^2
(a) filtration experiment			
2.67	0.104±0.008	150±11	0.99
2.91	0.054±0.008	77±11	0.96
3.26	0.028±0.002	40±3	0.99
3.54	0.0090±0.0007	13±1	0.99
3.82	0.0032±0.0003	4.6±0.4	0.98
(b) dialysis experiment (Chapter 2)			
5.50	--------	$8.19\pm0.32\times10^{-2}$	0.98
5.75	--------	$6.26\pm0.16\times10^{-2}$	0.99
6.01	--------	$5.72\pm0.42\times10^{-2}$	0.94
6.25	--------	$4.29\pm0.34\times10^{-2}$	0.93
6.50	--------	$2.25\pm0.15\times10^{-2}$	0.95
6.50	--------	$2.86\pm0.14\times10^{-2}$	0.97
6.80	--------	$1.58\pm0.10\times10^{-2}$	0.96
7.57	--------	$1.61\pm0.22\times10^{-2}$	0.82
8.06	--------	$1.33\pm0.20\times10^{-2}$	0.79

The error values of dissolution rate constant at each pH were estimated from the standard deviations of the slope obtained by using a least-squares linear regression of the filtration data (pH 2.67-3.82) from 5 to 30 min (Fig. 5-6) and the dialysis data (pH 5.50-8.06) in Chapter 2.

Table 5-3. Iron dissolution rate constants of $Fe_5O_7(OH).4H_2O$ in seawater at 20°C by adding acetic acid or HCl.

pH	Dissolution rate constant (k_2)		
	min^{-1}	day^{-1}	r^2
1.02 (0.1 N HCl)	0.0153±0.0007	22.0±1.0	0.99
1.37 (0.05 N HCl)	0.0095±0.0002	13.7±0.3	1.00
1.73	0.0065±0.0001	9.4±0.1	1.00
2.04	0.0038±0.0001	5.5±0.1	0.99
2.35	0.0021±0.0001	3.02±0.15	0.99

The error values of dissolution rate constant at each pH were estimated from the standard deviations of the slope obtained by using a least-squares linear regression of the filtration data from 5 to 90 min (Fig. 5-9).

Table 5-4. Iron dissolution rate constants of α-FeOOH in seawater at 20°C by adding HCl.

pH		Dissolution rate constant (k_2) day^{-1}	r^2
-0.21	(2N HCl)	0.1531±0.0038	1.00
-0.05	(0.96 N HCl)	0.0261±0.0021	0.96
0.29	(0.48 N HCl)	0.0175±0.0022	0.92
0.59	(0.24 N HCl)	0.0151±0.0019	0.93
0.97	(0.1 N HCl)	0.0103±0.0014	0.92

The error values of dissolution rate constant at each pH were estimated from the standard deviations of the slope obtained by using a least-squares linear regression of the filtration data from 3 hr to 6 day (Fig. 5-11).

Table 5-5. The nH^+ values and the estimated dissolution rate constants of ferric oxides at pH 7.0.

Material	nH^+ (r^2)	Dissolution rate constant k_2 a) day^{-1}	k_2 b) day^{-1}
amorphous	-0.96±0.03 (0.99) c)	0.0080 c)	0.015±0.002
γ-FeOOH	-0.80±0.02 (1.00) c)	0.0065 c)	0.005±0.001
$Fe_5O_7(OH).4H_2O$	-0.64±0.04 (0.99)	0.0036	-------
α-FeOOH	-0.38±0.04 (0.98)	0.000052	-------

The nH^+ values of amorphous and γ-FeOOH were calculated from filtration and dialysis data, while those of $Fe_5O_7(OH).4H_2O$ and α-FeOOH were only from filtration data. a): k_2 obtained by extrapolating to pH 7.0, b): average k_2 obtained by dialysis data (at pH 6.80-8.06 for amorphous and pH 7.00-8.20 for γ-FeOOH), c) values estimated from both filtration and dialysis data.

Table 5-6. Iron dissolution rate constants of amorphous hydrous ferric oxide (pH 3.26), γ-FeOOH (pH 2.60), $Fe_5O_7(OH).4H_2O$ (pH 1.02) and α-FeOOH (pH -0.21) in seawaters at various temperatures.

Temperature		amorphous	γ-FeOOH	$Fe_5O_7(OH).4H_2O$	α-FeOOH
°C	1/T (x1000)	(pH 3.26)	(pH 2.60)	(pH 1.02)	(pH -0.21)
		Dissolution rate constant (k_2), day^{-1} (r^2)			
2.5	3.6278	------	------	------	0.015±0.002 (0.92)
5	3.5952	20.6±0.2 (1.00)	7.3±0.1 (1.00)	5.7±0.2 (0.99)	------
10	3.5317	26.7±0.7 (1.00)	10.7±0.1 (1.00)	9.6±0.2 (0.99)	0.054±0.002 (0.99)
15	3.4704	27.8±1.6 (0.99)	17.4±0.3 (1.00)	15.6±0.2 (1.00)	------
20	3.4112	39.8±3.0 (0.99)	22.2±0.1 (1.00)	22.0±1.0 (0.99)	0.153±0.004 (1.00)
25	3.3540	------	30.2±1.0 (0.99)	31.3±1.4 (0.99)	------

The error values of dissolution rate constant at each temperature were estimated from the standard deviations of the slope obtained by using a least-squares linear regression of the filtration data from 5 to 30 min for amorphous hydrous ferric oxide and from 5 to 90 min for others (Fig. 3-12 and 5-14, 5-15 and 5-16, respectively).

Table 5-7. Activation energies for the dissolution of ferric oxides.

Material	Dissolution conditions	Activation energy kcal/mol	(r^2)
amorphous	pH 3.26 (acetic acid) 5, 10, 15 and 20°C	6.5±1.4	(0.92)
γ-FeOOH	pH 2.60 (acetic acid) 5, 10, 15, 20 and 25°C	11.8±0.7	(0.99)
$Fe_5O_7(OH).4H_2O$	pH 1.02 (HCl) 5, 10, 15, 20 and 25°C	14.0±0.6	(0.99)
α-FeOOH	pH -0.21 (HCl) 2.5, 10 and 20°C	21±3	(0.98)

The error values of activation energies were estimated from the standard deviations of the slopes by using a least-squares linear regression of the slope of log k_2 vs. 1/T plot (Fig. 5-17).

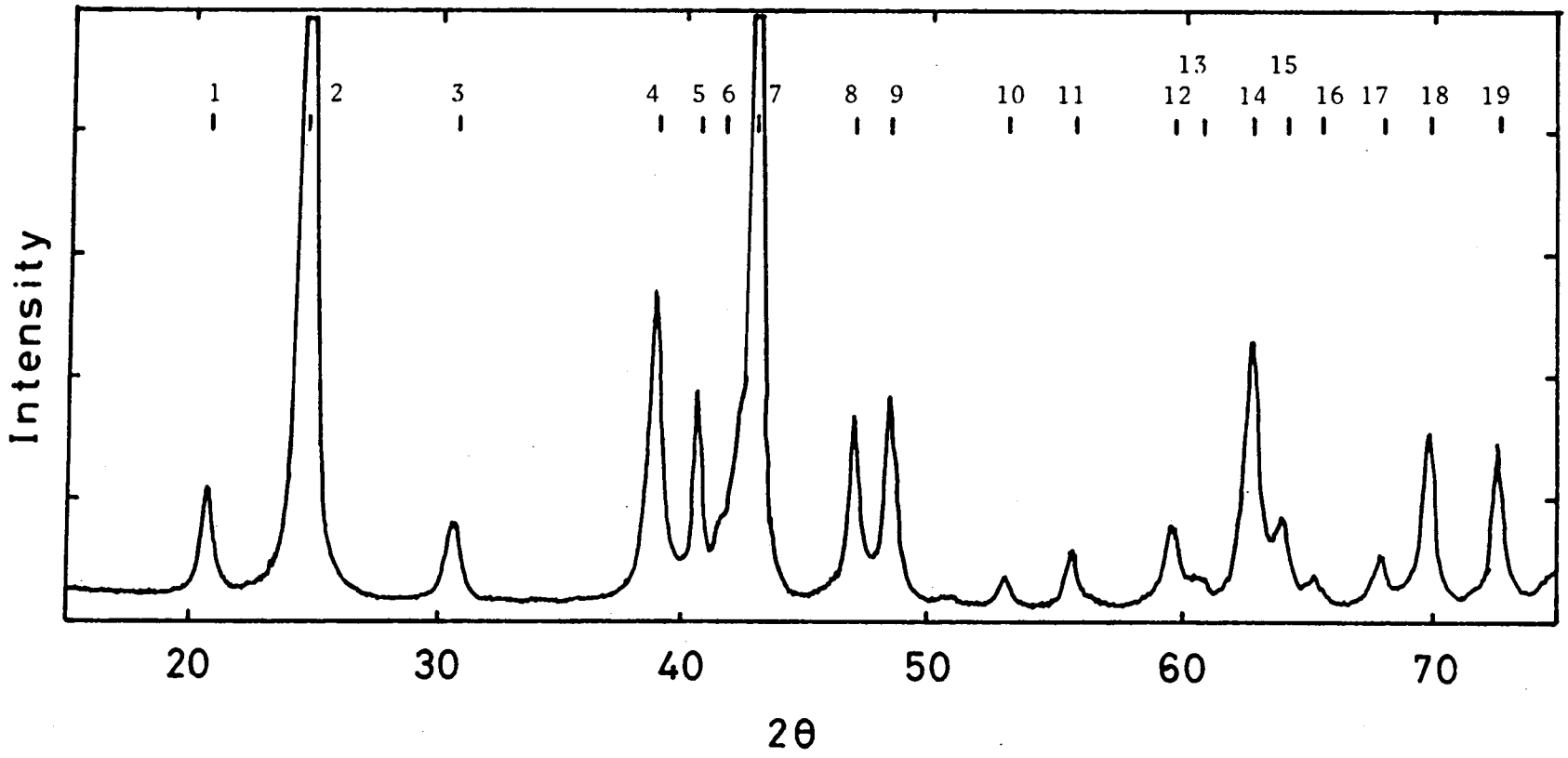

Fig. 5-1 X-ray diffractogram of iron oxyhydroxide defined as α-FeOOH (Table 5-1)

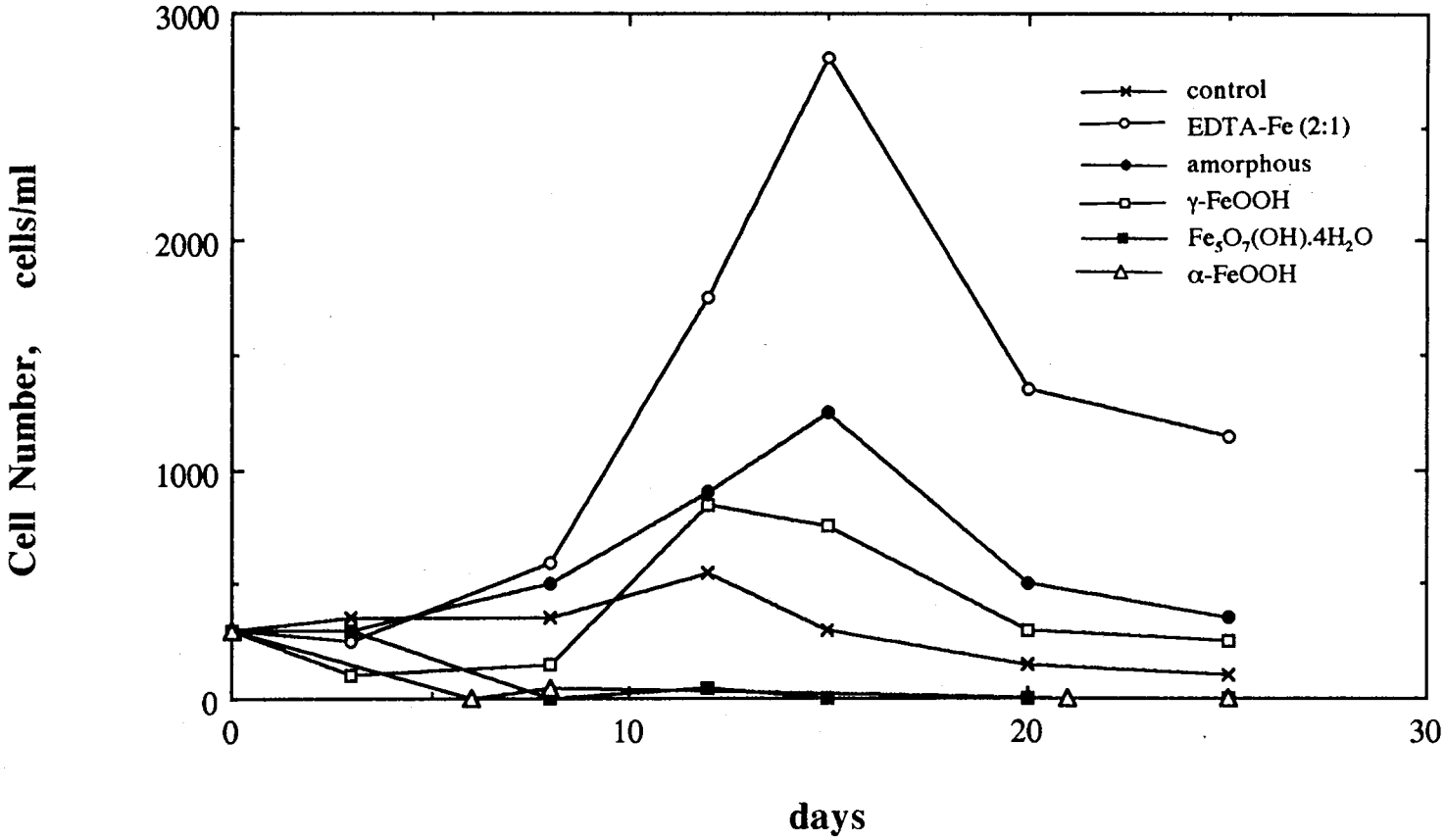

Fig. 5-2 Cell numbers of C. marina in cultures supplied with various ferric oxide forms

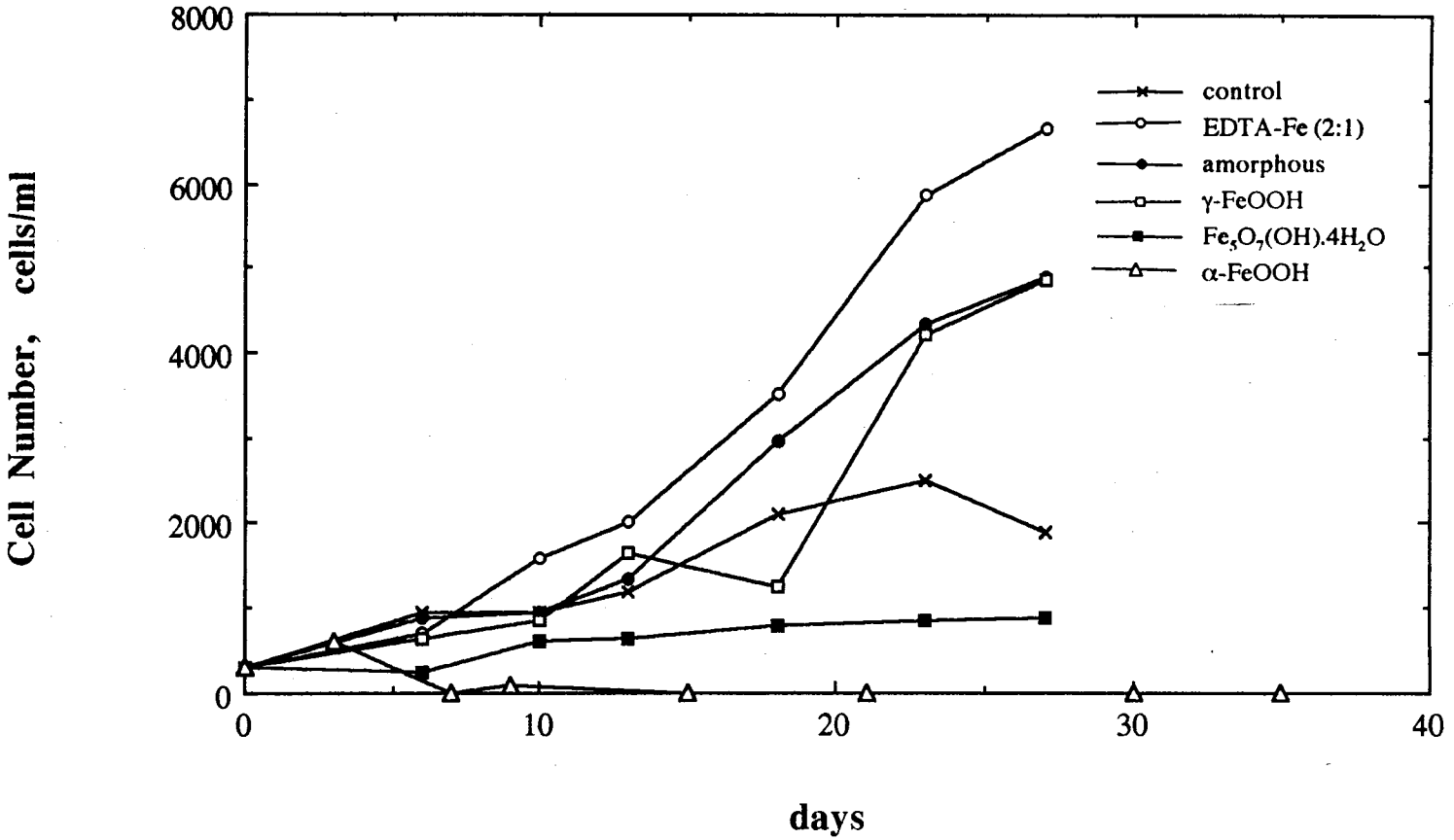

Fig. 5-3 Cell numbers of G. nagasakiense in cultures supplied with various ferric oxide forms

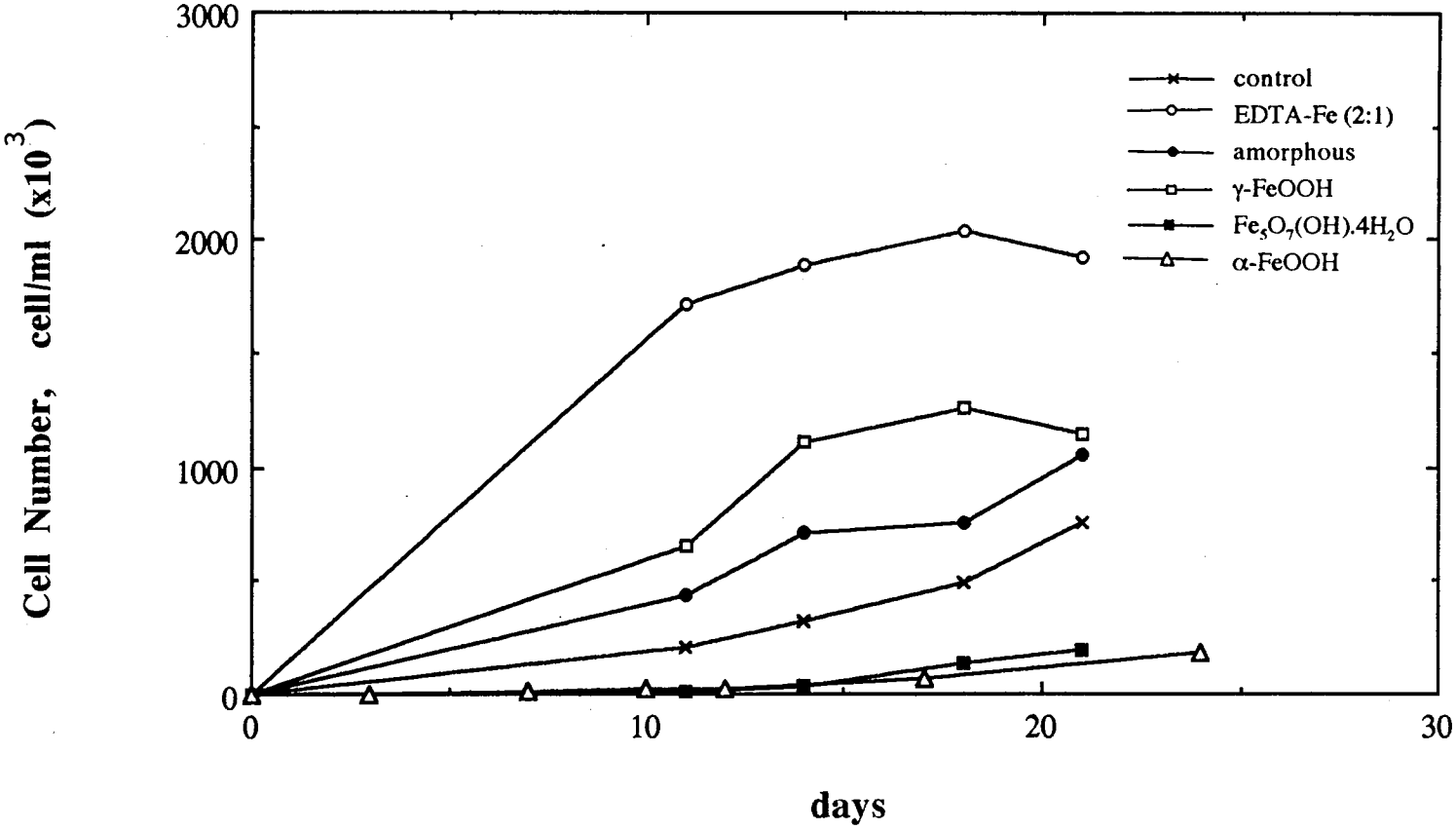

Fig. 5-4 Cell numbers of P. tricornutum in cultures supplied with various ferric oxide forms

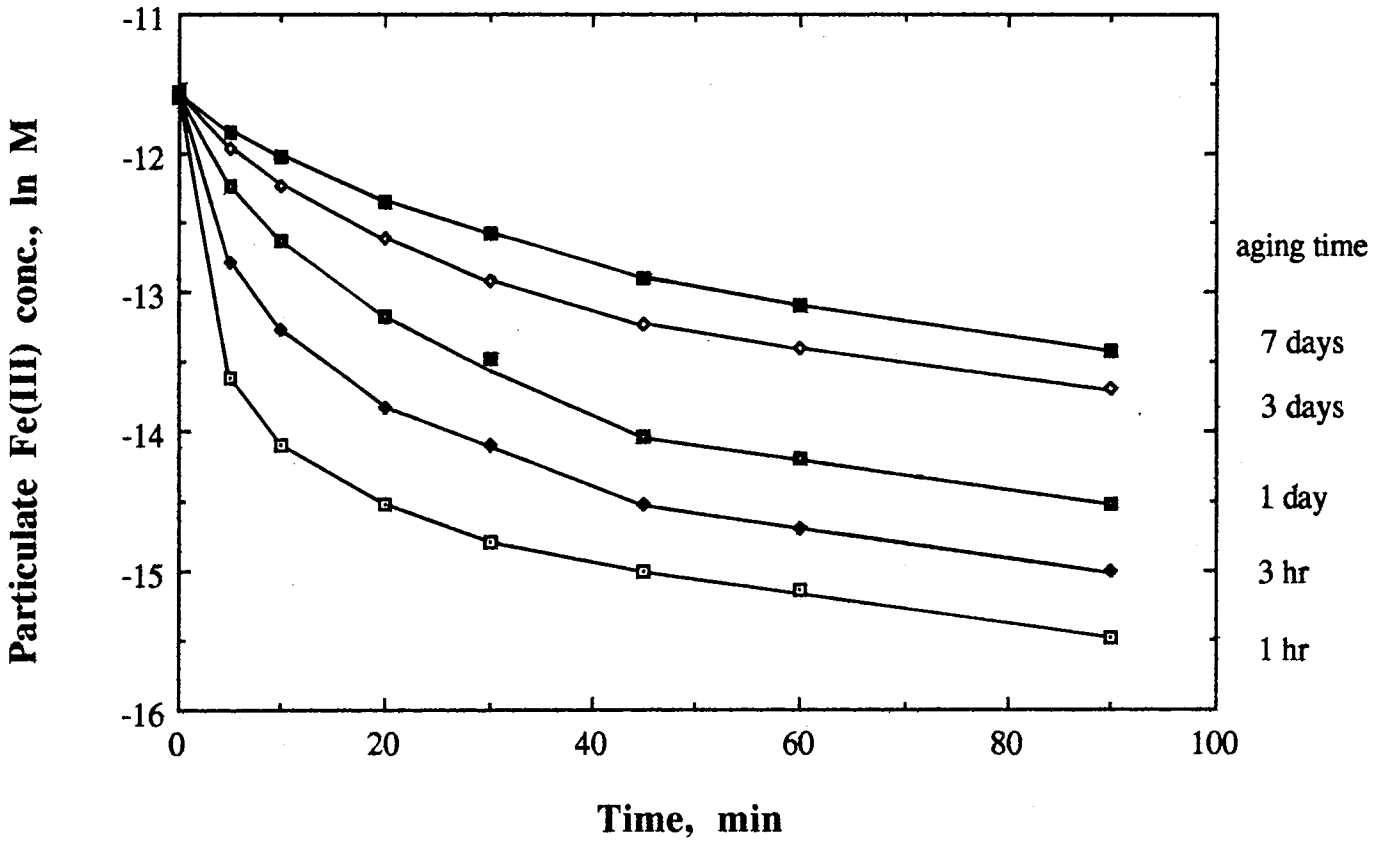

Fig. 5-5 Fe(III) dissolution rate of amorphous phase, aged for various time, in acidic seawater (pH 2.91) at 20°C obtained by filtration experiments

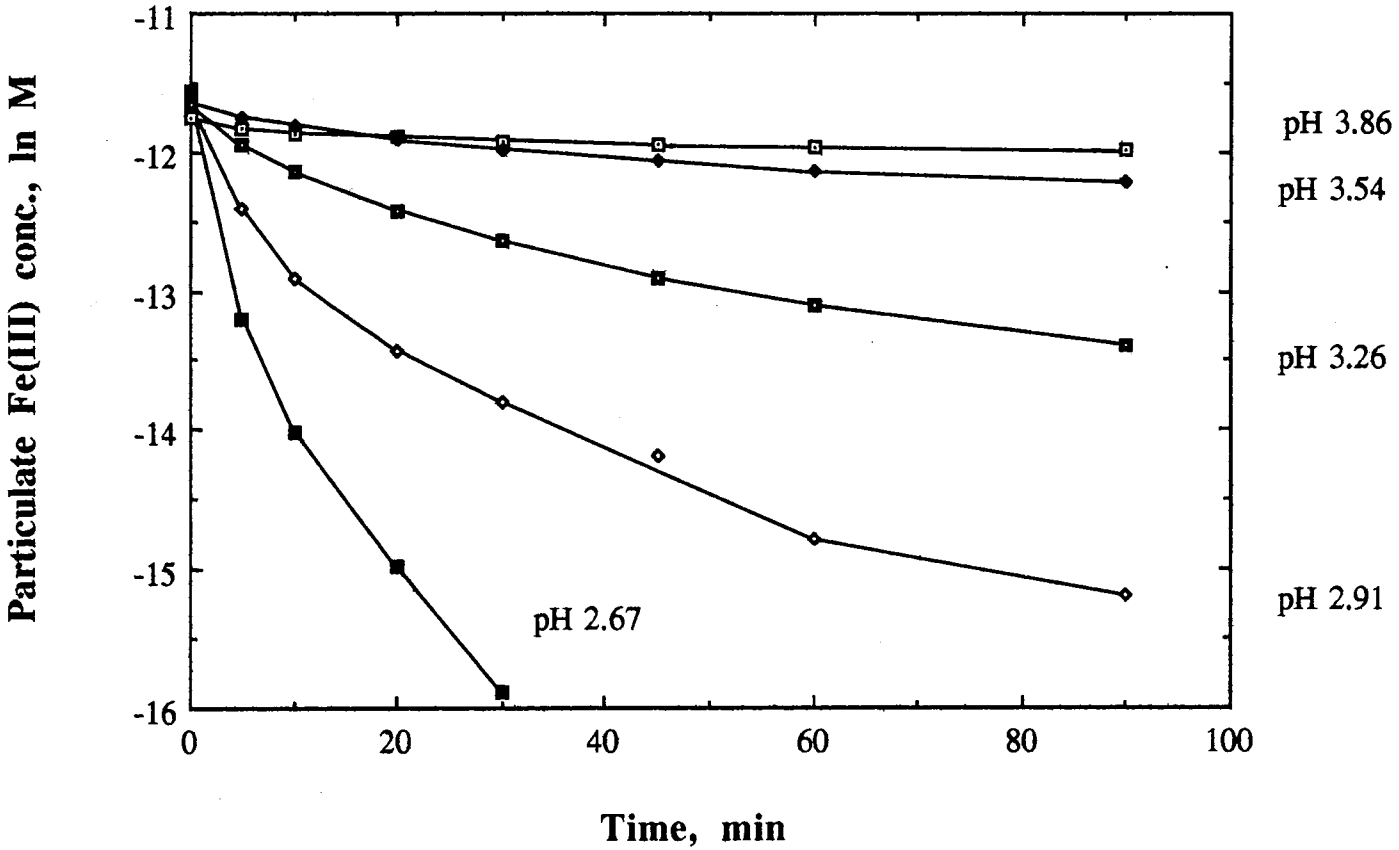

Fig. 5-6 Fe(III) dissolution rate of amorphous phase in seawater at various pH (20°C) obtained by filtration experiments

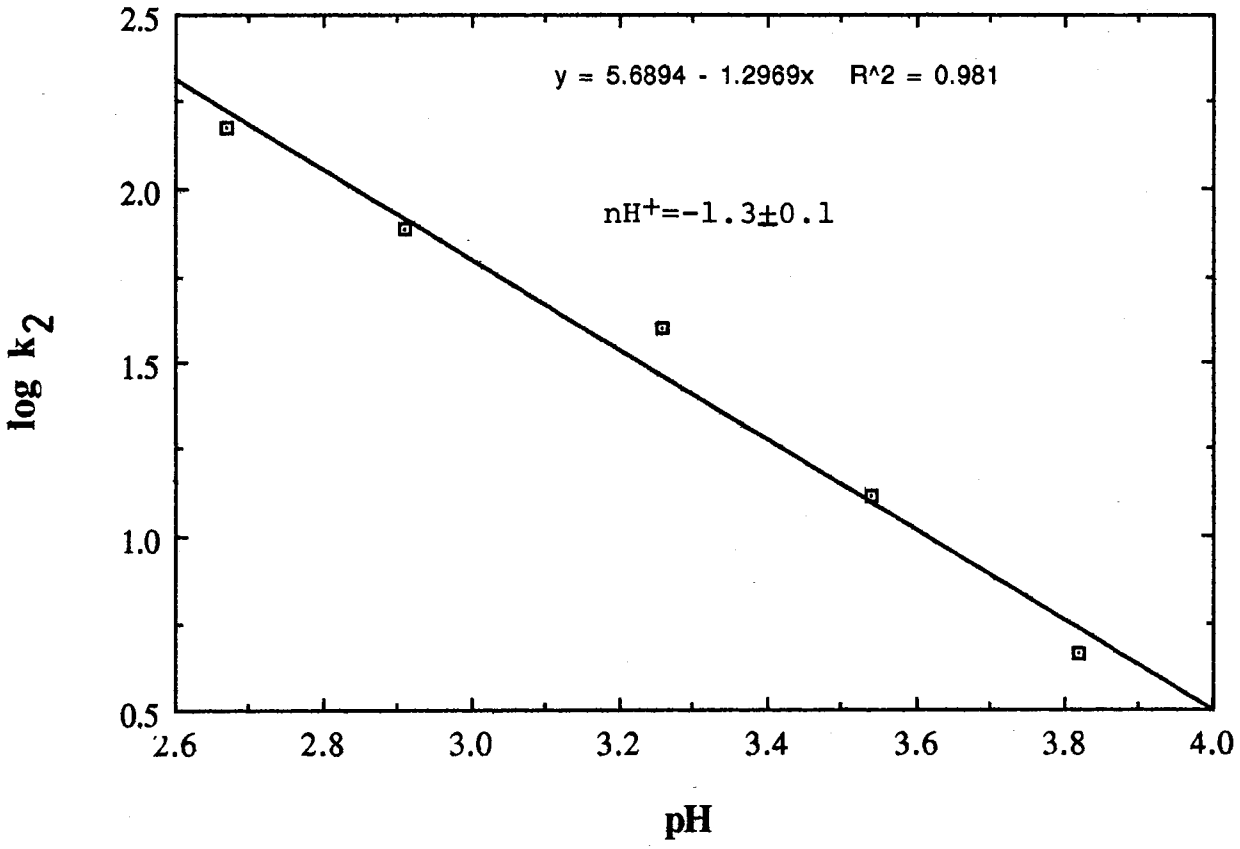

Fig. 5-7 Dissolution rate constant of amorphous phase vs. pH in seawater at 20°C

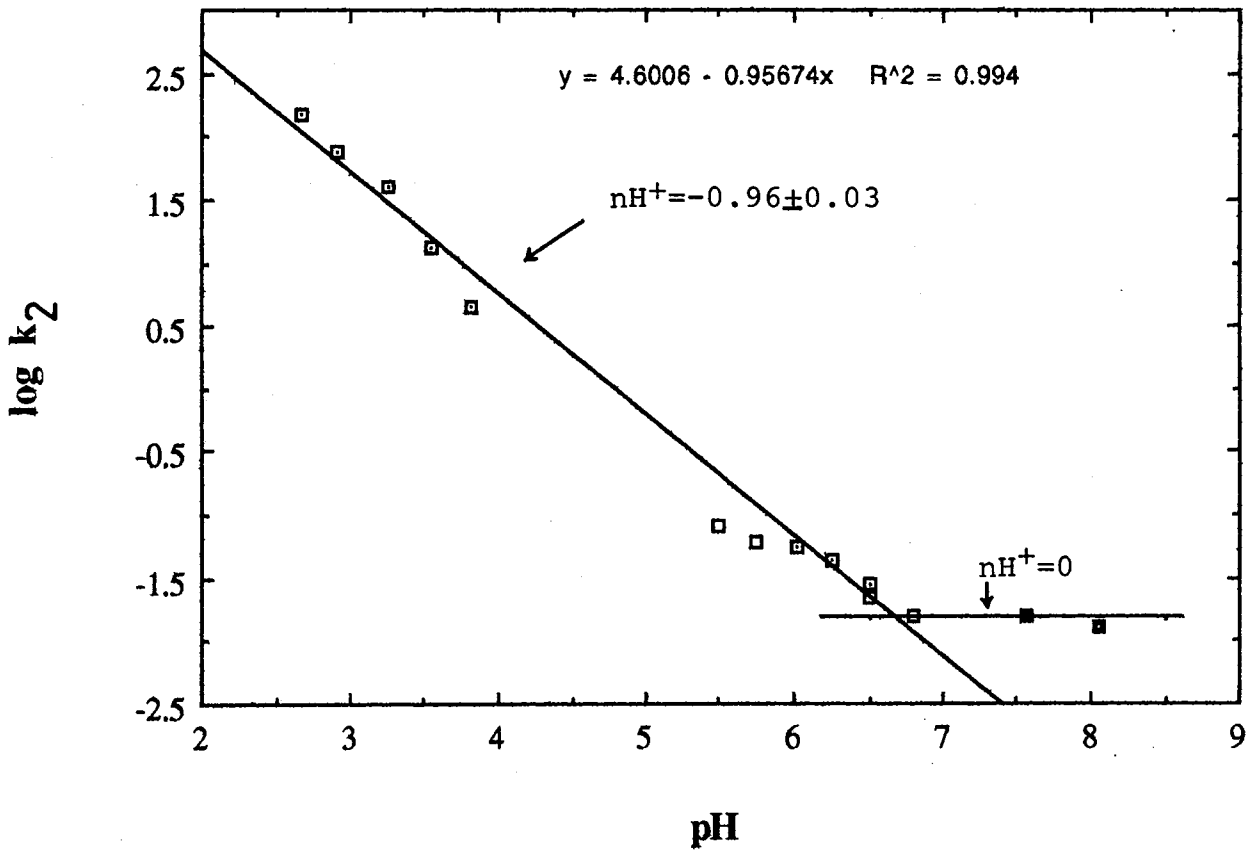

Fig. 5-8 Dissolution rate constant of amorphous phase vs. pH in seawater at 20°C obtained by filtration and dialysis experiments

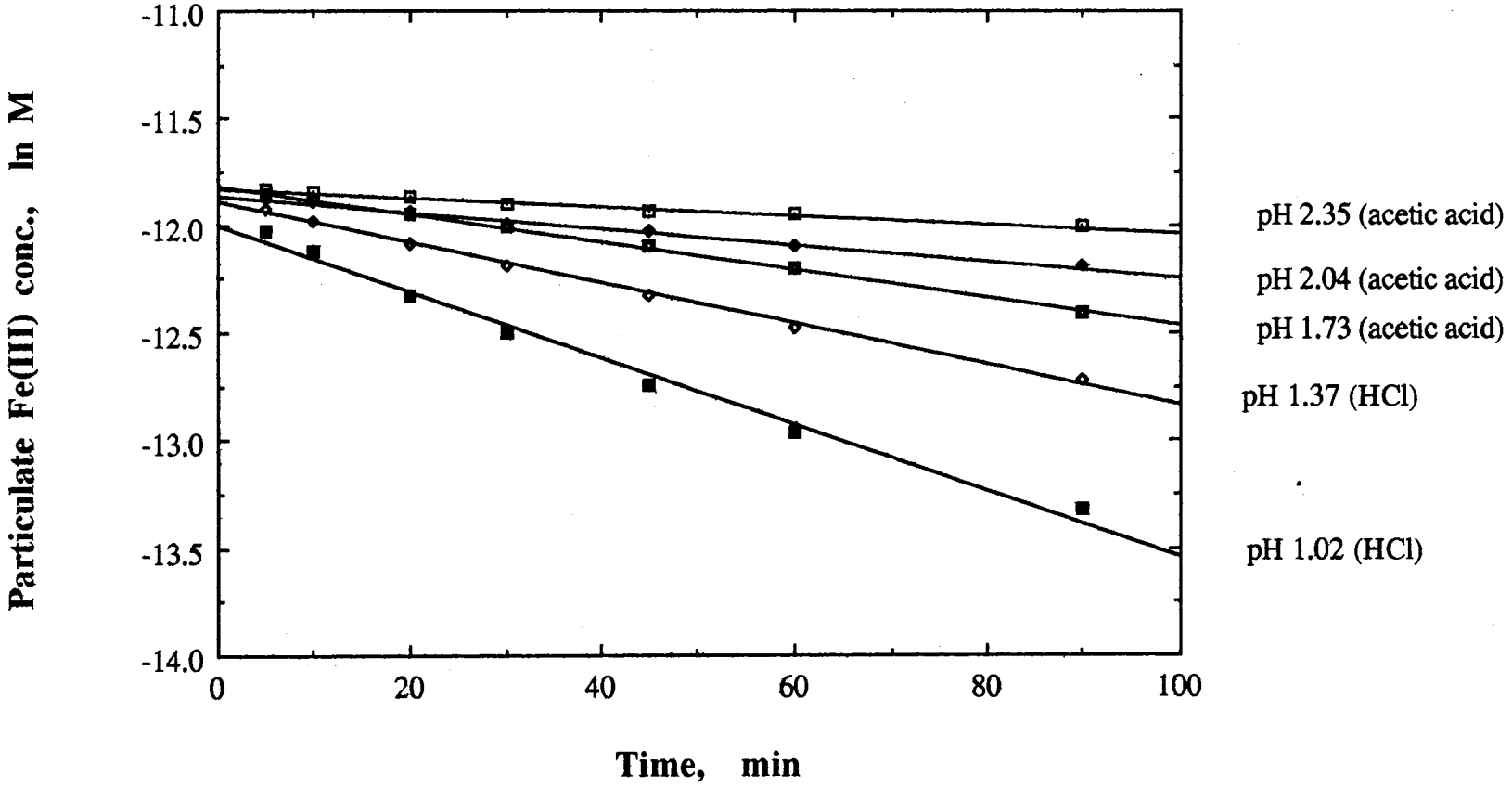

Fig. 5-9 Fe(III) dissolution rate of hydrated ferric oxyhydroxide polymer in seawater at various pH (20°C) obtained by filtration experiments

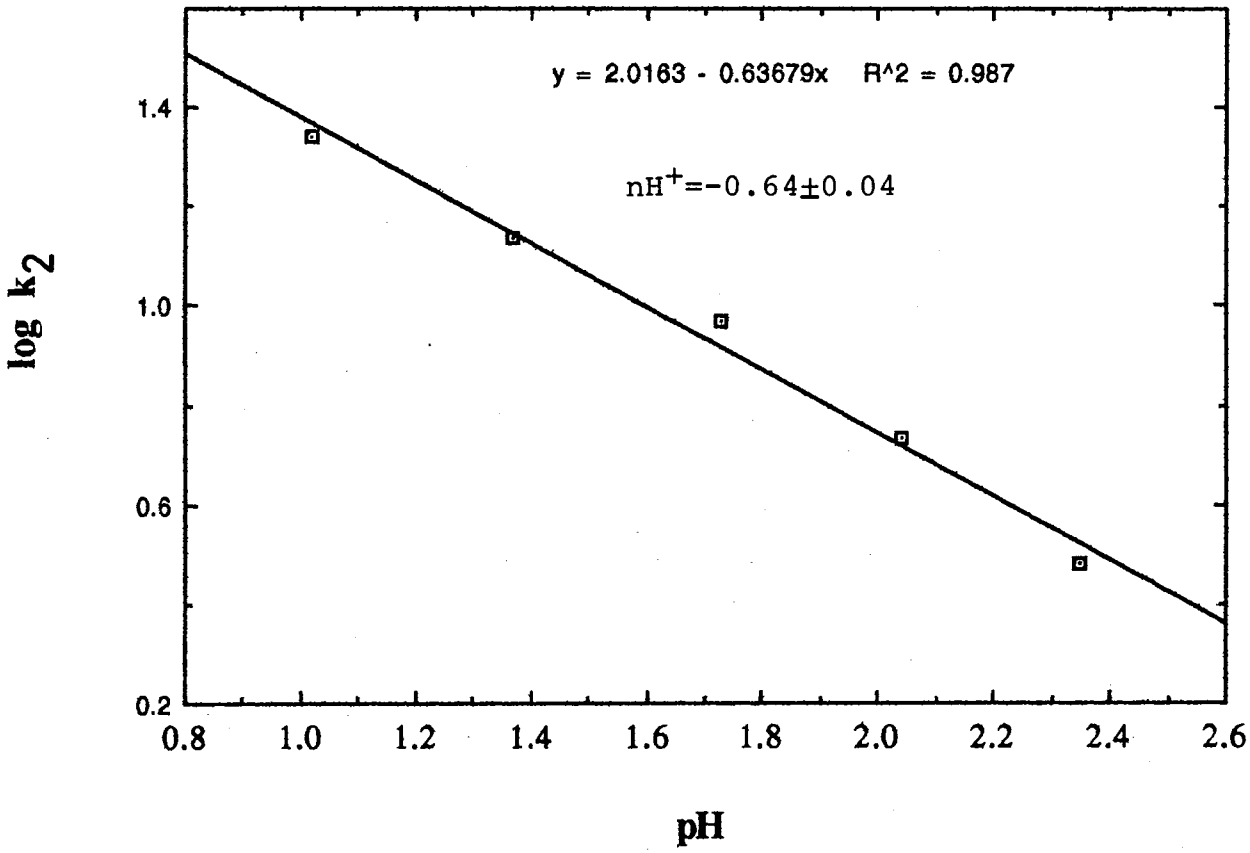

Fig. 5-10 Dissolution rate constant of hydrated ferric oxyhydroxide polymer vs. pH in seawater at 20°C obtained by filtration experiments

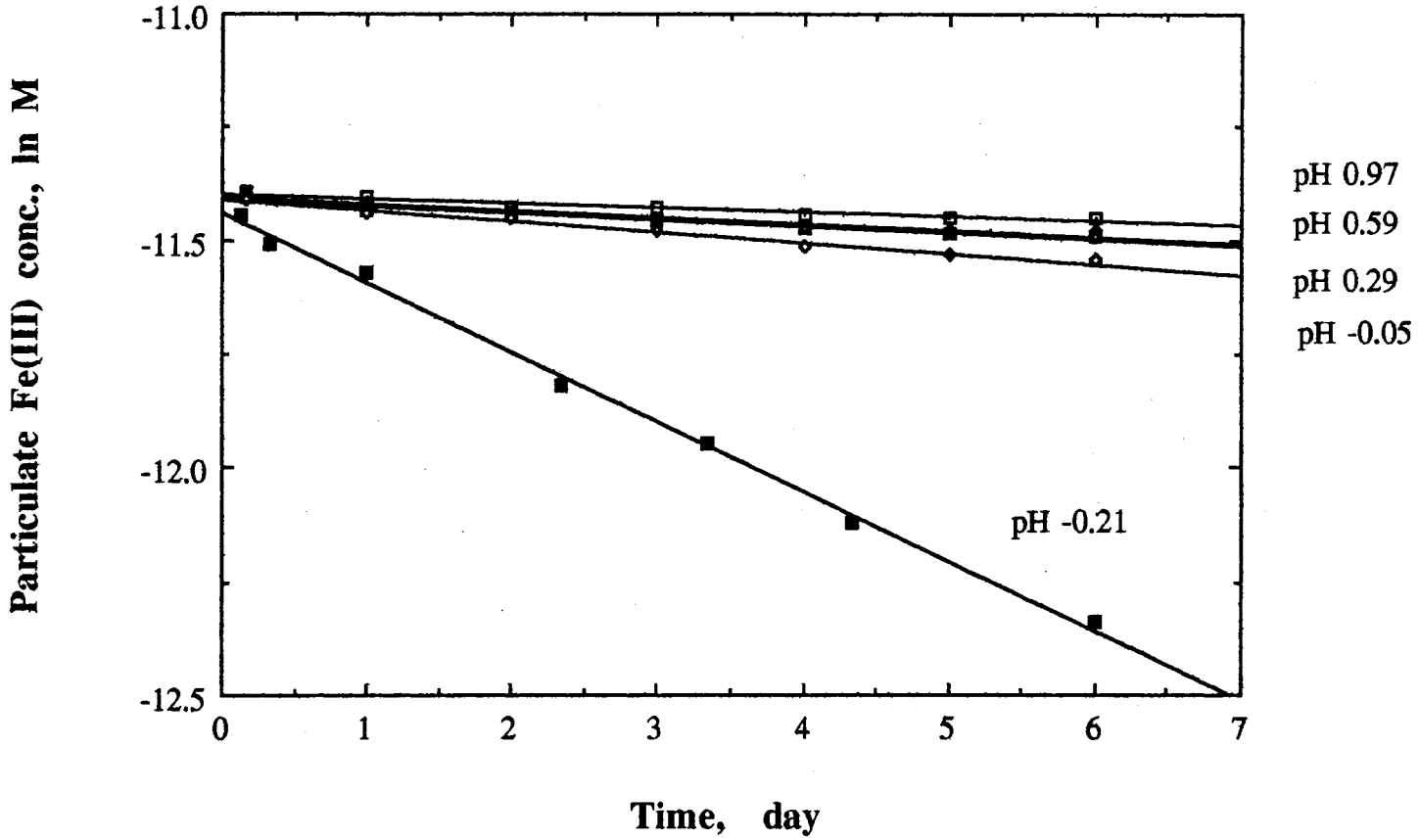

Fig. 5-11 Fe(III) dissolution rate of a-FeOOH in seawater (20°C) at various pH obtained by filtration experiments

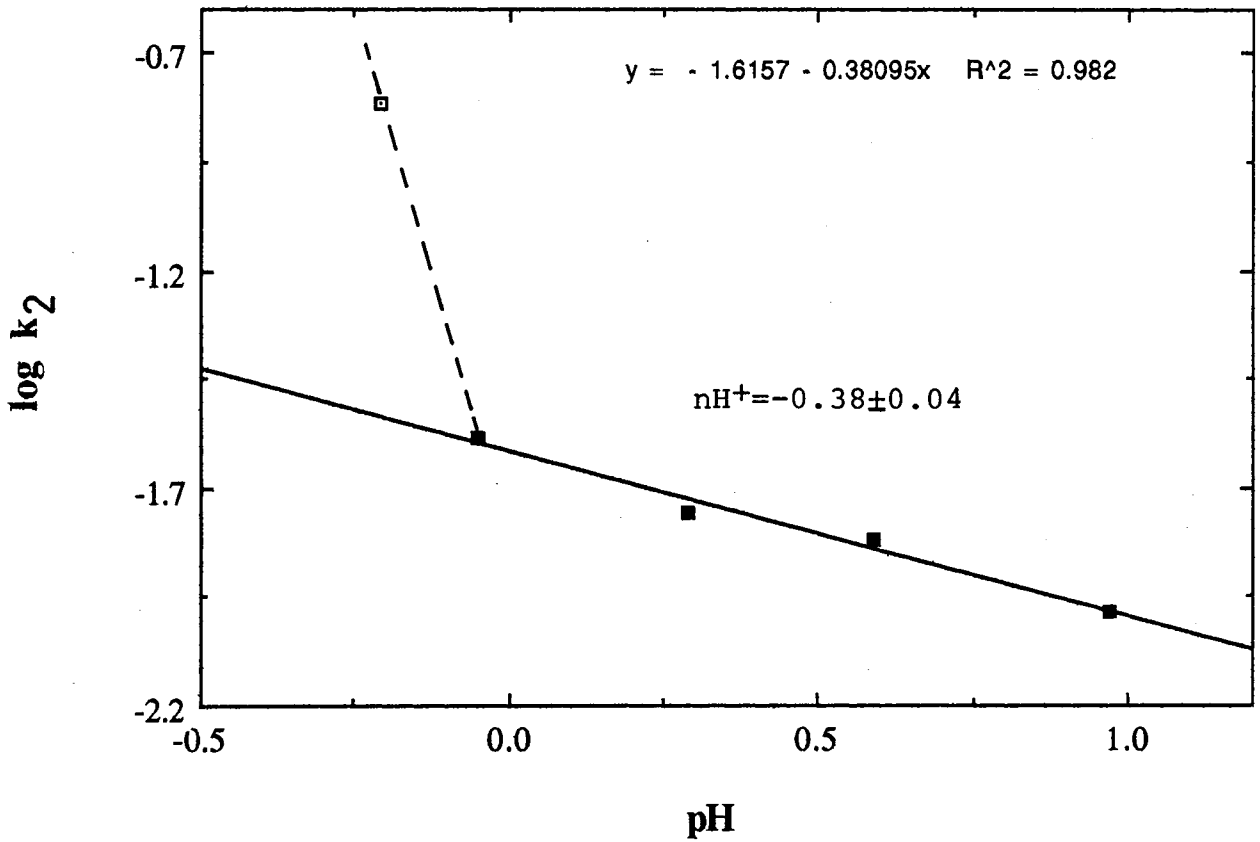

Fig. 5-12 Dissolution rate constant of a-FeOOH vs. pH in seawater at 20°C obtained by filtration experiments

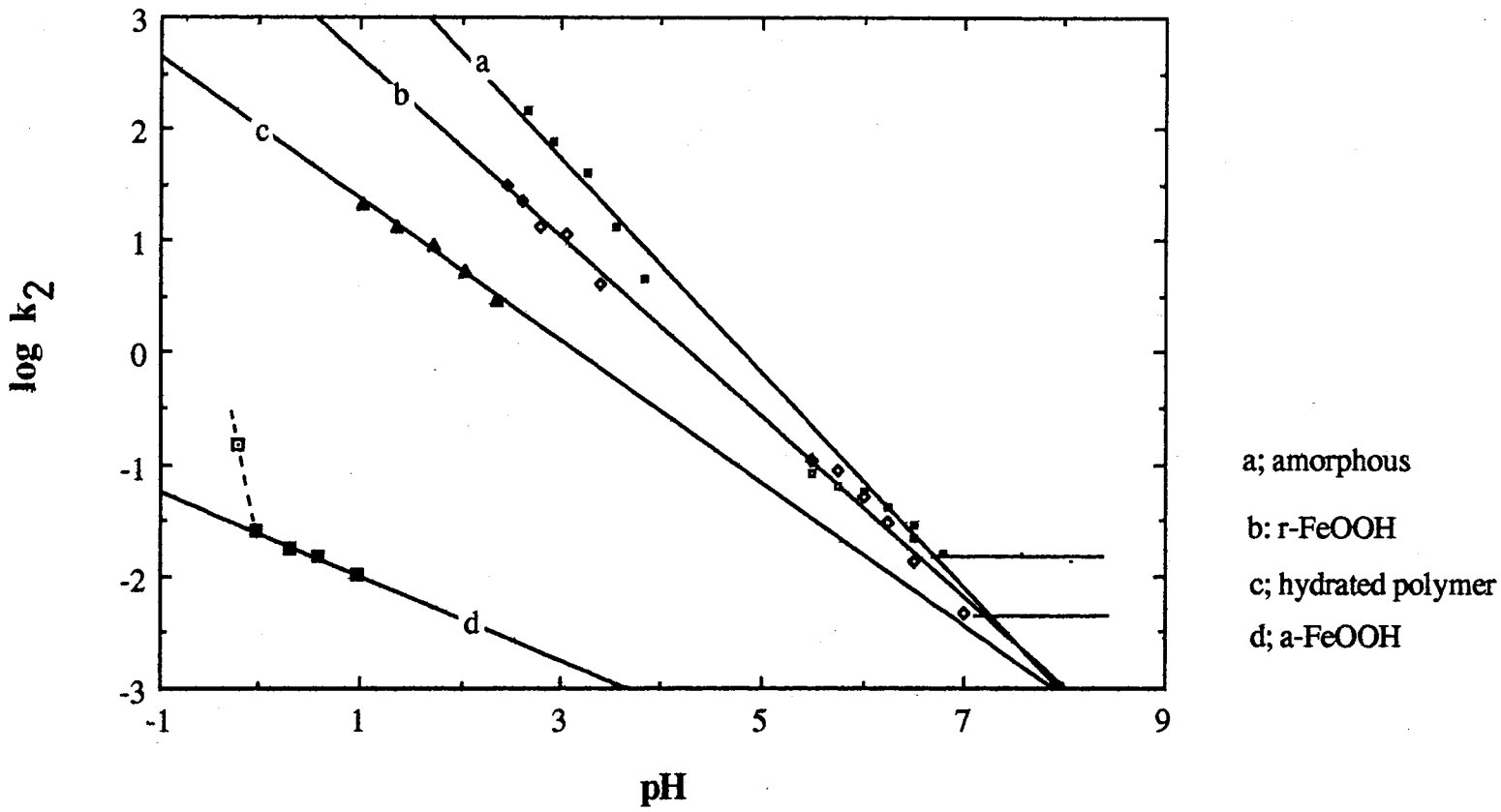

Fig. 5-13 Dissolution rate constant vs. pH in seawater at 20°C obtained by filtration and/or dialysis experiments

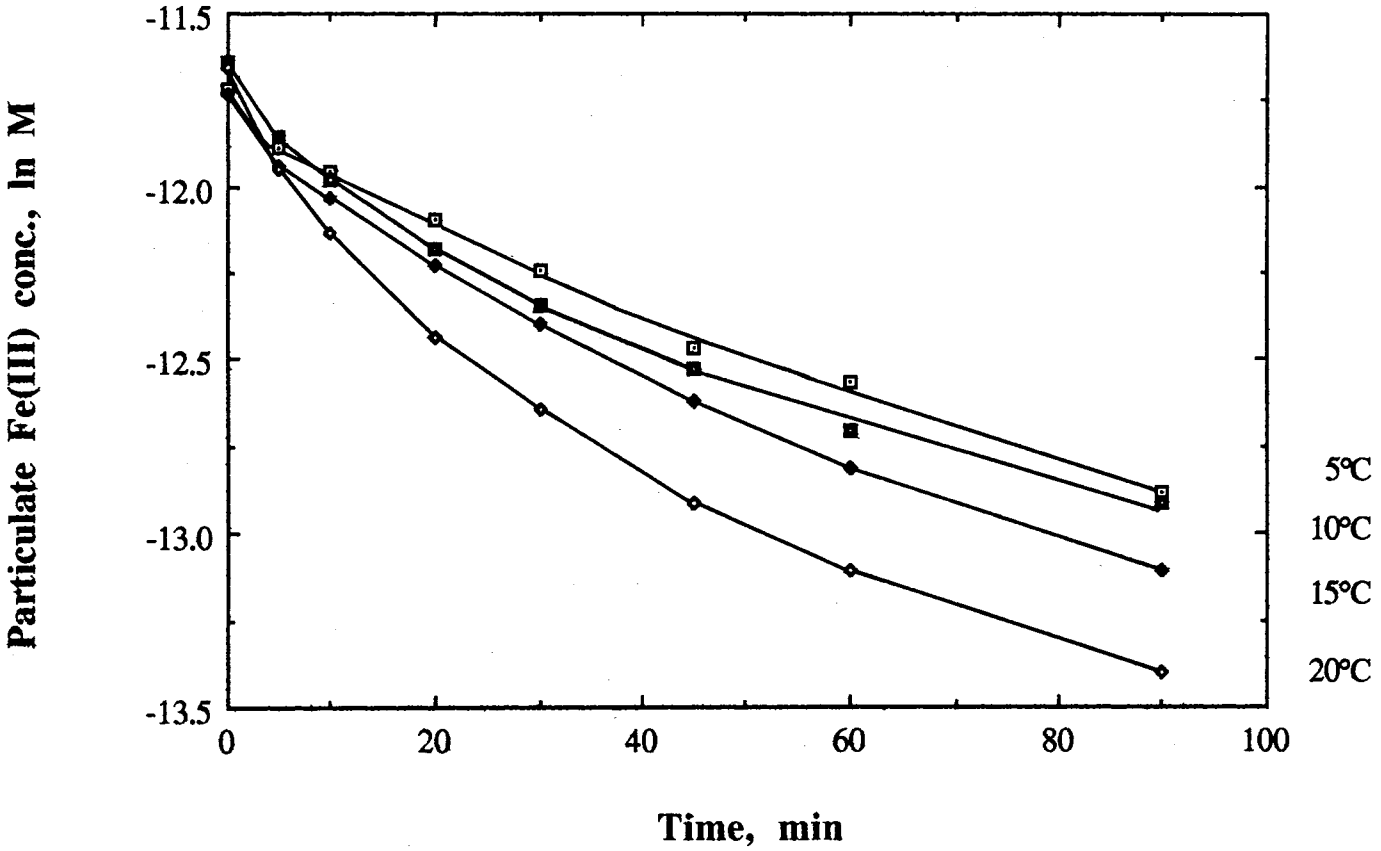

Fig. 5-14 Fe(III) dissolution rate of amorphous phase in seawater (pH 3.26) at various temp. obtained by filtration experiments

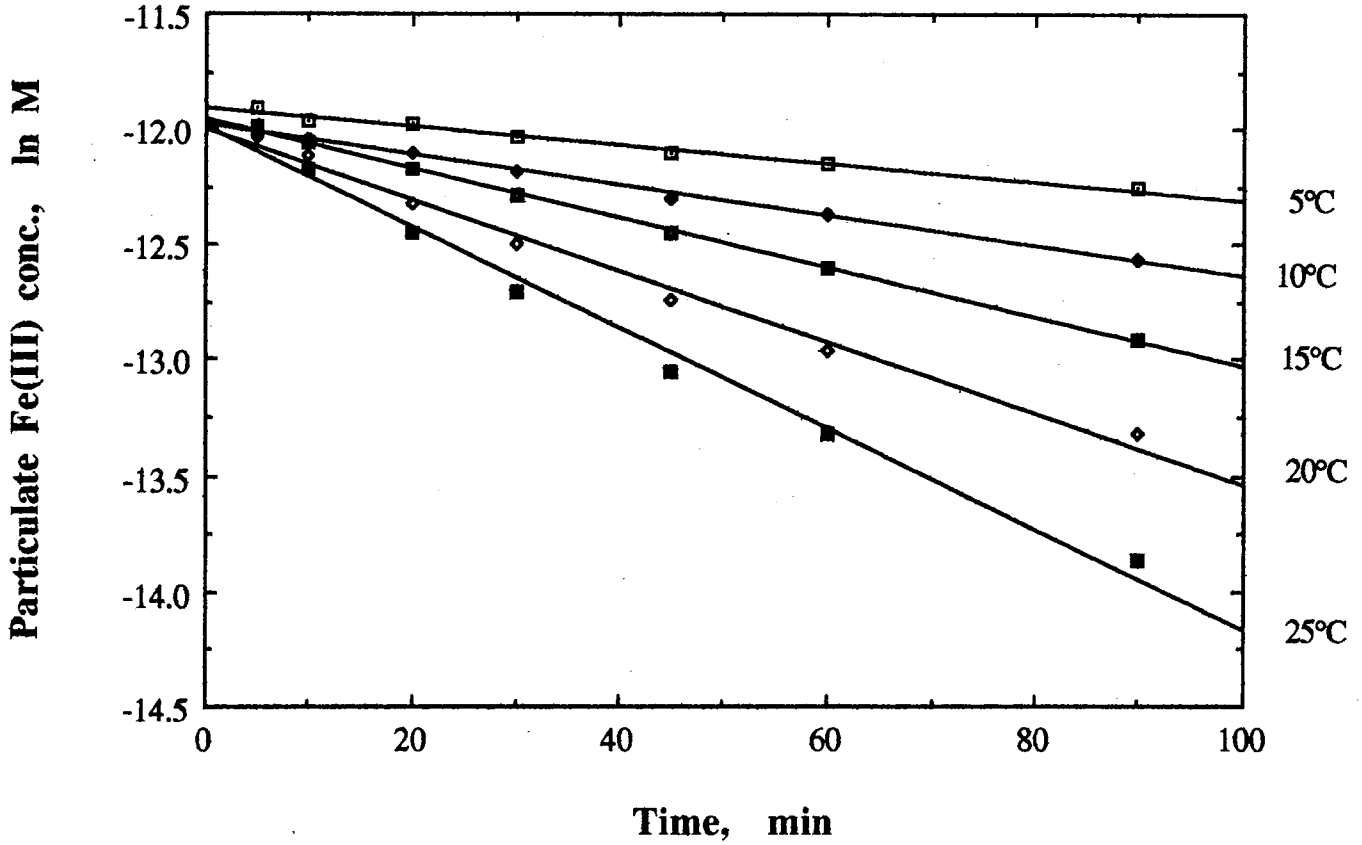

Fig. 5-15 Fe(III) dissolution rate of hydrated ferric oxyhydroxide polymer in seawater (pH 1.02) at various temp. obtained by filtration experiments

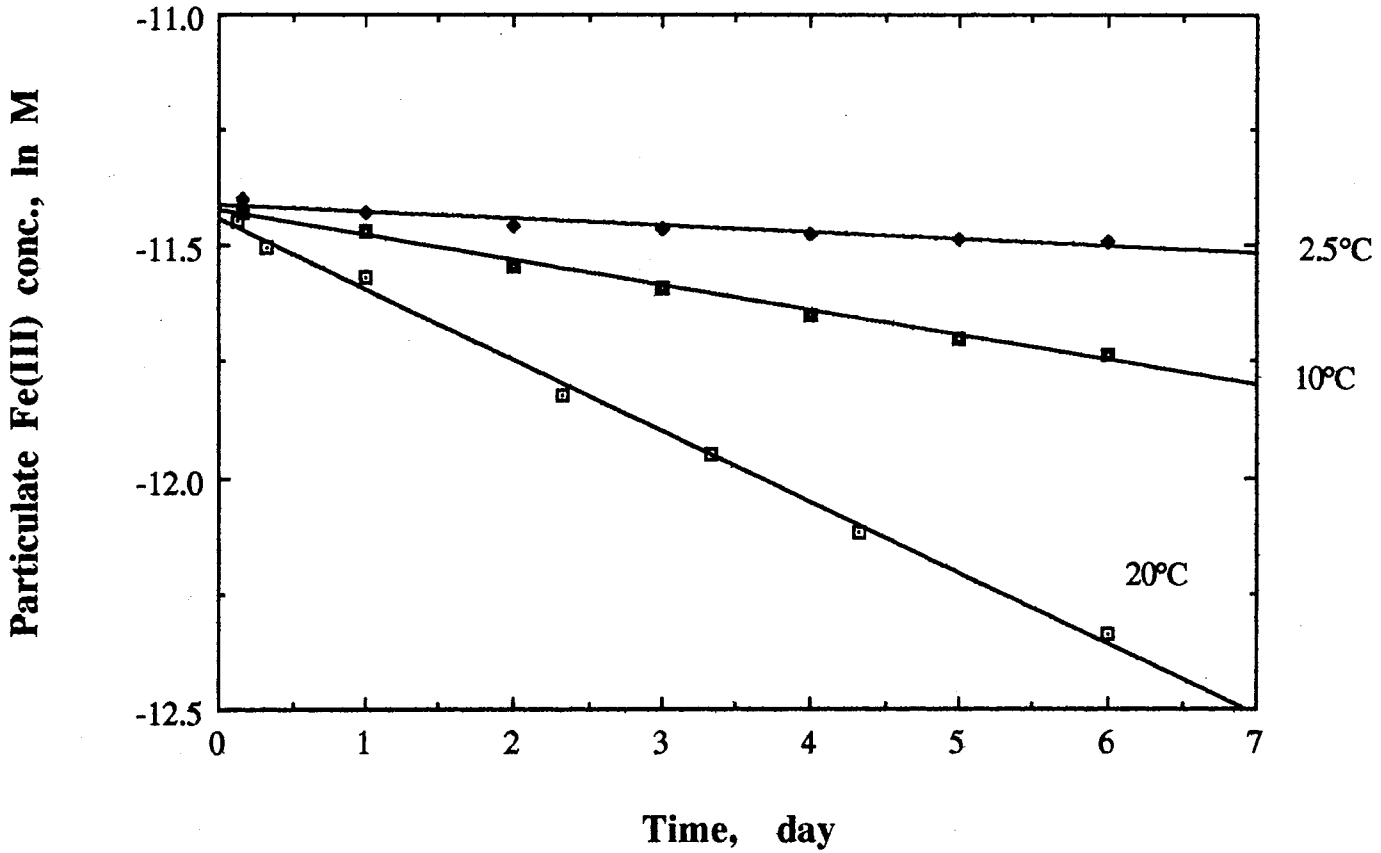

Fig. 5-16 Fe(III) dissolution rate of a-FeOOH in seawater (pH -0.21) at various temp. obtained by filtration experiments

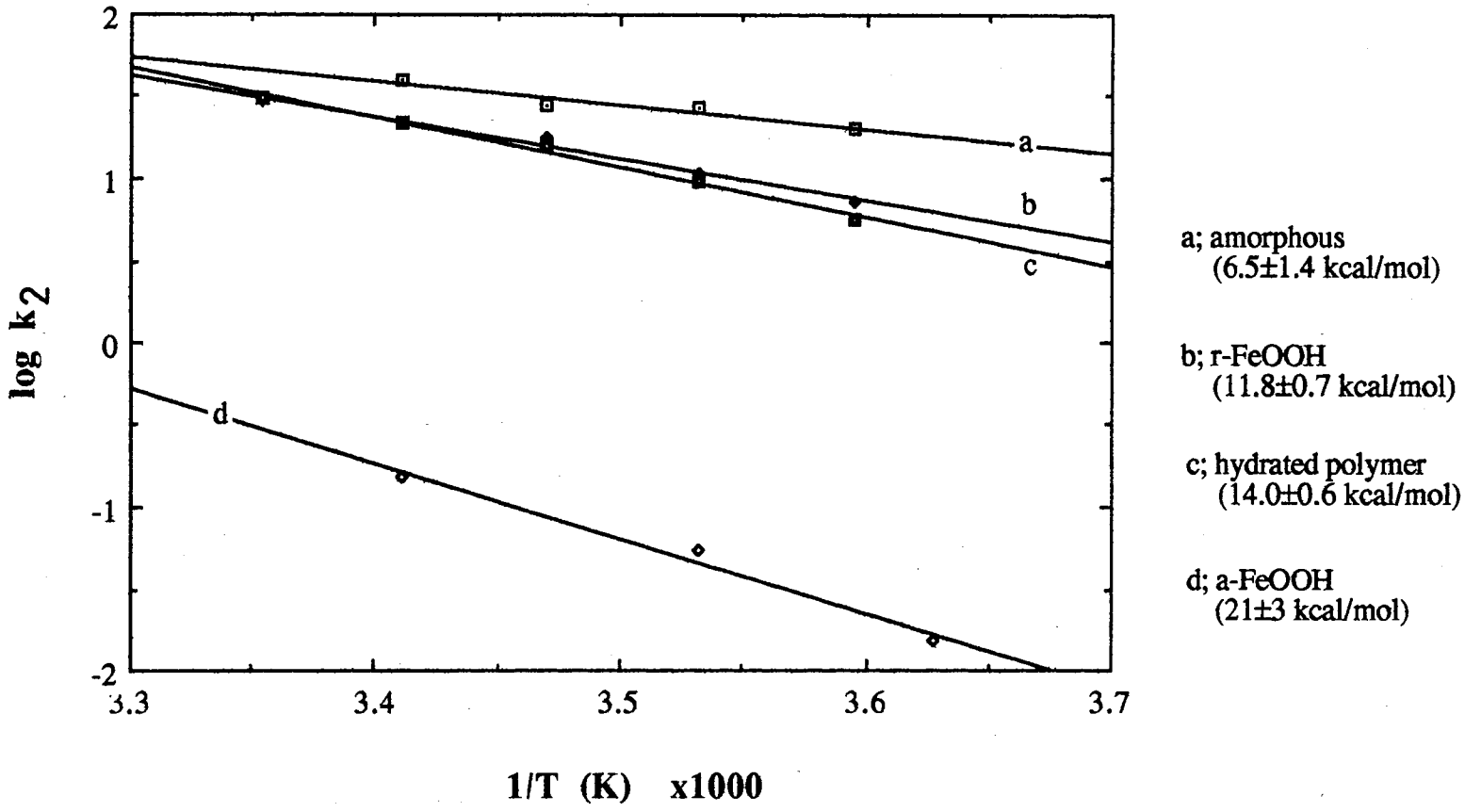

Fig. 5-17 The effect of temperature on the dissolution rate constant in acidic seawater obtained by filtration experiments

6 GENERAL CONCLUSIONS

6.1 General Conclusions

Solubilities of various colloidal ferric oxides, typical ferric oxides in natural waters and soils, in seawater at 20°C were experimentally determined by new dialysis techniques for amorphous hydrous ferric oxide and γ-FeOOH and/or by simple filtration experiments for amorphous phase, γ-FeOOH and $Fe_5O_7(OH).4H_2O$ involving γ-activity measurements of ^{59}Fe.

The results of dialysis experiments indicate that the logarithmic solubilities within the pH range 5.5-7.0 increased linearly with decreasing pH with a slope of -1.0, suggesting that $Fe(OH)_2^+$ is the dominant dissolved ferric species. In the normal pH range of seawater, the solubilities were independent of pH, indicating the existence of $Fe(OH)_3°$ in addition to $Fe(OH)_2^+$. The solubilities determined by dialysis experiments are consistent with those determined by simple filtration experiments with a 0.025 μm Millipore filter. The order of solubilities of various ferric oxides in seawater is amorphous hydrous ferric oxide (10 nM) > γ-FeOOH (1.4±0.4 nM) > $Fe_5O_7(OH).4H_2O$ (0.2-0.6 nM) > α-FeOOH (0.01 nM) since α-FeOOH, the most stable iron oxyhydroxide found in natural waters and soils, is about three orders of magnitude less soluble than amorphous phase. Recently, the dissolved iron concentrations measured at deep waters in the open ocean have been reported to be

0.3-0.7 nM as a constant value. The implication is that the deep waters in the open ocean may be in saturation equilibrium with the thermodynamically stable ferric oxide forms rather than metastable amorphous phase. The dissolved iron concentrations at the surface waters in the open ocean are controlled by atmospheric iron inputs (abundance in source media, solubility and dissolution rate depending on the iron solid form) and phytoplankton iron requirements. The iron solid form at deep waters, which is probably regenerated from oxidation of the biogenic organic flux and/or is less soluble atmospheric iron, may be less soluble ferric oxide than amorphous phase. However, to confirm this interpretation, the following several problems will have to be resolved; the operationally defined concept of a dissolved (filterable) fraction with 0.4 μm filter which can not quantitatively remove the smaller colloidal particles, qualitative and quantitative analyses for solid iron phases in seawaters, atmospheric dust and colloids from rivers, the crystallization mechanism of metastable to the stable forms in seawater, the adsorption mechanism of dissolved iron on the particles, etc.

The Fe(III) dissolution rates of various ferric oxides in seawater at 20°C were determined by the dialysis techniques for amorphous phase and γ-FeOOH and by the simple filtration experiments at acidic pH for amorphous phase, γ-FeOOH, $Fe_5O_7(OH).4H_2O$ and α-FeOOH.

The Fe(III) dissolution rate was defined as a first-order reaction in proportion to the concentration of particulate Fe(III) in seawater. Within the pH range 7-8, the dissolution rate constants, k_2, obtained from the dialysis experiments are relatively independent of pH with values of

0.015 and 0.005 day^{-1} for amorphous phase and γ-FeOOH, respectively. This suggests that only water is involved in breaking the Fe-O bond on the surface of ferric oxide to form an activated complex. On the assumption that the rate constants in the pH range 7-8 is independent of pH, the rate constants of various ferric oxides at pH 7.0, which estimated from both dialysis data and filtration data at acidic seawater, are in the order: amorphous hydrous ferric oxide (0.0080 day^{-1}) > γ-FeOOH (0.0065 day^{-1}) > $Fe_5O_7(OH).4H_2O$ (0.0036 day^{-1}) > α-FeOOH (0.000052 day^{-1}), a sequence that must be the result of differences in the chemical composition and crystal structure of these ferric oxides. On the basis of activation energies alone, dissolution rates should vary in reverse order. Actually, the activation energies required for the acid dissolution of various ferric oxides were in the order: α-FeOOH > $Fe_5O_7(OH).4H_2O$ > γ-FeOOH > amorphous phase. As the activation energy required for dissolution increases, the thermodynamic stability of ferric oxide increases. The order of cell yield in the culture experiments in the presence of various ferric oxide forms is amorphous phase > γ-FeOOH >> $Fe_5O_7(OH).4H_2O$ > α-FeOOH. This order is the same as those of the solubilities and dissolution rates of these ferric oxides in seawater. An increase in the thermodynamic stability may reduce the solubility and dissolution rate and hence the supply of biologically available iron by phytoplankton.

6.2 References

Aagaard P. and Helgeson H. C. (1982) Thermodynamic and kinetic constraints on reaction rates among minerals and aqueous solutions. I. Theoretical considerations. *Amer. J. Sci.* **282**, 237-285.

Anderson M. A. and Morel F. M. M. (1982) The influence of aqueous iron chemistry on the uptake of iron by the coastal diatom *Thalassiosira weissflogii*. *Limnol. Oceanogr.* **27**, 789-813.

Atkinson R. J., Posner A. M. and Quirk J. P. (1968) Crystal nucleation in Fe(III) solutions and hydroxide gels. *J. Inorg. Nucl. Chem.* **30**, 2371-2381.

Bruland K. W., Donat J. R. and Hutchins D. A. (1991) Interactive influences of bioactive trace metals on biological production in oceanic waters. *Limnol. Oceanogr.* **36**, 1555-1577.

Byrne R. H. and Kester D. R. (1976 a) Solubility of hydrous ferric oxide and iron speciation in seawater. *Mar Chem.* **4**, 255-274.

Byrne R. H. and Kester D. R. (1976 b) A potentiometric study of ferric ion complexes in synthetic media and seawater. *Mar. Chem.* **4**, 275-287.

Cornell R. M., Posner A. M. and Quirk J. P. (1976) Kinetics and mechanisms of the acid dissolution of goethite (α-FeOOH). *J. Inorg. Nucl. Chem.* **38**, 563-567.

Cornell R. M. and Giovanoli R. (1988) Acid dissolution of akaganeite and lepidocrocite: the effect on crystal morphology. *Clays & Clay Minerals* **36**, 385-390.

Crosby S. A., Glasson D. R., Cuttler A. H., Butler I., Turner D. R., Whitfield M. and Millward G. E.(1983) Surface area and porosities

of Fe(III)- and Fe(II)-derived oxyhydroxides. *Environ. Sci.Technol.* **17**, 709-713.

Duce R. A. (1986) The impact of atmospheric nitrogen, phosphorus, and iron species on marine biological productivity. In *The role of air-sea exchange in geochemical cycling* (Edited by Buat-Menard P.), pp. 497-529. Reidel.

Finden D. A. S., Tipping E., Jaworski G. H. M. and Reynolds C. S. (1984) Light-induced reduction of natural iron (III) oxide and its relevance to phytoplankton. *Nature* **309**, 783-784.

Fox L. E. (1988) The solubility of colloidal ferric hydroxide and its relevance to iron concentrations in river water. *Geochim.Cosmochim. Acta* **52**, 771-777.

Glover H. E. (1978) Iron in Maine coastal waters; seasonal variation and its apparent correlation with dinoflagellate bloom. *Limnol. Oceanogr.* **23**, 534-537.

Gordon R. M., Martin J. H. and Knauer G. A. (1982) Iron in north-east Pacific waters. *Nature* **299**, 611-612.

Guillard R. R. L. and Ryther J. H. (1962) Studies of marine planktonic diatoms. I. *Cyclotella nana* Hustedt and *Detonula confervacea* (Gleve) Gran. *J. Microbiol.* **8**, 229-239.

Hamada S. and Kuma K. (1976) Preparation of γ-FeOOH by aerial oxidation of iron(II) chloride solution. *Bull. Chem. Soc. Japan* **49**, 3695-3696.

Hamada S. and Kuma K. (1977) The coercive force of γ-Fe_2O_3 prepared from γ-FeOOH. *Bull. Chem. Soc. Japan* **50**, 1635-1636.

Helgeson H. C., Murphy W. M. and Aagaard P. (1984) Thermodynamic and kinetic constraints on reaction rates among minerals and

aqueous solution II. Rate constants, effective surface area, and the hydrolysis of feldspar. *Geochim. Cosmochim. Acta* **48**, 2405-2432.

Iwasaki H. and Iwasa K. (1982) Studies on the red tide flagellates - VII. *Prorocentrum micans* (*levantinoides* type) appeared in Ise Bay in 1978. *Bull. Fac. Fish., Mie Univ.* **9**, 49-56.

Kuma K., Nakabayashi S., Suzuki Y. and Matsunaga K. (1992 a) Dissolution rate and solubility of colloidal hydrous ferric oxide in seawater. *Mar. Chem.* **38**, 133-143.

Kuma K., Nakabayashi S., Suzuki Y., Kudo I. and Matsunaga K. (1992 b) Photo-reduction of Fe(III) by dissolved organic substances and existence of Fe(II) in seawater during spring blooms. *Mar. Chem.* **37**, 15-27.

Kuma K., Suzuki Y. and Matsunaga K. (1992 c) Solubility and dissolution rate of colloidal γ-FeOOH in seawater. *Water Res.* in press

Landing W. M. and Bruland K. W. (1987) The contracting biogeochemistry of iron and manganese in the Pacific Ocean. *Geochim. Cosmochim. Acta* **51**, 29-43.

Langmuir D. (1969) The Gibbs free energies of substances in the system Fe-O_2-H_2O-CO_2 at 25°C. U. S. Geol. Surv., Prof. Pap. 650-B, B180-B184.

Langmuir D. and Whittemore D. O. (1971) Variations in stability of freshly precipitated ferric oxyhydroxides, in Nonequilibrium systems in natural waters. *Advan. Chem. Ser.* **106**, 209-234.

Lewin J. and Chen C.-H. (1971) Available iron: a limiting factor for marine phytoplankton. *Limnol. Oceanogr.* **16**, 670-675.

Lewin J. and Chen C.-H. (1973) Changes in the concentration of soluble and particulate iron in seawater enclosed in containers.

Limnol. Oceanogr. **18**, 590-596.

Lindsay W. L. (1991) Iron oxide solubilization by organic matter and its effect on iron availability. In *Iron Nutrition and Interactions in Plants* (Edited by Chen Y. and Hadar Y.), pp. 29-36. Kluwer Academic Publishers, Netherlands.

Martin J. H. and Fitzwater S. E. (1988) Iron deficiency limits phytoplankton growth in the northeast Pacific subarctic. *Nature* **331**, 341-343.

Martin J. H. and Gordon R. M. (1988) Northeast Pacific iron distributions in relation to phytoplankton productivity. *Deep-Sea Res.* **35**, 177-196.

Martin J. H., Gordon R. M., Fitzwater S. E. and Broenkow W. W. (1989) VERTEX: phytoplankton/iron studies in the Gulf of Alaska. *Deep-Sea Res.* **36**, 649-680.

Martin J. H., Gordon R. M. and Fitzwater S. E. (1990) Iron in Antarctic waters. *Nature* **345**, 156-158.

Martin J. H., Gordon R. M. and Fitzwater S. E. (1991) The case for iron. *Limnol. Oceanogr.* **36**, 1793-1802.

Moore R. M., Milley J. E. and Chatt A. (1984) The potential for biological mobilization of trace elements from aeolian dust in the ocean and its importance in the case of iron. *Oceanol. Acta* **7**, 221-228.

Nakabayashi S., Kudo I., Kuma K., Toya K. and Matsunaga K. (1989) Existence of dissolved Fe^{2+} in a spring bloom at Funka Bay. *Bull. Jpn Soc. Fish. Oceanogr.* **53**, 128-130.

Nolting R. F., De Baar H. J. W., Van Bennekom A. J. and Masson A. (1991) Cadmium, copper and iron in the Scotia Sea, Weddell Sea

and Weddell/Scotia confluence. *Mar. Chem.* **35**, 219-243.

O'Sullivan D. W., Hanson A. K., Miller W. L. and Kester D. R. (1991) Measurement of Fe(II) in surface water of the equatorial Pacific. *Limnol. Oceanogr.* **36**, 1727-1741.

Price N. M., Anderson L. F. and Morel F. M. M. (1991) Iron and nutrition of equatorial Pacific plankton. *Deep-Sea Res.* **38**, 1361-1378.

Rich H. W. and Morel F. M. M. (1990) Availability of well-defined iron colloids to the marine diatom *Thalassiosira weissflogii*. *Limnol. Oceanogr.* **35**, 663-679.

Roekens E. J. and Van Grieken R. (1983) Kinetics of iron(II) oxidation in seawater of various pH. *Mar. Chem.* **13**, 195-202.

Schneider W. (1988) Iron hydrolysis and the biochemistry of iron - the interplay of hydroxide and biogenic ligands. *CHIMIA* **42**, 9-20.

Schwertmann U. (1991) Solubility and dissolution of iron oxides. In *Iron Nutrition and Interactions in Plants* (Edited by Chen Y. and Hadar Y.), pp. 3-27. Kluwer Academic Publishers, Netherlands.

Sidhu P. S., Gilkes R. J., Cornell R. M., Posner A. M. and Quirk J. P. (1981) Dissolution of iron oxides and oxyhydroxides in hydrochloric and perchloric acids. *Clays & clay Minerals* **29**, 269-276.

Sillen L. G. and Martell A. E. (1964) *Stability Constants of Metal Ion Complexes.* Chem. Soc. London, Spec. Publ., London, pp. 754.

Stookey L. L. (1970) Ferrozine - a new spectrophotometric reagent for iron. *Anal. Chem.* **42**, 779-781.

Stumm W. (1977) Chemical interaction in partical separation. *Environ. Sci. Tecnol.* **11**, 1066-1070.

Stumm W. and Morgan J. J. (1981) *Aquatic Chemistry*, Wiley-

Interscience, New York, pp. 780.

Sturgeon R. E., Berman S. S., Willie S. N. and Desaulniers J. A. (1981) Preconcentration of trace elements from seawater with silica-immobilized 8-hydroxyquinoline. *Anal. Chem.* **53**, 2337-2340.

Sulzberger B., Suter D., Siffert C., Banwart S. and Stumm W. (1989) Dissolution of Fe(III)(hydro)oxides in natural waters; Laboratory assessment on the kinetics controlled by surface coordination. *Mar. Chem.* **28**, 127-144.

Symes J. L. and Kester D. R. (1985) The distribution of iron in the northwest Atlantic. *Mar. Chem.* **17**, 57-74.

Waite T. D. and Morel F. M. M. (1984 a) Photoreductive dissolution of colloidal iron oxides in natural waters. *Environ. Sci. Technol.* **18**, 860-868.

Waite T. D. and Morel F. M. M. (1984 b) Photoreductive dissolution of colloidal iron oxides: effect of citrate. *J. Colloid Interface Sci.* **102**, 121-137.

Wells M. L., Zorkin N. G. and Lewis A. G. (1983) The role of colloid chemistry in providing a source of iron to phytoplankton. *J. Mar. Res.* **41**, 731-746.

Wells M. L. and Mayer L. M. (1991) The photoconversion of colloidal iron oxyhydroxides in seawater. *Deep-Sea Res.* **38**, 1379-1395.

Wells M. L., Mayer L. M., Donard O. F. X., De Souza Sierra M. M. and Ackelson S. G. (1991) The photolysis of colloidal iron in the oceans. *Nature* **353**, 248-250.

Westerlund S. and Ohman P. (1991) Iron in the water column of the Weddell Sea. *Mar. Chem.* **35**, 199-217.

Yamochi S. (1983) Mechanisms for outbreak of *Heterosigma akashiwo*

red tide in Osaka Bay, Japan. *J. Oceanogr. Soc. Jpn.* **39**, 310-316.

Zhuang G., Duce R. A. and Kester D. A. (1990) The dissolution of atmospheric iron in surface seawater of the open ocean. *J. Geophys. Res.* **95**, 16207-16216.

Zinder B., Furrer G. and Stumm W. (1986) The coordination of weathering: II. Dissolution of Fe(III) oxides. *Geochim. Cosmochim. Acta* **50**, 1861-1869.